

Scalar-Scaffolded Gluons and the Combinatorial Origins of Yang-Mills Theory

Nima Arkani-Hamed,^a Qu Cao (曹趣),^{b,c} Jin Dong (董晋),^{b,d} Carolina Figueiredo,^e
Song He (何颂)^{b,f,g}

^a*School of Natural Sciences, Institute for Advanced Study, Princeton, NJ, 08540, USA*

^b*CAS Key Laboratory of Theoretical Physics, Institute of Theoretical Physics, Chinese Academy of Sciences, Beijing 100190, China*

^c*Zhejiang Institute of Modern Physics, Department of Physics, Zhejiang University, Hangzhou, 310027, China*

^d*School of Physical Sciences, University of Chinese Academy of Sciences, No.19A Yuquan Road, Beijing 100049, China*

^e*Jadwin Hall, Princeton University, Princeton, NJ 08540, USA*

^f*School of Fundamental Physics and Mathematical Sciences, Hangzhou Institute for Advanced Study & ICTP-AP, UCAS, Hangzhou 310024, China*

^g*Peng Huanwu Center for Fundamental Theory, Hefei, Anhui 230026, P. R. China*

E-mail: arkani@ias.edu, qucao@zju.edu.cn, dongjin@itp.ac.cn,
cfigueiredo@princeton.edu, songhe@itp.ac.cn

ABSTRACT: We present a new formulation for Yang-Mills scattering amplitudes in any number of dimensions and at any loop order, based on the same combinatorial and binary-geometric ideas in kinematic space recently used to give an all-order description of $\text{Tr } \phi^3$ theory. We propose that in a precise sense the amplitudes for a suitably “stringy” form of these two theories are identical, up to a simple shift of kinematic variables. This connection is made possible by describing the amplitudes for n gluons via a “scalar scaffolding”, arising from the scattering of $2n$ colored scalars coming in n distinct pairs of flavors fusing to produce the gluons. Fundamental properties of the “ u -variables”, describing the “binary geometry” for surfaces appearing in the topological expansion, magically guarantee that the kinematically shifted $\text{Tr } \phi^3$ amplitudes satisfy the physical properties needed to be interpreted as scaffolded gluons. These include multilinearity, gauge invariance, and factorization on tree- and loop- level gluon cuts. Our “stringy” scaffolded gluon amplitudes coincide with amplitudes in the bosonic string for extra-dimensional gluon polarizations at tree-level, but differ (and are simpler) at loop-level. We provide many checks on our proposal, including matching non-trivial leading singularities through two loops. The simple counting problem underlying the u variables autonomously “knows” about everything needed to convert colored scalar to gluon amplitudes, exposing a striking “discovery” of Yang-Mills amplitudes from elementary combinatorial ideas in kinematic space.

Contents

1	Introduction and Summary	1
2	Review of Surfaceology	7
2.1	The $\text{Tr } \phi^3$ theory	8
2.2	Defining the surface	9
2.3	Kinematical data and curves on the surface	10
2.4	From curves on the fat graph to words	13
2.5	From words to u -variables	13
2.6	Summary of u facts	16
2.7	“Stringy” amplitudes	19
3	Scalar-Scaffolded Gluons	24
3.1	From $2n$ scalars to n gluons	25
3.2	Polarizations and momenta of the gluons	27
3.3	Unified form of gauge invariance and multi-linearity	28
3.4	Dictionary: From scalar to gluon kinematics	31
3.5	3-point gluon amplitude in scalar language	32
4	Tree-level Gluon Amplitudes	32
4.1	Connection to the bosonic string	33
4.2	The scaffolding residue	35
4.3	Scaffolding residue \Rightarrow Gauge invariant and multi-linear amplitude	37
4.4	Tree-level factorization	40
4.5	Computing scaffolding residues for general n	43
4.6	Consistency check: From $4n$ -scalars to $2n$ -scalars	48
4.7	Examples	49
4.8	Further comments	52
5	Loop-level Gluon Amplitudes	55
5.1	Loop scaffolding form	55
5.2	Surface gauge invariance	57
5.3	Example: 1-loop 2-point	59
5.4	A well-defined Yang-Mills integrand	60
6	Leading Singularities	61
6.1	Linearized u 's	62
6.2	Tree level	64
6.3	Loop level	67

7	Loop Cut and Matching with Tree-level Gluing	69
7.1	Set up	70
7.2	Gluing in the forward limit	71
7.3	Loop-cut	75
8	Outlook	77
A	Scaffolding residues using worldsheet variables of bosonic string	79
B	Complete results for 1-loop 4-point box leading singularity	80
C	Matching of the loop-cut with gluing of tree in the forward limit	82
C.1	Matching of the D -dependent part	82
C.2	Matching of variables of tree triangulation	83
C.3	Matching of loop variables	84
C.4	Matching of curves $X_{1,j}$	88
C.5	Matching the tadpole part	89
C.6	Difference between loop-cut and tree-gluing as a total derivative	90

1 Introduction and Summary

Scattering amplitudes are the “boundary observables” in flat space. The observations of the asymptotic states are made at infinity, while the interior of the spacetime serves as an auxiliary arena allowing us to incrementally build up the final amplitude in terms of interactions at and propagation between spacetime points. But given that the observable is anchored at infinity, it is natural to take the holographic point of view and ask: is there a way of calculating scattering amplitudes that jettisons the interior of the spacetime entirely, formulated purely in the kinematic space describing the scattering amplitude?

Tackling this question has turned out to involve ideas very far from the much more familiar (and so far more successful) instantiations of holography in Anti-de-Sitter space. The reason is simple: the “kinematic space” that labels boundary correlation functions in AdS space is simply all the points in the one lower-dimensional spacetime on the boundary, with a conventional notion of locality, time, and quantum mechanical evolution. By contrast, the kinematic space labeling scattering processes has none of this familiar structure: for n particle scattering we have the space of n on-shell momenta, without any of the familiar properties of the arenas in which physics is usually described.

But over the past decade, it has become apparent that in a number of cases, there is just enough structure in this seemingly barren kinematic space to discover entirely new mathematical questions to which the scattering amplitudes, with all their richness and complexity, are the answer. The emerging picture is that kinematic space contains elementary but deep combinatorial structures that in turn specify a tower of related mathematical objects above them, ultimately giving a completely autonomous definition of amplitudes. In

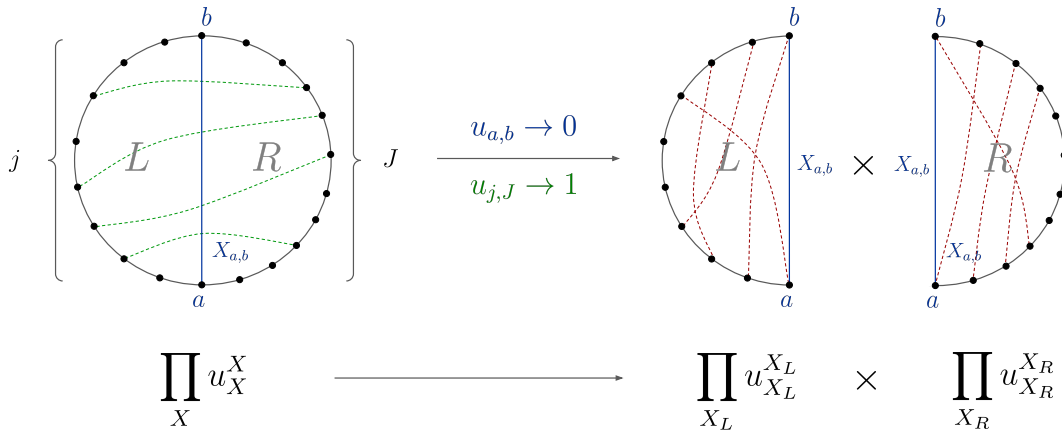


Figure 1: Binary behaviour of u -variables and factorizations.

this way, the usual foundational principles of locality and unitarity can be seen as derivative notions, ultimately arising from this fundamentally combinatorial rubric.

The first example of this sort of structure was seen with the discovery of the amplituhedron for $\mathcal{N} = 4$ SYM in the planar limit [1]. The integrand for the planar amplitude, at any loop order, is given as the “canonical form” [2] of a certain region in the kinematic space of momentum(-twistor) data [3], entirely specified by topological winding number and positivity properties [4]. There is no mention of diagrams, locality, or unitarity anywhere in sight, instead in this example, these very simple but rather alien and more abstract combinatorial and geometric concepts bring the physics of spacetime and quantum mechanics to life, along the way manifesting the hidden infinite Yangian symmetry enjoyed by the scattering amplitudes. However, the very special nature of planar $\mathcal{N} = 4$ SYM—its maximal supersymmetry and integrability—might be thought of as a dissuasion from the thought that such structures generalize to more realistic theories, instead perhaps being an artifact of studying the most special toy model we know of.

In the past few years, however, morally similar but technically quite different structures have been seen in a completely different setting, for the simplest theory of colored scalars with cubic self-interactions—the $\text{Tr } \phi^3$ theory—at all loop orders and to all orders in the topological ’t Hooft expansion [5, 6] [7, 8]. This “curve-integral” formalism features a simple counting problem defined at any order in the topological expansion, which defines a set of variables, u_C , defined for all propagators/ curves C on a surface, satisfying the remarkable non-linear equations $u_C + \prod_D u_D^{\#\text{int}(C,D)} = 1$. These equations define a “binary geometry” [9, 10]: if we set $u_C \geq 0$ they also force $0 \leq u_C \leq 1$, and as we approach a boundary where $u_C \rightarrow 0$ all the “incompatible” curves \mathcal{D} that cross C have $u_{\mathcal{D}} \rightarrow 1$. The amplitudes are defined by $\mathcal{A} = \int \omega \prod_C u_C^{P_C^2}$, where ω is a simple canonical form with logarithmic singularities on the boundaries where $u_C \rightarrow 0$, and P_C^μ is the momentum associated with C . The binary character of the u_C variables tells us that the “curve integral” for \mathcal{A} deserves to be called an “amplitude”, by guaranteeing the correct patterns of factorization near singularities as in figure 1 at tree-level. The curve integral can give us both “stringy” amplitudes, or, via

“tropicalization”, directly amplitudes in the field theory limit. There is no trace of the idea of “summing over all spacetime processes” in these formulas. Instead, the simple counting problem attached to curves on surfaces magically converts combinatorial geometry into local and unitary physics in this model.

But in the same way that $\mathcal{N} = 4$ SYM theory seems “too special” to offer a hope for connecting combinatorial geometry to real-world physics, the $\text{Tr } \phi^3$ theory might seem too simple. While the singularities/poles/“denominators” of $\text{Tr } \phi^3$ are universal and shared by all theories of colored particles, real-world amplitudes for e.g. colored gluons differ in a crucial way, in their numerator structure. However, so far the connection between amplitudes and geometry has centered on long-distance singularities captured only by the “denominators”, which are simple poles associated in many settings with the simplest “logarithmic” singularities. This is reflected in the ubiquity of “canonical forms with dlog singularities on boundaries of positive geometries” in this world of ideas. Interesting numerators are instead associated with new singularities at infinite momentum, not captured by “dlog” singularities. This basic fact has been a thorn in the side of the “amplitudes=combinatorial geometry” program for over a decade, going back to “poles at infinity” seen in non-supersymmetric BCFW shifts, and non-dlog forms in the Grassmannian required to describe leading singularities in non-supersymmetric gauge theory [11]. Clearly the realistic non-supersymmetric Yang-Mills theory demands a move away from such “dlog forms”, but in what setting, and how? Until very recently, there was no plan of attack to make progress on this fundamental mystery.

But in [12] we reported a wonderful surprise that has transformed the situation. Far from the toy model it appears to be, the “stringy” $\text{Tr } \phi^3$ amplitudes secretly *contains* the scattering amplitudes for pions [13], as well as non-supersymmetric gluons, in any number of dimensions. The amplitudes for the different theories are given by one and the same function, related by a simple shift of the kinematics. Working at tree-level, the stringy $\text{Tr } \phi^3$ amplitude is given as

$$\mathcal{A}^{\text{Tr}\phi^3} = \int_0^\infty \prod \frac{dy_i}{y_i} \prod_{i,j} u_{i,j}^{\alpha' X_{i,j}}, \quad (1.1)$$

where $X_{i,j} = (p_i + p_{i+1} + \dots + p_{j-1})^2$ are the natural planar variables occurring as poles in the amplitude. This same function remarkably determines Yang-Mills amplitudes by a simple kinematical shift:

$$\mathcal{A}^{\text{gluons}}(X) = \mathcal{A}^{\text{Tr}\phi^3}(X_{e,e} \rightarrow X_{e,e} + 1/\alpha', X_{o,o} \rightarrow X_{o,o} - 1/\alpha', X_{e,o} \rightarrow X_{e,o}), \quad (1.2)$$

where $X_{e,e}, X_{o,o}, X_{e,o}$ refer to $X_{i,j}$ where the pair of indices (i, j) are both even, both odd, or one of each respectively.

To be more precise, this kinematical shift gives us the amplitude for what we call “scaffolded gluons”: an amplitude for $2n$ colored scalars coming in n pairs of distinct flavors. As we will explain in detail, completely general amplitudes for n gluons, with arbitrary choices of (null) polarizations, are captured by these “scaffolded” amplitudes the “scaffolding residues” are taken, corresponding to factorizing this amplitude on the channel where the pairs of same-species scalar fuse into gluons. This will turn out to be a simple

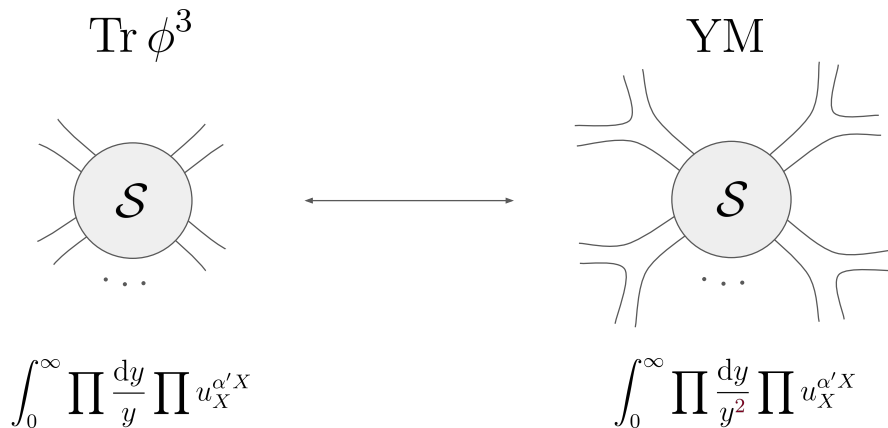


Figure 2: From colored scalars to scalar-scaffolded gluons.

and powerful picture both for presenting gluon amplitudes in an entirely canonical way free of the familiar annoying redundancies, as well as seeing their hidden relationships with other theories.

Our kinematic shift can equivalently be described by multiplying the $\text{Tr } \phi^3$ integrand by a factor $(\prod u_{e,e}^{+1} u_{o,o}^{-1})$. This factor has a beautiful interpretation directly in terms of the y variables, if we choose a particularly natural triangulation for our $2n$ -gon surface. We simply choose any triangulation/fat graph we like for the “inner” n -gon, and turn it into a “scaffolding triangulation” by splitting each of the n external legs in two, just as suggested from the scalar scaffolding picture. Quite beautifully, this product $(\prod u_{e,e}^{+1} u_{o,o}^{-1}) = \prod_i y_i^{-1}$. This means that the entire effect of the kinematical shift for the $2n$ scalar problem is to replace the dlog-form measure $\prod dy_i/y_i \rightarrow \prod dy_i/y_i^2$ (see figure 2)! Note this is no longer a dlog form, as had long been anticipated was necessary for non-supersymmetric Yang-Mills theory.

As shown in [12] and discussed at further length in this paper, at tree level this kinematic shift precisely matches gluon amplitudes in the bosonic string, choosing the momenta to lie in d dimensions and pairs of polarizations to live in n extra dimensions. In this paper we will go much further, and propose that, appropriately interpreted, this expression gives us a definition for the amplitudes of non-supersymmetric Yang-Mills theory at all loop orders, in any number of spacetime dimensions. But where does this strange kinematic shift come from? And why on earth should it have had anything to do with describing gluon amplitudes?

We will see striking answers to these questions throughout this paper. Clearly generic functions of X ’s for a $2n$ problem can not be interpreted as amplitudes for scaffolded gluons. Instead as we will see these functions must have a symmetry under certain linear shifts of the $X_{i,j}$, guaranteeing both **gauge invariance** and **multilinearity** of the gluon amplitudes they are describing. These properties emerge magically from the shifted integral with the dy/y^2 measure, when the scaffolding residue to land on gluon amplitudes is taken.

We have already remarked that the fundamental “binary” property of the u variables—that when $u_{\mathcal{C}} \rightarrow 0$ the $u_{\mathcal{D}} \rightarrow 1$ for \mathcal{D} intersecting \mathcal{C} —is responsible for factorization and therefore the right to call the curve integral an “amplitude” for the scalar $\text{Tr } \phi^3$ theory. Shifting to the dy/y^2 form and taking the scaffolding residue ends up also probing the behavior of the u ’s in the first-order neighborhood of where they vanish, which takes us beyond the most basic “binary” properties. Amazingly, fundamental identities relating u variables of the inner n -gon and outer $2n$ -gon problems give exactly the needed first-order behavior to force the integral to have the symmetries needed for gauge invariance and multilinearity!

This is already strong evidence that we must be describing gluons, but to clinch the case we have to show consistent factorization on gluon poles, both for tree-like factorization, as well the loop-level “single cut”. As we will see, once again properties of the u variables that follow transparently from their definition in terms of the counting problem, give precisely the needed identities for these “tree-cut” and “loop-cut = forward limit” factorizations to arise exactly as needed. All of these properties hold not just in the field theory limit but also at finite α' .

We find it fascinating that elementary but deep properties of the u variables, ultimately deriving from the simple counting problem associated with curves on surfaces that define them [7, 8], contain exactly the magical properties needed to produce functions that can be interpreted as scattering amplitudes for gluons enjoying gauge invariance. This mirrors the famous “discovery of gluons” arising from Möbius invariance of correlators for the spin-one vertex operators in string theory. But in this new picture there is no worldsheet, no conformal field theory living on it, and no vertex operators. Instead we have pure combinatorics, with the magical ability to produce “gluon amplitudes” seemingly out of thin air!

In the course of these explorations we will also see that merely asking for our new integrals to have any kind of natural factorization properties on the poles, dictates how to more precisely interpret the $2n$ scaffolded formula. At loop level the product over curves \mathcal{C} must include open curves with up to one self-intersection per loop. It must also include a product over closed curves Δ with exponents u_{Δ}^{1-D} where D is the number of spacetime dimensions, which is where the dependence on spacetime dimensionality, absent in the $\text{Tr } \phi^3$ theory, makes an appearance for gluons. The need for including curves with one self-intersection per loop is very interesting, and shows a pronounced difference with what is expected of string theory at one-loop. For $\text{Tr } \phi^3$ theory it is already known that matching (bosonic) string theory at loop-level from the curve-integral formalism [14] asks us to consider the product over *all* curves, including those with arbitrarily high intersection numbers. It is fascinating that in order to have consistent factorization on massless gluon poles—guaranteeing that we are describing Yang-Mills theory at low energies—we must make the curve-integral “slightly more stringy” by including curves with a finite number of self-intersections. Of course, this is still vastly simpler than the infinite set of curves that string theory demands even to describe the scalar $\text{Tr } \phi^3$ theory.

The consistent factorization of “loop-cut = forward limit” [15, 16] is especially non-trivial, where not only algebraic relations but total derivative identities are needed to establish the correspondence; nonetheless, they all fall out naturally from the counting

problem formulae for the u variables. As we will emphasize, this solves a long-standing conceptual problem afflicting all attempts to date to make sense of the notion of “the Yang-Mills integrand” at loop-level for non-supersymmetric theories. The well-known problem is again a very basic one. The Feynman diagrams have diagrams with “tadpoles” and hence $1/0$ propagators at the level of the integrand. But a general feature of the curve-integral formalism already for $\text{Tr } \phi^3$ theory allows us the flexibility to give any values we like to the X variables—in particular, nothing mandates that the variables corresponding to tadpoles (or massless external bubbles) be set equal to zero. Leaving them free then lets us work with completely well-defined integrands. Remarkably, it is precisely these well-defined integrands that satisfy the exact “loop-cut = forward limit” formula! So the surface formalism *defines* objects for us that naturally enjoy a “surface” notion of gauge-invariance, and also factorize precisely onto themselves. Amongst other things, this opens the door to finding all-loop recursion relations for pure Yang-Mills amplitudes in any number of dimensions [17].

We believe that the remarkable link between $\text{Tr } \phi^3$ theory, pions, and gluons reported in [12], extended to all loops in the present paper and [13] represents a major step forward in the adventure of describing real-world scattering processes in the radically new language of combinatorial geometry. Our goal in this paper is to initiate an exploration of the new world of physical and mathematical ideas involved in this “combinatorial discovery” of pure Yang-Mills theory, and present the most basic checks on our proposal, leaving many interesting and important questions for future work.

We will begin in section 2 with a review of “surfaceology” and the curve integral formalism. This is intended as a crash-course introduction to all the formulas needed to understand the surface picture for kinematic space, a user manual for computing u variables and using them to construct stringy amplitudes, and a compendium of important facts about u variables we will use throughout this paper. This short section is meant as a self-contained summary of the facts we will need from the curve-integral formalism, whose origin and conceptual underpinning are presented in a different series of papers beginning with [7, 8]; the review of u variables will borrow results to appear in [18]. We next move on in section 3 to describing the picture of scalar-scaffolded gluons, establishing the simple dictionary between gluon and scalar variables, and understanding how the basic gluonic kinematic facts of on-shell gauge-invariance and linear dependence on polarization-vectors are given a unified description in scalar terms. We discuss gluon amplitudes at tree level in section 4, beginning by showing how our proposal precisely matches gluon amplitudes in the open bosonic string, with an appropriate choice of extra-dimensional polarizations. We will see how the unified statements of gauge-invariance and multilinearity arise from simple properties of the u variables. The same properties also imply consistent factorization of the amplitude on massless gluon poles. We present an explicit n -point formula for scaffolding residues, and see how the interpretation of the scalar-scaffolded amplitudes as those of extra-dimensional polarization gluons is naturally discovered in our language. We also give simple examples of three- and four-point string/particle amplitudes. We move on to present our proposal at loop-level in section 5, where a number of essential new ingredients first make an appearance, and the difference with standard string amplitudes becomes

stark. This includes the need for keeping minimally self-intersecting curves as well as closed curves encoding the dependence on the number of spacetime dimensions we have alluded to above. Finally, we present a series of checks we have performed on our proposal. In section 6, we compute leading singularities corresponding to gluing together on-shell three-gluon amplitudes for arbitrary graphs: in our picture this turns into a simple residue computation in the y variables, and we present non-trivial examples through two loops, and we find perfect matching with the gluing computation includes both the Yang-Mills and F^3 three-particle amplitudes. Of course this computation of leading singularities using residues in y variables bears no resemblance at all to the direct gluing of three-particle amplitudes, and is also much more efficient. We then proceed to our most fundamental and important check in section 7, showing how the single one loop-cut magically matches the tree-forward limit, at full “stringy” level, following from many further fundamental properties of u variables hardwired into their combinatorial definition. We finally end with an outlook on obvious avenues for future exploration immediately following from the developments we discuss in this paper.

2 Review of Surfaceology

A recent series of papers [7] has introduced the curve integral formalism for describing both “stringy” $\text{Tr } \phi^3$ amplitudes, as well as the closely related “tropical” representation of these amplitudes in the field theory limit, at all orders in the ‘t Hooft topological expansion. The kinematic space for the amplitude at any order in the topological expansion is associated with a surface \mathcal{S} , which is specified by providing a triangulation or what is the same, a single “fat graph” \mathcal{F} , whose vertices are associated with triangles of the triangulation, glued to each other as dictated by the edges. All the kinematic variables at this order in the topological expansion are naturally associated with curves that can be drawn on the surface or equivalently, paths that can be drawn on \mathcal{F} . This space of curves on \mathcal{S} specifies the kinematic arena for $\text{Tr } \phi^3$ amplitudes. The heart of the curve integral formalism lies in the existence of a remarkable set of “ $u_{\mathcal{C}}$ -variables” attached to any curve \mathcal{C} on surface \mathcal{S} . As already mentioned in the introduction, these variables non-trivially satisfy the beautiful equations

$$u_{\mathcal{C}} + \prod_{\mathcal{D}} u_{\mathcal{D}}^{\#\text{int}(\mathcal{C}, \mathcal{D})} = 1. \quad (2.1)$$

These equations define a variety whose dimensionality is given by the number of internal edges of \mathcal{F} , or more fancily, the dimensionality of the Teichmuller space of \mathcal{S} . There are a variety of ways of presenting the solution space of these equations. One uses ideas from the hyperbolic geometry of \mathcal{S} . A more surprising and deeper presentation is fundamentally combinatorial, expressing $u_{\mathcal{C}}$ ’s as the solution to a certain extremely simple counting problem associated with the curve \mathcal{C} as drawn on the fat-graph \mathcal{F} , giving $u_{\mathcal{C}}(y_i)$ as a ratio of polynomials in variables y_i associated with all the internal edges of \mathcal{F} .

The u variables are the stars of the $\text{Tr } \phi^3$ show in [7], playing many crucial roles. They manifest a “binary” property, where asking $u_{\mathcal{C}} \geq 0$ also forces $0 \leq u_{\mathcal{C}} \leq 1$. This also implies that if some $u_{\mathcal{C}} \rightarrow 0$, all the $u_{\mathcal{D}} \rightarrow 1$ for the curves \mathcal{D} that cross \mathcal{C} . Mathematically,

this gives us a completely algebraic characterization of all possible degenerations of the surface. Said in more fancy (but not more contentful) language, the u_C variables give a new, practical, algebraic, and “global” definition of the compactification of the Teichmuller space of \mathcal{S} . This is extremely useful: all the usual ways of choosing coordinates for the surface are “local”; as such they make some degenerations/singularities easy to see, but others are always more complicated, needing a detailed analysis and manual “blow-ups” as the boundaries of the co-ordinate chart are approached. But the u variables do all the blowups for us, once and for all.

This “binary” property also has a crucial physical interpretation. If we consider a product of the form $\prod_X u_X^{P_X^2}$, then as any particular $u_{X^*} \rightarrow 0$, the product factorizes exactly to the same product on the smaller surface we get by cutting the big surface along X^* . This precisely reflects the factorization of scattering amplitudes when the propagator $P_{X^*}^2 \rightarrow 0$ goes on-shell. This is what allows the curve integral formulas for both the “stringy” and field-theoretic $\text{Tr } \phi^3$ theory to be interpreted as “amplitudes” for these models.

Amazingly, the u/y variables turn out to have a number of further properties, well beyond the “binary” property manifested in the u equations, that allow simple kinematic shifts to transmute the seemingly “dull” amplitudes of $\text{Tr } \phi^3$ theory into the amplitudes of gluons. The central goal of this paper is to show how this magic happens.

But our goal in this section is to provide a self-contained introduction to all aspects of “surfaceology” needed for the reader to follow all of our arguments, without needing to have previously read the series of papers associated with [7, 8]. As such our purpose is to simply present the logical connection between various important concepts, and provide recipes for concrete computations, without explaining where the concepts and formulas come from. The reader interested in these conceptual underpinning as well as many concrete examples of full amplitudes computed using the curve integral formalism is encouraged to consult [7, 8]. Our review of the properties of the u/y variables borrows from the complete account that will be given in [18].

2.1 The $\text{Tr } \phi^3$ theory

Let ϕ be an $N \times N$ matrix, the Lagrangian of the theory is:

$$\mathcal{L} = \text{Tr} (\partial\phi)^2 + g \text{Tr } \phi^3. \quad (2.2)$$

so ϕ is a massless field that interacts through cubic interactions with the coupling constant g ¹. We use the double line notation to keep track of the color indices in the interactions.

Since this is a scalar theory, the data of a scattering process in this theory is simply the momentum of the particles, p_i . As for the amplitude, since it has to be a Lorentz-invariant function, it will only be a function of the **Mandelstam invariants**: $p_i \cdot p_j$.

As we will explain in the next sections, the surface provides a very useful way of organizing the kinematic data of the problem. In addition, we can use it to read off the building blocks of string amplitudes – the **u-variables**.

¹It is trivial to add a mass term, but to keep things as simple as possible with our ultimate aim of describing gluons in mind, we will stick with the massless $\text{Tr } \phi^3$ theory.

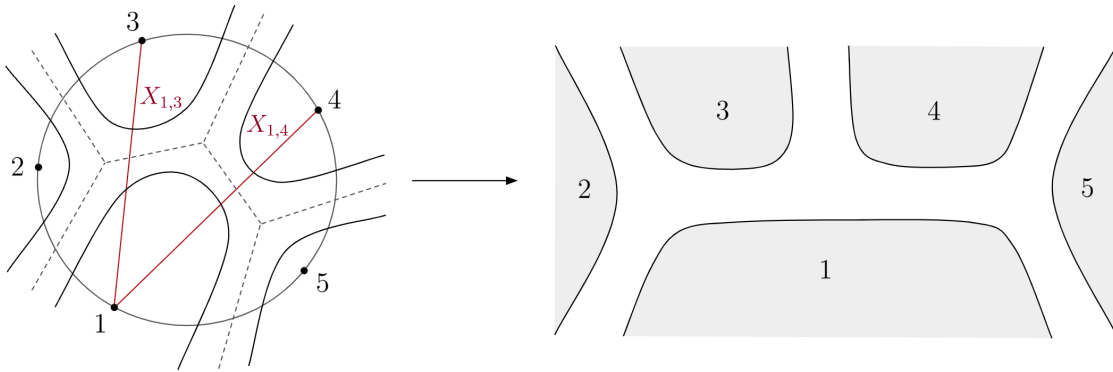


Figure 3: Triangulation of the disk with 5 marked points on the boundary and corresponding dual fat graph.

2.2 Defining the surface

The first step consists of defining the surface. By doing so, we specify both the scattering process and the order in the topological expansion we are considering.

A surface is defined as a collection of triangles together with a rule on how to glue the edges of the triangles together. So, one way of defining it is by providing a diagram, as it uniquely determines a triangulation via duality.

For the most part in this paper, the surfaces we will be considering are disks with n marked points on the boundary, and l punctures – corresponding to single-trace amplitudes of n particles at l loop order in the planar limit—though of course all surfaces corresponding to all orders in the ‘t Hooft topological expansion can be chosen.

2.2.1 Tree-level

At tree level let us consider the case of a 5-pt amplitude, which corresponds to a disk with 5 marked points on the boundary. Taking into account the diagram with propagators $X_{1,3}$ and $X_{1,4}$, we obtain the triangulation presented in Figure 3 (left).

The color graph, or ribbon graph, can be obtained from the Feynman diagram by fattening the edges of the graph and assigning arrows that keep track of the contraction of the color indices. However for our purposes, we only need the color graph without the color indices – we call it the **fat graph**, as shown in figure 3 (right). The fat graph is then dual to a triangulation of the surface and thus uniquely defines the surface. In fact, one can explicitly go from the fat graph to the surface: for example, in the 5-point case presented in figure 3, we can recover the disk with marked points on the boundary by shrinking the shaded regions to points.

2.2.2 Loop-level

Let us now consider a loop example, a 1-loop amplitude at 4 points. The corresponding surface is now a disk with a puncture and four marked points on the boundary, for which we choose a box triangulation. We denote the four chords of this triangulation by Y_i ,

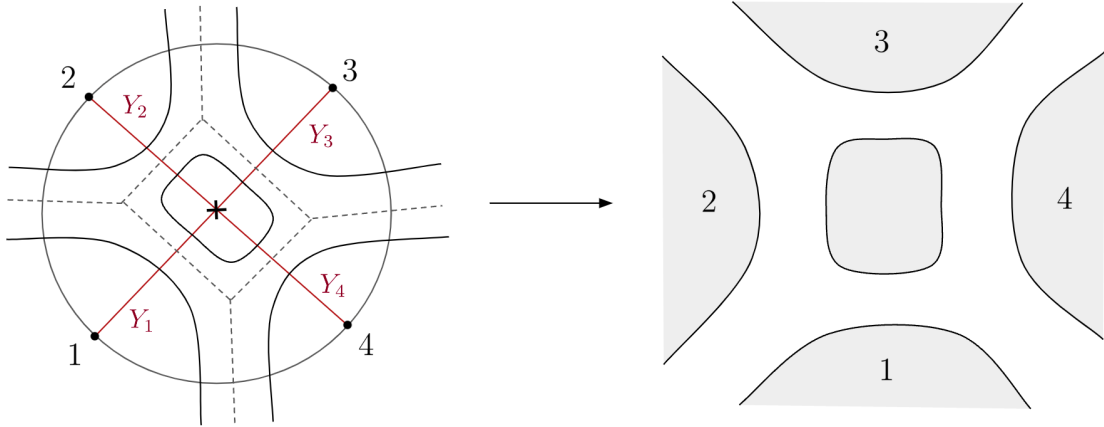


Figure 4: Box triangulation of the punctured disk with 4 marked points on the boundary and corresponding dual fat graph.

(instead of X) because they end on the puncture. (see Figure 4 for triangulation (left) and corresponding fat graph (right)). Similarly, by shrinking the shaded regions of the fat graph, we can recover the punctured disk with 4 marked points on the boundary.

2.3 Kinematical data and curves on the surface

Next, we need to understand how the kinematics, the data of the scattering problem is encoded in the surface.

The mapping can be summarized as follows:

Kinematical Data	→	Surface
Propagators	→	Chords/Curves, $[X_C]$
Feynman Diagrams	→	Triangulations $\{X_{i_1, j_1}, \dots, X_{i_{n-3}, j_{n-3}}\}$

The scalar amplitudes we are considering are purely functions of the propagators, so, according to the mapping, all the data of the problem is encoded on the curves we can draw on the surface. Of course, naively, there seems to be an infinite number of curves one can draw on a surface, so we need to understand which ones we need to consider.

The answer is: we consider all curves that are not homologous to each other. Now we need to say how to consistently assign momenta to these curves.

2.3.1 Tree-level

At tree level, we start by assigning momentum to the boundary curves of the disk, corresponding to the momentum of the external particles. Now the planar variables associated with the boundary curves are $X_{i, i+1} = p_i^2$, so for boundary curves, we have: $X_{i, i+1} = 0$, for massless particles.

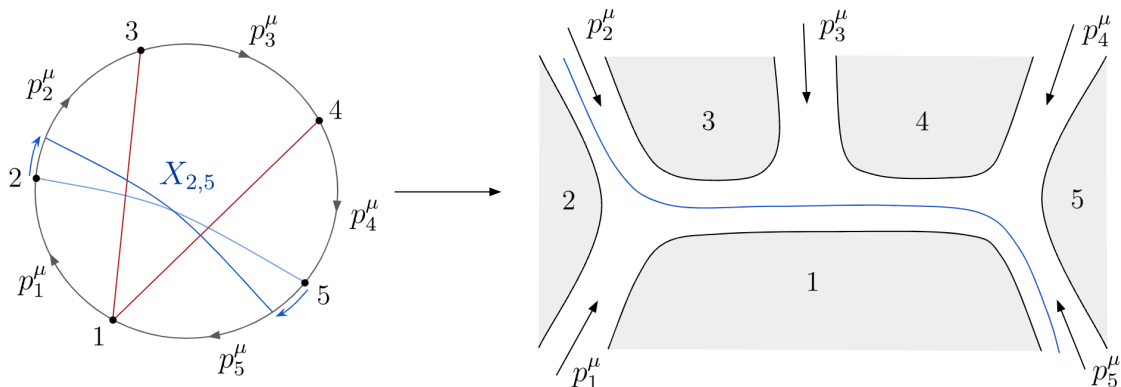


Figure 5: Determining momentum of curve $X_{2,5}$.

Now, at tree-level, we can read off the momentum assigned to a non-boundary curve, $X_{i,j}$, by deforming it into the boundary, where it can be seen as the union of the boundary curves from i to $i+1, \dots, j-1$ to j . So then the momentum of this curve is just the sum of the momentum of these boundary curves, and thus we get $X_{i,j} = (p_i + \dots + p_{j-1})^2$, as we expect for the planar propagators.

Alternatively, we can read off the momentum of a curve by using the fat graph. Let's go back to our 5-point example and consider the curve $X_{2,5}$, which on the surface side is connecting the marked points 2 and 5. In order to draw this curve on the fat graph, we first need to slightly rotate the ends of this curve **clock-wise** (see figure 5 (left)), this new curve goes by the name of a **lamination**. Laminations start and end in the boundaries of the disk, instead of marked points. These boundaries correspond to the edges of the fat graph, and this is why laminations are the objects that are naturally defined in the fat graph. From now on we will refer to the edges of the fat graph as **roads**, since, as opposed to 1-dimensional edges of graphs, the roads of the fat graph are crucially 2-dimensional. Therefore, the momentum of the boundaries of the disk, p_i^μ , determines the momentum associated with the external roads of the fat graph.

Thus to each curve on the surface, there is a unique lamination which is also defined in the fat graph. The distinction between a curve and a lamination will not be important for most of the matters we will encounter, so we will refer to curves and laminations interchangeably, and highlight the situations in which the difference is important.

So as a lamination, we can draw curve $X_{2,5}$ on the fat graph as shown in figure 5 (right). To read off the momentum, we follow the curve and start by writing down the momentum of the road in which the curve enters the graph – so for $X_{2,5}$, we would write down p_2^μ . Now each time the curve reaches an intersection and turns **right**, we add the momentum of the road coming from the **left** – so for $X_{2,5}$, it turns right in the first intersection, so we add p_3^μ , and right in the second intersection, so we also add p_4^μ . If, instead, the curve turns left at an intersection, we don't add anything. In the end, the momentum of the curve is simply the sum of momentum obtained squared – so for $X_{2,5}$ we get $(p_2 + p_3 + p_4)^2$, as

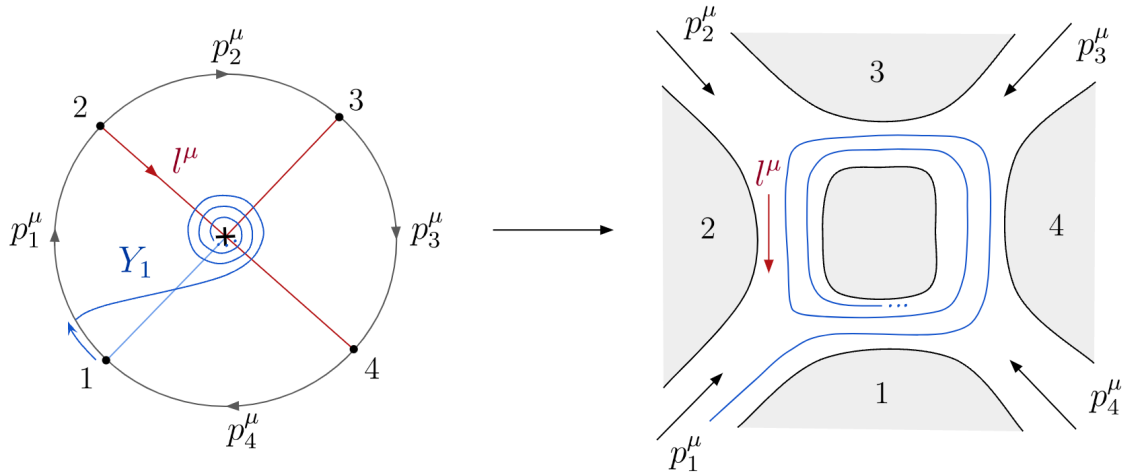


Figure 6: Determining momentum of curve Y_1 .

expected.

2.3.2 Loop-level

At loop level, we also start by assigning momentum to the boundary curves. However, because of the presence of the puncture, we can now draw curves that are **not homologous** to any boundary, for example, any curve going from a boundary-marked point to the puncture. Therefore we need to assign a momentum to one of such curves – this is exactly the loop momentum l^μ (see figure 6, left).

As opposed to the case of tree-level, at loop-level we now have a genuine infinite family of curves that are not homologous to each other. One way of seeing all such curves is to consider a curve starting and ending in some boundary-marked points. At tree-level, all such curves are unique, but in the presence of the puncture we can consider curves that start and end in the same points but that wind around the puncture n times and thus self-intersecting n times. In addition, another curve we can draw in the punctured disk is a **closed** curve. This closed curve is homologous to the full boundary and so has zero momentum. In any case, we will associate a variable, Δ , to this curve and it will turn out to play an important role later.

Just like in the tree-level case, we can read off the momentum of any curve using the fat graph. To do so we go from the curve to the lamination – note that for curves that end in the puncture, the corresponding laminations spiral **counter-clockwise** around the puncture an infinite number of times (see figure 6). Then we follow exactly the same rule as in the tree-level case: so for Y_1 , we start by writing down p_1^μ , then it turns right in the first intersection, so we add the momentum coming from the left which in this case is l^μ , the loop momentum. Finally, it spirals around forever, and keeps turning left while doing so, which means we don't have to add any more momentum. Therefore we are left with $Y_1 = (p_1 + l)^2$.

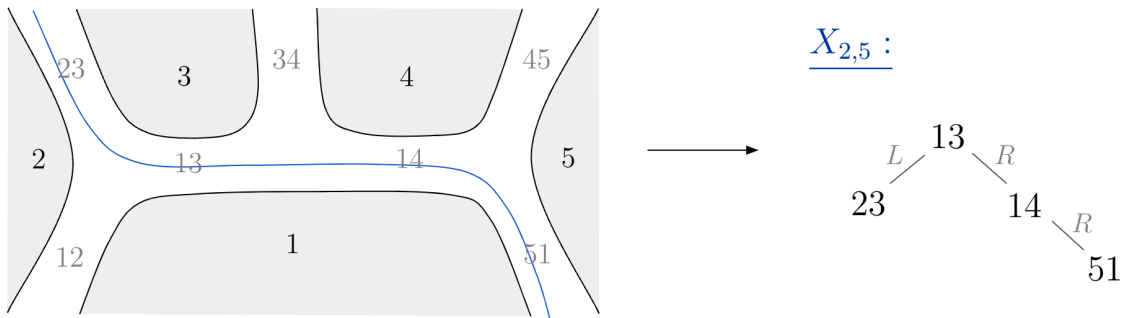


Figure 7: From curve to word: curve $X_{2,5}$.

Having defined the mapping between the surface variables and the kinematic invariants, we now have to understand what operation we need to do on the surface that gives us the amplitude in terms of these variables.

2.4 From curves on the fat graph to words

In this step, we want to find a way of encoding the information about the curves on the surface of some new objects. These objects should be such that using them one is fully able to reconstruct the surface as well as the curve in question.

To do this we use the fat graph defining the surface, and start by labelling its **roads** according to the sides they touch (see figure 7 (left)).

Making use of this labelling, we can record the path of a given curve along the fat graph by keeping track of the roads it goes through as well as whether it turns right or left each time it reaches an intersection. So let's establish the rule that for each left-turn we go up, while for each right turn, we go down. By following this rule we build up a mountainscape uniquely associated with the curve we follow, we call this object the **word**.

As an example, let's consider a 5-point process at tree-level. Let's pick the fat graph with propagators $X_{1,3}$ and $X_{1,4}$, and look at the curve from 2 to 5 (see figure 7 (left)). Following the curve, we see it enters the graph in road 23, then it turns **left** to 13, then **right** to 14, and finally **right** to 45. Following the rule described in the previous paragraph, we get the word for curve $X_{2,5}$ (see figure 7 (right)).

The words are the most basic objects defined on the surface that encode all the kinematic data. The last step is to understand what manipulation we need to do on these words to obtain the amplitude. This involves building the **u-variables**.

2.5 From words to u -variables

At tree-level, the u -variables are well-studied objects in the literature, appearing already in the earliest days of the dual resonance model in the work of Koba and Nielsen [19], in the work of Francis Brown on the study of ζ values from stringy integrals [20], and directly in the context of binary geometries in [9]. One of the central discoveries of the curve integral

formalism [7] is the generalization of u -variables to all surfaces. There are a number of ways of doing this, either framed in the language of hyperbolic geometry, or more abstractly, in terms of a simple counting problems associated with the words attached to curves on surfaces. This counting problem approach is both the more elementary and deeper one, and was summarized in [7]. A more systematic exposition of all the different ways of thinking about u variables from both the counting problem and hyperbolic geometry viewpoints, aimed at physicists, will be given in [14, 18].

To each curve, \mathcal{C} , on the surface we can associate a u -variable, $u_{\mathcal{C}}$, that satisfies the **u-equation**:

$$u_{\mathcal{C}} + \prod_{\mathcal{D}} u_{\mathcal{D}}^{\#\text{int}(\mathcal{C}, \mathcal{D})} = 1, \quad (2.3)$$

where the product is taken over all other curves \mathcal{D} and $\#\text{int}(\mathcal{C}, \mathcal{D})$ the intersection number between the two curves. For positive u 's, we see that all u 's are bounded by 1. In addition, from equation (2.3), when $u_{\mathcal{C}}$ goes to zero, all the $u_{\mathcal{D}}$, for the curves \mathcal{D} that intersect \mathcal{C} , have to go to one. This **binary** behavior is crucial to ensure that amplitudes build out of the u 's satisfy **factorization** near poles.

The u -equations form a non-linear set of equations that make it obvious that the u -variables are not independent of each other. So it is useful to find a good parametrization of the space of solutions of the u -equations. This is a non-trivial problem for which the surface gives a very nice answer.

As we explained in 2.2, in order to define the surface one has to provide a fat graph, dual to a triangulation of the surface. Of course, there are multiple fat graphs that describe the same surface, in particular for an n -point tree, there are Catalan_{n-2} such possibilities. Each choice of fat graph corresponds to a **positive parametrization** of the u -variables that automatically satisfies the u -equations.

To obtain this parametrization we start by assigning variables to the internal roads of the fat graph – the ones corresponding to the propagators, y_i . Now the u 's will be functions of the y_i 's, in particular, will be ratios of polynomials in the y_i 's. To get these functions we define two matrices:

$$M_L(y_i) = \begin{bmatrix} y_i & y_i \\ 0 & 1 \end{bmatrix} \quad ; \quad M_R(y_i) = \begin{bmatrix} y_i & 0 \\ 1 & 1 \end{bmatrix}, \quad (2.4)$$

where L and R stand for left and right. To build the u -variable from some word, W_C of some curve C , all we need to do is multiply these matrices in the order the curve tells us to, *i.e.* each time it turns left/right at some road y_i we multiply by $M_L(y_i)/M_R(y_i)$, respectively. Any non-boundary curve starts in some boundary road and then turns left or right into some internal road, since there is no y associated with the starting boundary road, the first matrix appearing M_L or M_R should be evaluated at 1. By the end of this, we have a 2×2 matrix, whose entries are polynomials in the ys , $m_{i,j}(y)$. The u -variable for the curve is simply:

$$u_C = \frac{m_{1,2} \cdot m_{2,1}}{m_{1,1} \cdot m_{2,2}}. \quad (2.5)$$

Let's go through an example to see how the rule works in practice. Consider the 5-pt tree level amplitude, so the disk with 5 punctures, and let's get the u -variable for curve $X_{2,5}$ (figure 7). In this case, the sequence of L/R matrices is:

$$M_L(1)M_R(y_{1,3})M_R(y_{1,4}) = \begin{bmatrix} 1 & 1 \\ 0 & 1 \end{bmatrix} \begin{bmatrix} y_{1,3} & 0 \\ 1 & 1 \end{bmatrix} \begin{bmatrix} y_{1,4} & 0 \\ 1 & 1 \end{bmatrix} = \begin{bmatrix} 1 + y_{1,4} + y_{1,3}y_{1,4} & 1 \\ 1 + y_{1,4} & 1 \end{bmatrix}. \quad (2.6)$$

Hence from (2.5), we have:

$$u_{2,5} = \frac{1 + y_{1,4}}{1 + y_{1,4} + y_{1,3}y_{1,4}}. \quad (2.7)$$

The u variables for the “spiraling curves” into punctures are interesting. Let us denote the chords in the triangulation hitting the puncture read counterclockwise as $y_1^{(p)}, y_2^{(p)}, \dots, y_r^{(p)}$. Then any word corresponding to a spiraling curve will end with the infinite repeating upward sequence:

$$\begin{array}{c} \dots \\ y_1^{(p)} \\ \diagup \\ y_2^{(p)} \\ \dots \\ y_r^{(p)} \\ \diagup \\ y_1^{(p)} \\ \dots \end{array} \quad (2.8)$$

So at the end of the word, we encounter the matrix $M_{\text{spiral}} = M_L(y_1^{(p)})M_L(y_2^{(p)})\dots M_L(y_r^{(p)})$, which is raised to the N 'th power with N sent to infinity. Now

$$M_{\text{spiral}}^N = \begin{pmatrix} Y_{\text{spiral}}^N & F_{\text{spiral}}(1 + Y_{\text{spiral}} + \dots + Y_{\text{spiral}}^{N-1}) \\ 0 & 1 \end{pmatrix}, \quad (2.9)$$

where

$$Y_{\text{spiral}} = (y_1^{(p)} \dots y_r^{(p)}), \quad F_{\text{spiral}} = y_1^{(p)} + y_1^{(p)} y_2^{(p)} + \dots + y_1^{(p)} \dots y_r^{(p)}. \quad (2.10)$$

Note that as $N \rightarrow \infty$, in order for the geometric series in the matrix above ($1 + Y_{\text{spiral}} + Y_{\text{spiral}}^2 + \dots$) to be convergent we must have that the product $Y_{\text{spiral}} \leq 1$. This is an extra restriction above and beyond the positivity of the y 's. If we call the matrix product for the part of the word before we begin spiraling as:

$$M_{\text{before}} = \begin{pmatrix} a & b \\ c & d \end{pmatrix}, \quad (2.11)$$

then if we take the u variable associated with the matrix $M_{\text{before}}M_{\text{spiral}}^N$ and send $N \rightarrow \infty$ we have

$$u_{\text{spiraling}} = \frac{aF_{\text{spiral}} + b(1 - Y_{\text{spiral}})}{cF_{\text{spiral}} + d(1 - Y_{\text{spiral}})}. \quad (2.12)$$

2.5.1 u -variable for closed curve

The rules described above allow us to obtain the u variables for all curves defined on the surface. We will also have occasion to define u variables for closed curves around the punctures, Δ , for which we put:

$$u_{\Delta_I} = \left(1 - \prod_i y_i^{(p_I)} \right), \quad (2.13)$$

where Δ_I stands for the closed curve around puncture I , and $y_i^{(p_I)}$ are the y 's present in the underlying triangulation that go from one boundary point, i , and end in the puncture, I . For example, let's consider again the punctured disk with 4 marked points on the boundary – the 4-point one-loop amplitude. Choosing the box triangulation of figure 4, means we have four chords going from the boundary to the puncture, Y_1, Y_2, Y_3 and Y_4 . So in this case, the u -variable for the closed curve is:

$$u_{\Delta} = \left(1 - y_1^{(p)} y_2^{(p)} y_3^{(p)} y_4^{(p)} \right). \quad (2.14)$$

Note this $u_{\Delta} \rightarrow 0$ precisely when the product Y_{spiral} we encountered for spiraling u variables hits the boundary $Y_{\text{spiral}} \rightarrow 1$ we just saw above. So it is natural to have u_{Δ} detect this boundary.

Using the relation between the y and u variables we will review just below, it is easy to see that this definition is independent of the choice of triangulation; we have that $\prod_i y_i^{(p)} = \prod_Y u_Y$ where the Y denote all the curves spiraling at the puncture.

2.6 Summary of u facts

Here present a summary of a few facts about the u variables that will be useful throughout the rest of the paper. These results are all borrowed from [18] where a systematic understanding of these and many other properties of u/y variables will be given.

2.6.1 u 's of sub-surfaces

Suppose we have a surface \mathcal{S} , and a subsurface s contained inside it. (We can concretely define a subsurface s simply by giving its fat-graph as a subgraph of the parent fat-graph for \mathcal{S}). It is natural to wonder whether we can build out of the u variables $u_c^{(\mathcal{S})}$ for curves \mathcal{C} variables on the big surface \mathcal{S} , a set of objects $u_c^{(s)}$ that satisfy the u equations labelled by curves c on the smaller surface s . This question has a beautiful and natural answer: we can build u variables for the small surface out of simple monomials in the u variables for the big one. Given a curve c in s , we simply consider *all* ways of extending c into curves on the big surface, \mathcal{C}_c . Then we have

$$u_c^{(s)} = \prod_{\text{all curves } \mathcal{C}_c, \text{ extending } c \text{ into } \mathcal{S}} u_{\mathcal{C}_c}^{(\mathcal{S})}. \quad (2.15)$$

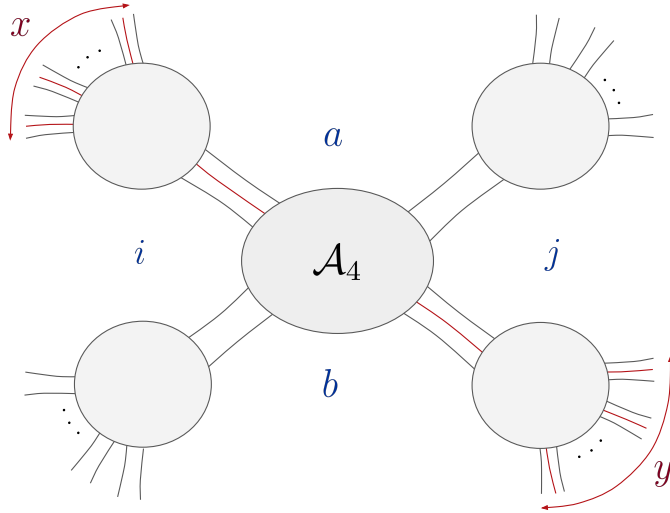


Figure 8: Smaller 4-point inside bigger surface.

2.6.2 Generalized u -equations

We have just seen that the u variables for smaller surfaces s can be expressed as monomials in the u variables of the big surface \mathcal{S} . Thus the u equations for the smaller surface s turn into new equations when these are expressed as monomials in the original surface \mathcal{S} —these are the *generalized u equations*. For instance for the disk at tree-level, we can consider the subsurface given by a 4-point fatgraph bounded by regions i, a, j, b as in figure 8. The curve (i, j) in this 4-point subsurface extends to the bigger tree into all the curves (x, y) with x in the set between $(i, a - 1)$ and y in the set between $(j, b - 1)$. Then we have $u_{i,j}^{(4)} = \prod_{x \in (i, a-1), y \in (j, b-1)} u_{x,y}$. Similarly the curve (a, b) in the subsurface extends to all the (w, z) with w between $(a, j - 1)$ and z between $(b, i - 1)$, so $u_{a,b}^{(4)} = \prod_{w \in (a, j-1), z \in (b, i-1)} u_{w,z}$. Then from the trivial 4-point u equations we get a non-trivial expression for sums of monomials in the parent u 's:

$$u_{i,j}^{(4)} + u_{a,b}^{(4)} = 1 \rightarrow \prod_{x \in (i, a-1), y \in (j, b-1)} u_{x,y} + \prod_{w \in (a, j-1), z \in (b, i-1)} u_{w,z} = 1. \quad (2.16)$$

All the extended u equations at tree-level can be summarized by a simple picture: we divide all the indices going around the disk into four consecutive sets (A, B, C, D) . Then the extended equations are $U_{A,C} + U_{B,D} = 1$, where $U_{A,C}$ is the product of all the $u_{i,j}$ with i in A and j in C , and $U_{B,D}$ is the product of all $u_{k,l}$ with k in B and l in D . The special case where A is the single i and C is the single j , with B, D filling out the complementary indices, gives us the standard u equation for $u_{i,j}$. As an example of a new generalized u equations for $n = 6$ we can take $A = (1, 2), B = (3), C = (4), D = (5, 6)$, then we have $u_{1,4}u_{2,4} + u_{3,5}u_{3,6} = 1$.

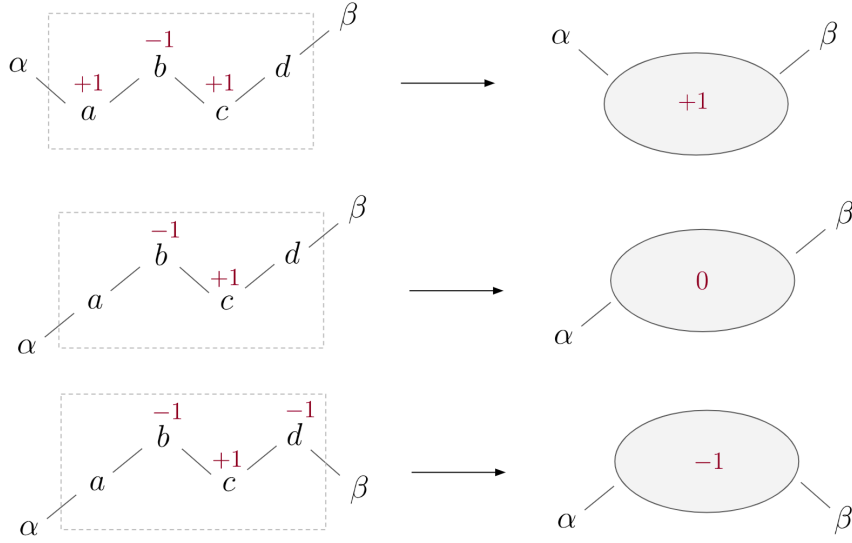


Figure 9: P_X for different words.

2.6.3 y 's and u 's

We now explain how to express the product of all the y 's in terms of u 's, for any given triangulation of the surface.

We can write each y as a product of u 's in the following way:

$$y_i = \prod_X u_X^{g_X^{(i)}}, \quad (2.17)$$

where $g_X^{(i)}$ stands for the i -th component of the **g -vector** corresponding to curve X . We can get g_X by looking at the corresponding word describing the curve. This word is a mountainscape with some roads appearing as peaks, \mathcal{P} , and others as valleys, \mathcal{V} . These peaks and valleys are always roads associated with the propagators of the underlying triangulation/ internal edges of the underlying fat-graph. To each such internal road we assign a vector, \vec{g}_i , then the g -vector of some curve, X , can be written as a linear combination of \vec{g}_i as follows:

$$\vec{g}_X = - \sum_{I \in \mathcal{P}} \vec{g}_I + \sum_{J \in \mathcal{V}} \vec{g}_J. \quad (2.18)$$

Therefore we have that $g_X^{(i)}$ will either be ± 1 depending on whether i appears as a valley or a peak in the word for X . Ultimately, the product of all the y 's is simply:

$$\prod_i y_i = \prod_X u_X^{p_X}, \quad p_X \equiv \sum_i g_X^{(i)}. \quad (2.19)$$

From (2.18), we have that $p_X = \#$ (valleys) - $\#$ (peaks), appearing in the word for curve X . It turns out that p_X is completely determined by what the word looks like at

the boundaries since the net number of right/left turns in the middle must even out (see figure 9). In summary, we have:

$$\prod_I y_I = \prod_X u_X^{p_X}, \quad \text{with } p_X = \begin{cases} +1, & \text{if } X \text{ turns } R \text{ at the start and } L \text{ at the end,} \\ -1, & \text{if } X \text{ turns } L \text{ at the start and } R \text{ at the end,} \\ 0, & \text{otherwise.} \end{cases} \quad (2.20)$$

2.7 “Stringy” amplitudes

Now we want to explain how we can use the variables defined from the surface, such as the curves and respective u -variables, to build string amplitudes.

2.7.1 Tree-level

String amplitudes are given as integrals over possible configurations of the string worldsheet. An n -point string tree-level amplitude corresponds to an integral over the moduli-space of real points z_1, \dots, z_n on the boundary of the disk [19, 21]:

$$\mathcal{A}_n^{\text{tree,tachyon}}(1, 2, \dots, n) = \int \frac{dz_1 \dots dz_n}{\text{SL}(2, \mathbb{R})} \times \underbrace{\prod_{i < j} (ij)^{2\alpha' k_i \cdot k_j}}_{\text{Koba-Nielsen factor}}, \quad (2.21)$$

with $z_1 < z_2 < \dots < z_n$, so that $(ij) = z_j - z_i > 0$ for $i < j$, k_i are the particle momenta and α' is the string constant. The worldsheet $\text{SL}(2, \mathbb{R})$ invariance demands that $\alpha' k_i^2 = -1$ and so the external states are tachyons with $m^2 = -(\alpha')^{-1}$.²

It turns out that the z_i 's also define a parametrization of the solution to the u equations in which each u variable is an $\text{SL}(2, \mathbb{R})$ invariant cross-ratios of the (ij) 's defined as follows:

$$u_{i,j} = \frac{(i-1, j)(i, j-1)}{(i, j)(i-1, j-1)}. \quad (2.22)$$

We can now express the integrand in terms of u 's, finding [5, 9, 10]:

$$\mathcal{A}_n^{\text{tree,tachyon}}(1, 2, \dots, n) = \int \frac{d^n z_i / \text{SL}(2, \mathbb{R})}{(12)(23)(34)\dots(n1)} \prod_{i < j} u_{i,j}^{\alpha'(x_{i,j}-1)}, \quad (2.23)$$

where the $x_{i,j} = (k_i + \dots + k_{j-1})^2$ are the planar-variables made from the external tachyon momenta. We will find it convenient to instead interpret this expression not as scattering amplitudes for tachyons but for massless external scalars with momenta p_i with $p_i^2 = 0$, simply by identifying the planar kinematic invariants for the massless problem $X_{i,j} = (p_i + \dots + p_{j-1})^2$ with those of the tachyons $x_{i,j}$ via $X_{i,j} = x_{i,j} - 1$. Thus we study finally

$$\mathcal{A}_n^{\text{tree}}(1, 2, \dots, n) = \int \frac{d^n z_i / \text{SL}(2, \mathbb{R})}{(12)(23)(34)\dots(n1)} \prod_{i < j} u_{i,j}^{\alpha' X_{i,j}}, \quad (2.24)$$

This is useful for talking about a “low-energy field theory limit”, something which doesn't make sense for tachyons whose mass is set by the string scale, but does make sense for

²We use the mostly-plus signature so that $k^2 = -m^2$.

the massless $X_{i,j}$ kinematics (where we also set $X_{i,i+1} = 0$). Indeed the low-energy limit of these “Parke-Taylor” or “Z-theory” amplitudes [22–24], where $\alpha' X_{i,j} \ll 1$, are just those of massless $\text{Tr } \phi^3$ theory (2.2). For this reason we will refer to this as the bosonic string $\text{Tr } \phi^3$ amplitude in the rest of this paper.

We can easily convert between the z_i and y_i variables that have both been used to give parametrizations of the same $u_{i,j}$ variables. Doing this we find that the “Parke-Taylor” measure written in terms of the z_i variables simplifies to a “dlog form” in the y_i , and the string integral takes it’s simplest form as:

$$\mathcal{A}_n^{\text{tree}}(1, 2, \dots, n) = \int_0^\infty \prod_i \frac{dy_i}{y_i} \prod_C u_C^{\alpha' X_C}, \quad (2.25)$$

where the product is taken over all the curves C on the disk with n -marked points on the boundary, and u_C are the corresponding u -variables parametrized by the y_i .

2.7.2 Loop-level

The n -point 1-loop amplitude in terms of surface variables is given exactly by (2.25) but where the product is taken over all the curves of the punctured disk with n marked points on the boundary. As pointed out before, at 1-loop, there are now an infinite number of curves coming from curves that self-intersect infinitely often. So we can rewrite this product as follows:

$$\mathcal{A}_n^{1\text{-loop}}(1, 2, \dots, n) = \int_0^\infty \prod_i \frac{dy_i}{y_i} \prod_C u_C^{\alpha' X_C} \times \prod_{C' \in \text{S.I.}} u_{C'}^{\alpha' X_{C'}} \times u_\Delta, \quad (2.26)$$

where the first product includes a finite number of terms corresponding to curves that never self-intersect. The second product is an infinite product over all the self-intersecting curves with different numbers of self-intersections. At last, we have the closed curve contribution, Δ .

A precise matching between this form of the amplitude and the conventional presentation of tachyon bosonic string amplitudes through 1-loop will appear in [14]. But as stressed in [7], at loop-level there are more options for “stringy” presentations of amplitudes at least so long as we are primarily interested in matching the correct field theoretic low energy limit. In particular, the contributions from the self-intersecting and closed curves are irrelevant to the field theory or “tropical” limit of the amplitudes; indeed these curves don’t even occur dually as propagators in any $\text{Tr } \phi^3$ diagrams. This means that if we are only interested in the field theory limit, we can effectively use a truncated integrand where we only keep the first product over non-self-intersecting curves. We emphasize again that this truncated object is **not** the full string amplitude at loop level, rather it is a simpler but still “stringy” object that correctly gives $\text{Tr } \phi^3$ amplitudes at low-energies.

2.7.3 Higher loops

Beyond single-trace amplitudes at one loop, an important novelty appears with the first non-planar amplitudes. For instance in the double-trace one-loop amplitudes, we have infinitely many curves that we can draw on this fat graph: they differ from one another

only in how many times they wind around the graph. This is a consequence of the *mapping class group* of the surface, which acts by increasing the winding of curves. In fact, this infinity of windings is the heart of the well-known difficulty in defining a loop integrand for non-planar amplitudes. Fortunately as described explicitly in [7, 8], it is easy to *mod out* by the action of the mapping class group, using the “*Mirzakhani trick*” [25]. This is a version of the familiar Fadeev-Popov idea for modding out by gauge redundancies in the path integral, and is accomplished by inserting a “*Mirzakhani Kernel*” $K(u)$ into the integration over the y variables. We will not display these factors explicitly in the rest of this paper, and they will not be relevant for the explicit two-loop computations we will perform for leading singularities.

2.7.4 Integration Contour

The stringy $\text{Tr } \phi^3$ integral is defined naively on the integration contour where $0 < y_i < \infty$. But this form only converges when the $X_{i,j} > 0$; continuing to the physically interesting region where we see resonances and the amplitude has poles, where $X_{i,j} < 0$, is carried out by analytic continuation.

This is a frustrating state of affairs. For four-point, the explicit expression in terms of the Beta function $(\Gamma(X_{1,3})\Gamma(X_{2,4}))/\Gamma(X_{1,3} + X_{2,4})$ gives us the analytic continuation and allows us to compute the amplitude everywhere, but for general n -point scattering no analytic formula is known and so the analytic continuation is not handed to us.

More conceptually, we would like to find the correct integration contour on which to define this integral. The contour should agree with the naive one for $0 < y_i < \infty$ when the integral is convergent, but give us the correct analytic continuation everywhere.

This is essentially the subject of defining the $i\epsilon$ prescription for string amplitudes, and a prescription for this contour was given by Witten in [26]. This prescription is essentially “local” in character, describing a deformation of the contour in the neighborhood of all possible singularities of the amplitude, ultimately associated with all the possible degenerations of the surface equivalent to Feynman diagrams, and so involves a local analysis of the integration domain with an amount of work that grows exponentially with the number of particles.

Now we know that one of the purposes in life of the u variables and their y parametrization is to explicitly “blow up” all possible degenerations of the surface, and thereby generate these exponentially many degenerations from objects that are described only by at most $O(n^2)$ variables. As will be described in much greater length [27], for this reason, the u, y formalism is ideally suited to define the $i\epsilon$ contour in a one-shot “global” way. In practice, this gives us a concrete contour prescription that can be written down once and for all, for all n , on which all the integrals in our paper are convergent returning well-defined amplitudes. We defer a detailed discussion of this contour to [27], contenting ourselves here only with illustrating how things work in the simplest case of four-particle scattering. Setting $u_{1,3} = y_{1,3}/(1 + y_{1,3})$ and $u_{2,4} = 1/(1 + y_{1,3})$, we have one of the classic forms of the beta function integral

$$\mathcal{A}_4 = \int_0^\infty \frac{dy_{1,3}}{y_{1,3}} y_{1,3}^{X_{1,3}} (1 + y_{1,3})^{-(X_{1,3} + X_{2,4})}. \quad (2.27)$$

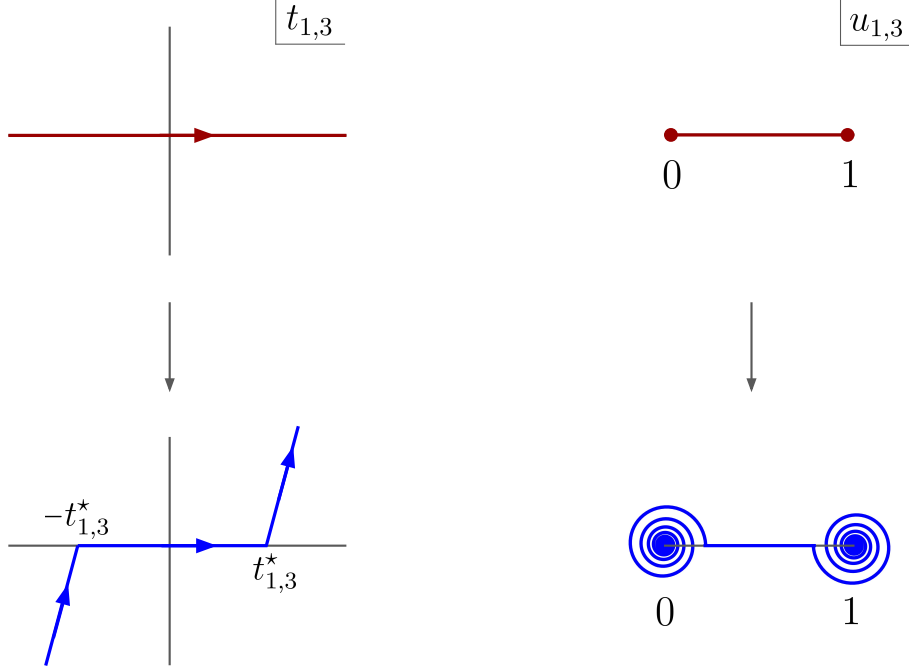


Figure 10: $i\epsilon$ contour for the 4-point amplitude.

To define the analytic continuation we imagine giving $X_{1,3}, X_{2,4}$ small imaginary parts, i.e. setting $X_{1,3} \rightarrow X_{1,3}^* + i\epsilon_{1,3}$ and $X_{2,4} \rightarrow X_{2,4}^* + i\epsilon_{2,4}$ where $X_{1,3}^*, X_{2,4}^*$ are real. It is useful to change from the y variables to the effective Schwinger parameter $y_{1,3} = e^{-t_{1,3}}$. The naive contour $0 < y_{1,3} < \infty$ is then given by an integration over the entire real $t_{1,3}$ axis. It is important that the contour goes to $t_{1,3} \rightarrow +\infty$ to capture the pole in the amplitude as $X_{1,3} \rightarrow 0$, and similarly that it goes to $t_{1,3} \rightarrow -\infty$ to capture the pole in $X_{2,4}$. These are of course also the degenerations where $u_{1,3} \rightarrow 0$ and $u_{2,4} \rightarrow 0$, respectively.

Now, the $i\epsilon$ contour is very natural in this Schwinger parameterization language. After we proceed on the real axis for a little while, we tilt the contour up till it's nearly vertical in the complex $t_{1,3}$ plane for $\text{Re}(t_{1,3}) > 0$, but with a small tilt towards the right so it does reach $\text{Re}(t_{1,3}) \rightarrow \infty$. Similarly, we tilt it down in the complex plane for $\text{Re}(t_{1,3}) < 0$. In other words for some $t_{1,3} > t_{1,3}^*$, our contour can be parametrized as $t_{1,3}(\rho) = t_{1,3}^* + \rho(i + \delta)$ with $0 < \rho < \infty$, for small δ . The contour for negative values of $\text{Re}(t_{1,3})$ can be defined in a similar way. This contour is a smooth deformation of the original one, but now gives us a well-defined integral, provided δ is chosen to be small enough. For instance on the right, as ρ becomes large, the integrand scales as $\exp[(X_{1,3}^* + i\epsilon_{1,3})(\rho(i + \delta))]$. The real part of the argument of the exponential is $(X_{1,3}^*\delta - \epsilon_{1,3})\rho$. So no matter how negative $X_{1,3}^*$ becomes, we can make δ small enough for the $-\epsilon_{1,3}$ term to suppress the integrand as $\rho \rightarrow \infty$. The same thing holds for the left side of the contour. We can readily check that numerically integrating along this contour gives us the correct result. Note that this natural contour in $t_{1,3}$ translates in a pretty contour in $u_{1,3} = e^{-t_{1,3}}/(1 + e^{-t_{1,3}})$. The usual contour has $u_{1,3}$ covering the entire real line $0 < u_{1,3} < 1$. The new contour instead spirals around $u_{1,3} = 0, 1$,

exactly as in Witten’s prescription [26]. The original and deformed contours in both $t_{1,3}$ and $u_{1,3}$ are shown in figure 10.

This example is too simple to illustrate the real power of the u, y variables in defining the $i\epsilon$ contour, which we will explain in more detail in [27]. But briefly, the point is that essentially the same contour, only with some care taken in where the “turns” into the complex plane are taken, can be chosen for each y_i independently. The magic of the u, y variables then correctly implements the needed shifts to make the integrals convergent in all degenerate limits, for precisely the same reason that the $u_{i,j}$ ’s “blow up” all the singularities as $u_{i,j} \rightarrow 0$ and the $y_{i,j}$ furnish a positive parametrization of the $u_{i,j}$. For the purposes of this paper, this is enough to concretely specify a contour on which our scaffolded gluon amplitudes can be concretely evaluated.

2.7.5 Low Energy Limit

The u/y variable formalism makes it especially easy to take the low-energy limit $\alpha' X_{i,j} \ll 1$ of the stringy $\text{Tr } \phi^3$ integrals and extract the field theory limit of the amplitudes. The reason is simply that the singularities in the dy/y measure are logarithmic, regulated by the u_X^X factors.

Putting $y_i = e^{-t_i}$, the naive integration runs over all real t_i , and for $X \rightarrow 0$ we have divergences at infinity in t space. Thus for $\alpha' X \ll 1$ the integral is dominated by $|\vec{t}| \rightarrow \infty$. In this limit, the u variables simplify. Each u is a ratio of polynomials in the y , and the polynomials in turn simplify. In different cones in \vec{t} space, corresponding to a triangulation/diagram \mathcal{T} when a collection of compatible u variables all vanish together, exactly because the incompatible u ’s $\rightarrow 1$, the integral in t space becomes nothing than the Schwinger parametrization for \mathcal{T} and the integral is dominated by $\prod_{\mathcal{X} \in \mathcal{T}} (1/X)$ which is just the contribution to the amplitude from the diagram \mathcal{T} .

This shows that the field-theory limit of the stringy integrals matches the correct sum over diagrams. The fact that we have an analytic representation of u variables actually gives us much more: an integral expression for the amplitude directly in the field-theory limit, as an integral over a single object, just as the full stringy integral, but now interpreted as giving a “global Schwinger parametrization” for the sum over all diagrams at once. Returning to examining the stringy integrand as $|\vec{t}| \rightarrow \infty$, in different cones, one monomial in the polynomials defining the u ’s will dominate over others, and so $u_X \rightarrow \exp^{\alpha_X(t)}$, where α_X is a **piece-wise linear** function of the t_i that is called the “tropicalization” of u_X , which serves as the global Schwinger parameter for X . This variable was also called the “headlight function” in [7], to emphasize that it “lights up” in all the cones in t space compatible with the chord X . Replacing the full stringy integrand by this “tropicalized” version gives the correct field-theory limit. This gives a much more striking representation of the amplitude without any reference to sum over diagrams.

As an example at 5-points, consider the polynomial $(1 + y_{1,4} + y_{1,4}y_{1,3})$ appearing in the expression for the u variables. Seeing $y_{1,3} = e^{-t_{1,3}}$, $y_{1,4} = e^{-t_{1,4}}$, then as $|\vec{t}| \rightarrow \infty$ we have

$$(1 + e^{-t_{14}} + e^{-t_{14}}e^{-t_{13}}) \xrightarrow{|\vec{t}| \rightarrow \infty} e^{\max(0, -t_{14}, -t_{14}-t_{13})}, \quad (2.28)$$

and similarly for the other polynomials. In this way we can read off the α_X , for instance

$$u_{2,4} = \frac{1 + e^{-t_{1,4}} + e^{-t_{1,4}}e^{-t_{1,3}}}{(1 + e^{-t_{1,3}})(1 + e^{-t_{1,4}})} \xrightarrow{|t| \rightarrow \infty} e^{\alpha_{2,4}(t_{1,3}, t_{1,4})}, \quad (2.29)$$

where

$$\alpha_{2,4}(\vec{t}) = \max(0, -t_{1,4}, -t_{1,4} - t_{1,3}) - \max(0, -t_{1,3}) - \max(0, -t_{1,4}), \quad (2.30)$$

is the piece-wise linear global Schwinger parameter or “headlight function” associated with the curve (2,4). In this way the full 5-point tree amplitude can be written as a single “tropical” integral,

$$\mathcal{A}_5[X_{i,j}] = \int_{-\infty}^{+\infty} dt_{1,3} dt_{1,4} e^{\sum_{i,j} X_{i,j} \alpha_{i,j}(t)}. \quad (2.31)$$

Furthermore, at loop-level, as familiar from Schwinger parametrization, the loop integrations can be performed as Gaussian integrals, so we are left with a global Schwinger parametrization of the sum of all loop diagrams at any given order in the topological expansion.

3 Scalar-Scaffolded Gluons

In this paper, we are unveiling a hidden direct connection between the seemingly “boring” $\text{Tr } \phi^3$ theory and the much more exciting physics of gluon scattering amplitudes in Yang-Mills theory. Obviously the first order of business in making this connection is to answer the simplest possible question: how can the basic kinematics for these theories possibly be the same? After all, gluons have spin described by polarization vectors, which are obviously missing in $\text{Tr } \phi^3$ theory. So how can gluons and scalars possibly be related?

This has been a constant source of tension in attempting to connect the world of polytopes and curves on surfaces to real-world scattering amplitudes. The purely scalar $X_{i,j}$ variable description of kinematics played a crucial role from the very outset of the ABHY associahedron story, but there was seemingly no natural way to manually “add polarization vectors” to include gluons. For one thing, due to gauge-redundancy, there was no invariant way of doing this. And besides, adding any source of redundancy ran very much counter to the spirit of the $X_{i,j}$, one of whose virtues was in giving a non-redundant description of the momentum kinematics!

In this section we will describe an extremely simple but beautiful resolution to this basic problem. We will describe n gluon amplitudes in a purely scalar language using kinematic X variables, by imagining that we are scattering $2n$ colored scalars. There is always a pole of the amplitude where the scalars (1,2) fuse into an on-shell gluon₁, scalars (3,4) fuse to gluon₂, and so on. The residue on this pole then gives us the n -gluon amplitude³. For obvious reasons, we will refer to this as “the scaffolding residue”.

³Note that in order for the massless residue on $(p_i + p_{i+1})^2 \rightarrow 0$ to *only* be given by factorization on the gluon pole, we further have to assume that there are no cubic interactions between these scalars. This can be trivially arranged with the Z_2 symmetry flipping the sign of every scalar. It also automatically occurs from one of the natural origins for these scalars from higher-dimensional gluons

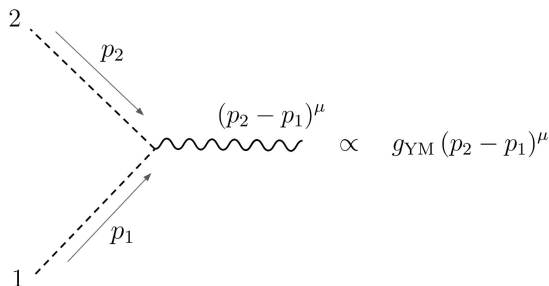


Figure 11: Three particle amplitude between two colored scalars and a gluon.

We will show explicitly how to describe gluon scattering amplitudes for any ⁴ polarizations in this scalar language. We will also discuss the constraints on functions of the $2n$ -gon X_{ij} variables, that allow us to interpret scaffolding residues as gluon amplitude, satisfying both the constraints of on-shell gauge-invariance and multilinearity in the polarization vectors. Despite the fact that these two properties are physically very different, we will see that they are both naturally unified in a single pretty mathematical statement.

We remark that the “scaffolding” method is a very general one, and can be used to describe particles of any mass and spin, since we can always imagine producing the spinning particles with a pair of scalars. We can for instance also “scaffold” gravitons, only the scaffolded avatar of the gauge-invariance/multilinearity conditions will change. Similarly we can scaffold massive string states, with some extra care to be taken to disentangle mass degeneracy in the string spectrum.

But while the basic strategy is essentially trivial, the scaffolding picture allows us to talk about seemingly very different amplitudes in the same kinematical language. It is this ability that allows us to bring the highly non-trivial relations between the amplitudes for very different theories to light.

3.1 From $2n$ scalars to n gluons

The scalars we consider interact with gluons via the unique three-point coupling: $g_{\text{YM}}(p_2 - p_1)^\mu$, as depicted in figure 11. If we start with a $2n$ -scalar scattering process and take n residues to make all the gluons (produced by adjacent scalars) on-shell, we land on the n -gluon amplitude.

Explicitly, to get the n -point gluon amplitude we take residues on the simple poles corresponding to $X_{1,3} = X_{3,5} = X_{5,7} = \dots = X_{2n-1,1} = 0$, or equivalently, in terms of the momentum, $(p_1 + p_2)^2 = (p_3 + p_4)^2 = (p_5 + p_6)^2 = \dots = (p_{2n-1} + p_{2n})^2 = 0$, which is exactly the condition to have the intermediate particles, in this case the gluons, on-shell. This procedure is illustrated in figure 12 for the case of a 5-point gluon amplitude.

At tree-level, making the external gluons on the shell is enough to ensure that all the internal particles are gluons as well. For this reason, by taking this residue we are

⁴Strictly speaking we will describe *null* polarization vectors $\epsilon^2 = 0$. Of course, these provide a basis for all possible polarizations.

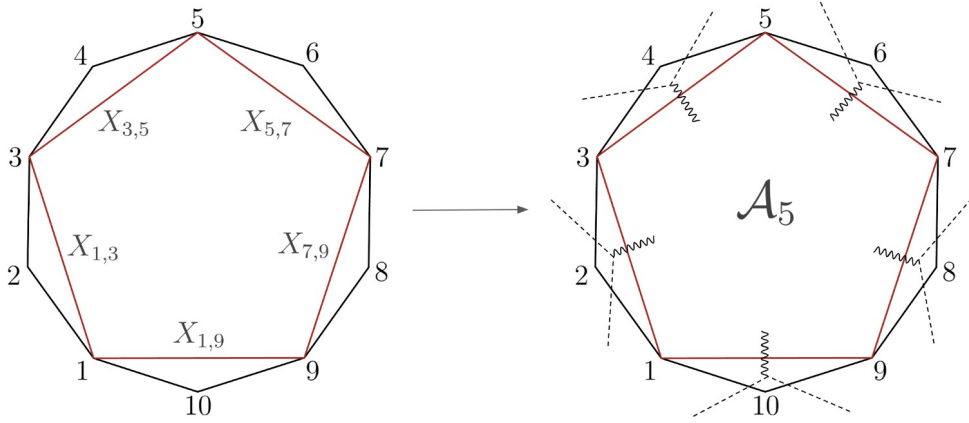


Figure 12: Scaffolding residue from 10-scalar amplitude to 5-gluon.

automatically left with the **tree-level pure gluon amplitude**. From this point onward, we will denote this residue that takes us from the scalar $2n$ -gon to the gluon n -gon, as the **scaffolding residue**, for purely pictorial reasons inspired by figure 12.

However, exactly because we are still starting from a scalar scattering, all the gluon information in the n -point amplitude left after taking the scaffolding residue is now encoded in scalar language, and so all the explicit dependence on polarizations characteristic of gluon amplitudes is less manifest. So we need to understand how we can extract this information from the starting scalar process.

For the rest of this section, we will explain how the information about the gluons is encoded in the $X_{i,j}$'s as well as understand how the properties of gluon amplitudes such as gauge invariance and multilinearity in each polarization are manifest in what we get from the scaffolding residue of the $2n$ -scalar amplitude.

3.1.1 Counting number of degrees of freedom

As a sanity check, let's start by checking that after taking the $2n$ scaffolding residue the number of degrees of freedom left in the scalar problem, matches that of an n -point gluon problem. Originally, for the scattering of these $2n$ -scalars, we have a total of $2n(2n-3)/2$ independent planar Mandelstams, $X_{i,j}$. After taking the scaffolding residue, we fix n of these variables to zero, so we have $2n(2n-3)/2 - n = 2n(2n-4)/2$ degrees of freedom left. For an n -point gluon problem, we have $n(n-3)/2$ independent planar Mandelstams, $n(n-1)/2$ possible $\epsilon_i \cdot \epsilon_j$, and $n(n-1) - n = n(n-2) = n(2n-2)/2$ different $\epsilon_i \cdot p_j$. So summing these three: $(4n^2 - 8n)/2 = 2n(2n-4)/2$, which agrees with the scaffolding residue, as expected.

Let's now proceed and see in detail how to extract the gluon amplitude from the $2n$ -scalar amplitude, via this residue.

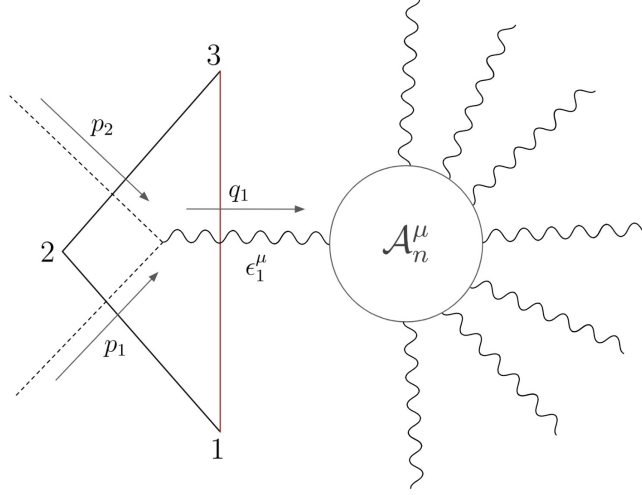


Figure 13: Polarization and momentum of scaffolded gluon.

3.2 Polarizations and momenta of the gluons

Let's now understand how the polarizations and momentum of the gluons are encoded in the planar variables $X_{i,j}$ of the scaffolding scalars. To do so, we focus on a single gluon of the full process, see figure 13. By momentum conservation, we can read off directly that the momentum of the incoming gluon is going to be $q_i^\mu = (p_{2i-1} + p_{2i})^\mu$, which satisfies $q_i^2 = 0$ on the scaffolding residue. So we have $q_1^\mu = (p_1 + p_2)^\mu$. By convention, we will always use q to denote the momentum of the gluons and p the momentum of the scaffolding scalars.

As for the polarization vector, ϵ_i , of course it isn't uniquely fixed but can be shifted by gauge transformations, whose geometric interpretation we will give in a moment. But one symmetrical choice for ϵ_i is the one familiar from the Feynman rule for the 3-point vertex between the scalars and the gluon, which gives us $\epsilon_i^\mu \propto (p_{2i} - p_{2i-1})^\mu$. On the scaffolding residue, it satisfies $\epsilon_i \cdot p_i = 0$, as necessary for on-shell gluons. It also satisfies $\epsilon_i^2 = 0$, so we are describing generalized "circular polarizations"; this is not a restriction since these furnish a basis for all possible polarization states.

To better understand the geometrical meaning of the polarizations, it is useful to label the edges of the momentum polygon by vectors X_i^μ , such that $p_i^\mu = (X_{i+1} - X_i)^\mu$. In terms of these variables we have:

$$\epsilon_1^\mu \propto (X_3 - X_2)^\mu - (X_2 - X_1)^\mu \propto X_2^\mu - \frac{(X_3 + X_1)^\mu}{2}. \quad (3.1)$$

So we can see that the information about the polarizations is also included in the momentum polygon: they correspond to the vectors going from the midpoint of the triangle to the extra edge in the scaffolding (see figure 14). Picking this particular representation of the polarization vectors gives a misleading significance to the midpoint, however, as we will see, invariance under gauge transformations tells us precisely that the polarization vector can be attached anywhere on this edge.

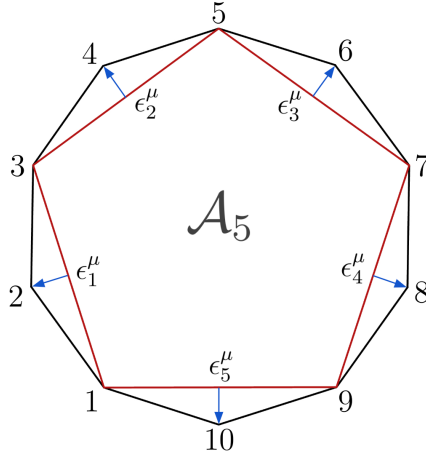


Figure 14: Polarizations of scaffolded gluons.

3.3 Unified form of gauge invariance and multi-linearity

We now want to see what the statements about gauge invariance and multi-linearity translate to in the scalar degrees of freedom, $X_{i,j}$. Let's start with **gauge invariance**. To avoid cumbersome indices, we will study gauge invariance for gluon 1, but all translate to the i th gluon by replacing 1 by $2i - 1$, 2 by $2i$, etc.

Invariance under gauge transformations tells us:

$$\epsilon_1^\mu \rightarrow \epsilon_1^\mu + \alpha q_1^\mu \quad \Rightarrow \quad \delta\mathcal{A} = 0 \quad \forall \alpha, \quad (3.2)$$

which can be phrased in terms of the momentum of the $2n$ -scalars as

$$(p_2 - p_1)^\mu \rightarrow (p_2 - p_1)^\mu + \alpha(p_1 + p_2)^\mu \quad \Rightarrow \quad \delta\mathcal{A} = 0 \quad \forall \alpha. \quad (3.3)$$

Now we want to understand what this shift means in terms of the $X_{i,j}$ since these are the variables the amplitude depends on. To do this, let's express the gauge transformations in terms of the variables X_i^μ :

$$\left(X_2 - \frac{X_1 + X_3}{2}\right)^\mu \rightarrow \left(X_2 - \frac{X_1 + X_3}{2}\right)^\mu + \alpha(X_3 - X_1)^\mu, \quad (3.4)$$

which is equivalent to simply shifting X_2^μ as follows:

$$X_2^\mu \rightarrow X_2^\mu + \alpha(X_3 - X_1)^\mu. \quad (3.5)$$

Geometrically, gauge invariance is then equivalent to the statement that we are allowed to move the base point of the polarization of gluon i along $X_{2i-1,2i+1}^\mu$, see figure 15.

Indeed, while we have emphasized a “top-down” picture of the scalar scaffolding, starting with the idea of using pairs of colored scalars to fuse into gluons, we can also very nicely motivate the scaffolding idea from the bottom-up. So let's start from the beginning just with the data for n gluons—their momenta p_i and polarization vectors ϵ_i . We can use the p_i

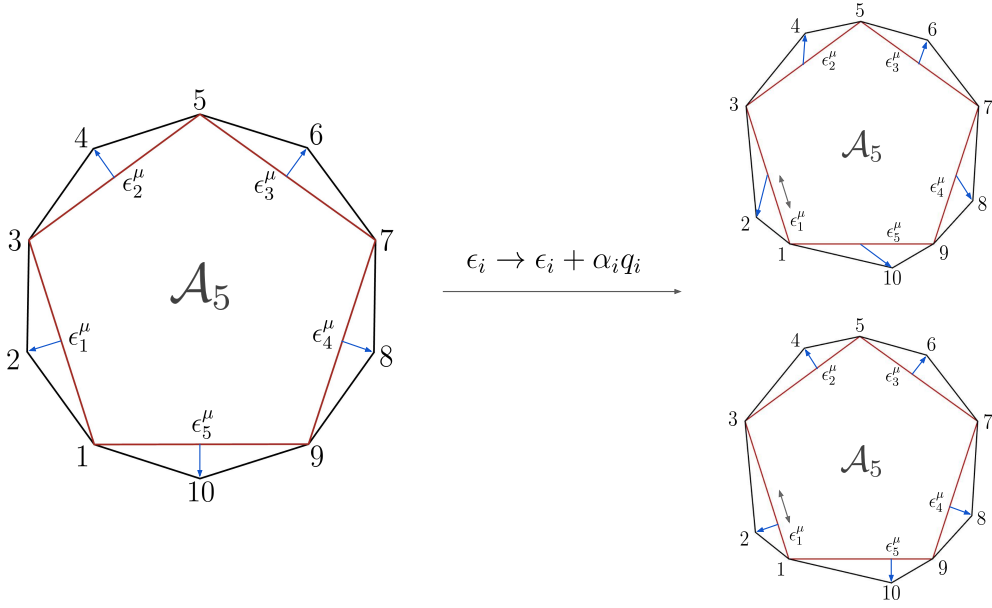


Figure 15: Gauge Transformations.

to draw the momentum polygon as usual. But it is also natural to record the information about the polarization vectors simply by placing the end of the vector ϵ_i somewhere on the edge p_i of the momentum polygon. This immediately defines our $2n$ -gon, on the locus where $X_{1,3}, X_{3,5}, \dots = 0$ reflecting $p_i^2 = 0$. Since there is no invariant place on the edge p_i to place ϵ_i , it is natural to demand that any question we ask of this $2n$ -gon should be invariant under shifting where we place the endpoint of ϵ_i , and of course very nicely shifting this endpoint is precisely gauge-invariance $\epsilon_i^\mu \rightarrow \epsilon_i^\mu + \alpha p_i^\mu$. As an aside, the on-shell field-strength $f_i^{\mu\nu} = p_i^\mu \epsilon_i^\nu - p_i^\nu \epsilon_i^\mu$ has an obvious and pretty geometric interpretation as well—it is simply the antisymmetric tensor determined by the plane formed, $(X_{2i-1}, X_{2i}, X_{2i+1})$.

Ultimately this transformation will produce a shift in the planar variables involving X_2^μ which can be derived as follows:

$$\begin{aligned}
(X_2^\mu - X_j^\mu) &\rightarrow (X_2^\mu - X_j^\mu) + \alpha(X_3^\mu - X_1^\mu) \\
\Rightarrow (X_2^\mu - X_j^\mu)(X_{2\mu} - X_{j\mu}) &\rightarrow (X_2^\mu - X_j^\mu)(X_{2\mu} - X_{j\mu}) + \alpha(X_3^\mu - X_1^\mu)(X_{2\mu} - X_{j\mu}) \quad (3.6) \\
&\Rightarrow X_{2,j} \rightarrow X_{2,j} + \alpha(X_{3,j} - X_{1,j}).
\end{aligned}$$

So we can state gauge invariance in gluon i th as

$$\mathcal{A}[X_{2i,j} \rightarrow X_{2i,j} - \alpha(X_{2i+1,j} - X_{2i-1,j})] - \mathcal{A}[X_{2i,j}] = 0. \quad (3.7)$$

In addition, we know the amplitude, A_{2n} , should be **multi-linear** in each polarization:

$$\epsilon_i^\mu \rightarrow \epsilon_i^\mu + \beta \epsilon_i^\mu \quad \Rightarrow \quad \delta \mathcal{A} = \beta \mathcal{A}. \quad (3.8)$$

Again, let's see what this translates to in scalar language for gluon 1. Rewriting this in terms of X_i^μ yields

$$\left(X_2 - \frac{X_1 + X_3}{2}\right)^\mu \rightarrow \left(X_2 - \frac{X_1 + X_3}{2}\right)^\mu + \beta \left(X_2 - \frac{X_1 + X_3}{2}\right)^\mu, \quad (3.9)$$

which is equivalent to

$$X_2^\mu \rightarrow X_2^\mu + \frac{\beta(X_2^\mu - X_1^\mu)}{2} + \frac{\beta(X_2^\mu - X_3^\mu)}{2}. \quad (3.10)$$

Proceeding as we did in (3.6), we get that the $X_{2,j}$ transform as

$$X_{2,j} \rightarrow X_{2,j} + \frac{\beta(X_{2,j} - X_{1,j})}{2} + \frac{\beta(X_{2,j} - X_{3,j})}{2}, \quad (3.11)$$

and so linearity in polarization i th can be restated as:

$$\mathcal{A}\left[X_{2i,j} \rightarrow X_{2i,j} + \frac{\beta}{2}(X_{2i,j} - X_{2i-1,j}) + \frac{\beta}{2}(X_{2i,j} - X_{2i+1,j})\right] - \mathcal{A}[X_{2i,j}] = \beta\mathcal{A}[X_{2i,j}]. \quad (3.12)$$

Combining **gauge invariance** and **multi-linearity** for gluon 1, we get:

$$\begin{aligned} & \mathcal{A}\left[X_{2,j} \rightarrow X_{2,j} + \frac{\beta(X_{2,j} - X_{1,j})}{2} + \frac{\beta(X_{2,j} - X_{3,j})}{2} + \alpha(X_{3,j} - X_{1,j})\right] - \mathcal{A}[X_{2,j}] = \beta\mathcal{A}[X_{2,j}] \\ \Leftrightarrow & \mathcal{A}\left[X_{2,j} \rightarrow X_{2,j} + \left(\frac{\beta}{2} + \alpha\right)(X_{2,j} - X_{1,j}) + \left(\frac{\beta}{2} - \alpha\right)(X_{2,j} - X_{3,j})\right] - \mathcal{A}[X_{2,j}] = \beta\mathcal{A}[X_{2,j}]. \end{aligned} \quad (3.13)$$

Picking $\alpha = \pm\beta/2$, we get:

$$\begin{aligned} & \mathcal{A}[X_{2,j} \rightarrow X_{2,j} + \beta(X_{2,j} - X_{1,j})] - \mathcal{A}[X_{2,j}] = \beta\mathcal{A}[X_{2,j}], \\ & \mathcal{A}[X_{2,j} \rightarrow X_{2,j} + \beta(X_{2,j} - X_{3,j})] - \mathcal{A}[X_{2,j}] = \beta\mathcal{A}[X_{2,j}]. \end{aligned} \quad (3.14)$$

This is then the unified form of the statements for both multilinearity and gauge invariance: we have a rescaling symmetry under shifting $X_{2,j}$ by either of its neighbors $X_{1,j}$ or $X_{3,j}$. The shift by $X_{1,j}$ tells us that the amplitude must be expressible as

$$\begin{aligned} \mathcal{A} &= \sum_{j \neq \{1,2,3\}} (X_{2,j} - X_{1,j}) \times \mathcal{Q}_{2,j}, \\ \mathcal{A} &= \sum_{j \neq \{1,2,3\}} (X_{2,j} - X_{3,j}) \times \tilde{\mathcal{Q}}_{2,j}, \end{aligned} \quad (3.15)$$

where $\mathcal{Q}_{2,j}, \tilde{\mathcal{Q}}_{2,j}$ some function of the kinematics, $X_{i,j}$, but **independent** of $X_{2,j}$. This tells us they are equal:

$$\mathcal{Q}_{2,j} = \tilde{\mathcal{Q}}_{2,j} = \partial_{X_{2,j}} \mathcal{A}. \quad (3.16)$$

In summary, translating this property for a general gluon i , we conclude that the amplitude **must** be of the form:

$$\begin{aligned} \mathcal{A}_n^{\text{gluon}} &= \sum_{j \neq \{2i-1, 2i, 2i+1\}} (X_{2i,j} - X_{2i-1,j}) \times \mathcal{Q}_{2i,j} \\ &= \sum_{j \neq \{2i-1, 2i, 2i+1\}} (X_{2i,j} - X_{2i+1,j}) \times \mathcal{Q}_{2i,j}. \end{aligned} \quad (3.17)$$

where $\mathcal{Q}_{2i,j}$ is function of the remaining kinematics, **independent** of $X_{2i,j}$. As pointed out before and is made clear in this section, gluon amplitudes expressed in terms of the scalar data have a **unique** form, that makes gauge invariance manifest, without introducing any redundancies in the representation.

3.4 Dictionary: From scalar to gluon kinematics

In this section we present a systematic way of mapping from the scalar kinematic invariants of the scaffolding $2n$ -gon into the momenta, q_i , and polarizations, ϵ_i , of the gluons we obtain after extracting the scaffolding residue.

Note that all the $X_{i,j}$ with i and j **odd**, $X_{o,o}$, correspond to chords living inside the n -gon, and thus are the planar variables of the n gluon problem:

$$X_{2i-1,2j-1} = (q_i + q_{i+1} + \cdots + q_{j-1})^2 \equiv X_{i,j}^g, \quad (3.18)$$

where $X_{2i-1,2i+1} = (p_{2i-1} + p_{2i})^2 = q_i^2 = 0$ on the scaffolding residue. As usual, these $n(n-3)/2$ planar variables are related to the same number of linearly independent Mandelstam variables of n gluons via

$$\begin{aligned} -2q_i \cdot q_j &= X_{i,j}^g + X_{i+1,j+1}^g - X_{i,j+1}^g - X_{i+1,j}^g \Leftrightarrow \\ -2(p_{2i-1} + p_{2i}) \cdot (p_{2j-1} + p_{2j}) &= X_{2i-1,2j-1} + X_{2i+1,2j+1} - X_{2i-1,2j+1} - X_{2i+1,2j-1}. \end{aligned} \quad (3.19)$$

Let's now work out the relations between the remaining planar variables: $X_{e,e}$ and $X_{e,o}$, and the gluon data, *i.e.* (linearly independent) products of the form $\epsilon_i \cdot \epsilon_j$, $\epsilon_i \cdot q_j$. In the previous section, we saw that the polarization of each gluon could be associated with a vector starting at the midpoint of the edge of the gluon n -gon and ending on the vertex of the scalar $2n$ -gon. However, gauge invariance tells us that the polarization vector does **not** have to lie at the midpoint, and can lie in any point along the gluon edge, allowing us to write:

$$\epsilon_i = (1 - \alpha)p_{2i} - \alpha p_{2i-1}, \quad (3.20)$$

for an arbitrary parameter α . Recall that $q_i^\mu = (p_{2i} + p_{2i-1})^\mu$, thus $\epsilon_i^2 = \epsilon_i \cdot q_i = 0$ exactly on the scaffolding residue. The choice of midpoint corresponds to $\alpha = 1/2$, but let us keep α generic. Both the momentum and polarization of the i th gluon can be expressed in terms of the vertices of the $2n$ -gon as

$$\epsilon_i^\mu \propto (1 - \alpha)(X_{2i+1} - X_{2i})^\mu - \alpha(X_{2i} - X_{2i-1})^\mu, \quad (3.21)$$

$$q_i^\mu \propto (X_{2i+1} - X_{2i})^\mu + (X_{2i} - X_{2i-1})^\mu = (X_{2i+1} - X_{2i-1})^\mu. \quad (3.22)$$

Note that q_i^μ only depends on ‘‘odd’’ vertices $X_1, X_3, \dots, X_{2n-1}$, thus $\epsilon_i \cdot q_j$ must depend on $X_{k,l}$ with at least one of k, l being odd. This means that the only dependence on $X_{e,e}$ is through $\epsilon_i \cdot \epsilon_j$ – this will be important shortly. The remaining Lorentz products can be expressed in terms of X 's as follows: Using (3.21) and (3.22) we can write the remaining gluon kinematics as

$$\begin{aligned} 2\epsilon_i \cdot \epsilon_j &= (1 - \alpha) \left(-(1 - \alpha)X_{2i+1,2j+1} - \alpha X_{2i-1,2j+1} - \alpha X_{2i+1,2j-1} + X_{2i,2j+1} + X_{2i+1,2j} \right) \\ &\quad - \alpha^2 X_{2i-1,2j-1} + \alpha X_{2i,2j-1} + \alpha X_{2i-1,2j} - X_{2i,2j}, \end{aligned} \quad (3.23)$$

$$2\epsilon_i \cdot q_j = (1 - \alpha)X_{2i+1,2j-1} - (1 - \alpha)X_{2i+1,2j+1} + \alpha X_{2i-1,2j-1} - \alpha X_{2i-1,2j+1} + X_{2i,2j+1} - X_{2i,2j-1}, \quad (3.24)$$

with $X_{1,3} = X_{3,5} = \dots = X_{2n-1,1} = 0$ and $X_{i,i} = X_{i,i+1} = 0$. Again by plugging in $\alpha = \frac{1}{2}$ we recover the special midpoint choice above. If, instead, we choose $\alpha = 0$ or 1 both equations simplify, *e.g.*, for $\alpha = 1$ we have

$$\begin{aligned} 2\epsilon_i \cdot \epsilon_j &= X_{2i,2j-1} + X_{2i-1,2j} - X_{2i-1,2j-1} - X_{2i,2j} = -c_{2i-1,2j-1}, \\ 2\epsilon_i \cdot q_j &= X_{2i,2j+1} - X_{2i,2j-1} + X_{2i-1,2j-1} - X_{2i-1,2j+1}. \end{aligned} \quad (3.25)$$

Note that if and only if an expression of Lorentz products is **gauge invariant** and **multilinear** in all ϵ 's, the corresponding expression in X 's becomes independent of the parameter α . On the other hand, by solving (3.23) and (3.24) we can express all $X_{e,e}$ and $X_{e,o}$ in terms of a basis of Lorentz products, and vice-versa.

3.5 3-point gluon amplitude in scalar language

To finish this section, we want to provide an example of a gluon amplitude written in this scalar language. So will consider the 3-point gluon amplitude that is extracted from a 6-point scalar process.

Using (3.23) and (3.24) for $n = 3$, *e.g.* with $\alpha = 1$ we have

$$\begin{aligned} 2\epsilon_1 \cdot \epsilon_2 &= X_{1,4} - X_{2,4}, & 2\epsilon_2 \cdot \epsilon_3 &= X_{3,6} - X_{4,6}, & 2\epsilon_3 \cdot \epsilon_1 &= X_{2,5} - X_{2,6}, \\ 2\epsilon_1 \cdot q_2 &= X_{2,5}, & 2\epsilon_2 \cdot q_3 &= X_{1,4}, & 2\epsilon_3 \cdot q_1 &= X_{3,6}. \end{aligned} \quad (3.26)$$

At 3-points we have two different types of interactions: the Yang-Mills (YM) vertex, $\mathcal{A}_3^{\text{YM}}$, and the F^3 vertex, $\mathcal{A}_3^{F^3}$. Using (3.26), we can write $\mathcal{A}_3^{\text{YM}}$ in terms of X 's as

$$\mathcal{A}_3^{\text{YM}}(1, 2, 3) = -(X_{2,5} - X_{2,6})X_{1,4} - (X_{3,6} - X_{4,6})X_{2,5} - (X_{1,4} - X_{2,4})X_{3,6}, \quad (3.27)$$

which become nicely

$$\mathcal{A}_3^{\text{YM}}(1, 2, 3) = -4(\epsilon_1 \cdot \epsilon_3 \epsilon_2 \cdot q_3 + \epsilon_2 \cdot \epsilon_3 \epsilon_1 \cdot q_2 + \epsilon_1 \cdot \epsilon_2 \epsilon_3 \cdot q_1). \quad (3.28)$$

Similarly, for the 3-point F^3 amplitude, $-X_{1,4}X_{2,5}X_{3,6}$, we find

$$\mathcal{A}_3^{F^3}(1, 2, 3) = -8 \epsilon_1 \cdot q_2 \epsilon_2 \cdot q_3 \epsilon_3 \cdot q_1. \quad (3.29)$$

4 Tree-level Gluon Amplitudes

Having learned how to describe the kinematics of gluon scattering amplitudes in a scalar language—thinking of each gluon as being “scaffolded” by a pair of colored scalars—we now turn to dynamics, and make our proposal for gluon scattering amplitudes.

We start at tree-level, and define a stringy integral representation of scaffolded gluon amplitudes as a very simple deformation of the stringy $\text{Tr } \phi^3$ as [12]:

$$\mathcal{A}_{2n}(1, 2, \dots, 2n)[X_{i,j}] = \int_0^\infty \underbrace{\prod_{\mathcal{C} \in \mathcal{T}} \frac{dy_{\mathcal{C}}}{y_{\mathcal{C}}} \prod_{i < j} u_{ij}^{\alpha' X_{i,j}}}_{\text{Integrand of (2.24)}} \left(\frac{\prod_{(i,j) \in \text{even}} u_{i,j}}{\prod_{(i,j) \in \text{odd}} u_{i,j}} \right), \quad (4.1)$$

where y_C corresponds to the positive parametrization associated with triangulation \mathcal{T} of the disk with $2n$ marked points in the boundary. Note that this deformation simply amounts to shifting the kinematics entering the stringy $\text{Tr } \phi^3$: $X_{o,o} \rightarrow X_{o,o} - 1/\alpha'$ and $X_{e,e} \rightarrow X_{e,e} + 1/\alpha'$.

In the rest of this section, we will explain *why* (4.1) describes the scaffolded gluons. At tree-level, we can “cheat” to be assured that we are describing gluons, by showing that this proposal precisely matches the amplitude for gluons in the open bosonic string, and we will begin by doing this.

We will then proceed to see why these expressions deserve to be called “gluon amplitudes” more intrinsically, by showing that the amplitudes defined in this way satisfy all the physical properties expected of gluons: on-shell gauge invariance, linearity in polarizations, as well as consistent factorization on massless gluon poles. These will all follow from simple but fundamental facts about the u variables summarized in our discussion of “surfaceology”. This more intrinsic understanding of the amplitudes directly in u variable language will be crucial in the extension of our proposal to loop-level we undertake in the next section, where (welcome!) stark differences with string loop amplitudes appear and we can no longer “cheat” by borrowing the (in)consistency of the bosonic string.

4.1 Connection to the bosonic string

At tree-level, gluon amplitudes in the bosonic string are given as a worldsheet integral [28]:

$$\mathcal{A}_n^{\text{tree}}(1, 2, \dots, n) = \int \frac{d^n z_i}{\text{SL}(2, \mathbb{R})} \left(\prod_{i,j} (ij)^{2\alpha' p_i \cdot p_j} \right) \exp \left(\sum_{i \neq j} 2 \frac{\epsilon_i \cdot \epsilon_j}{(ij)^2} - \frac{\sqrt{\alpha'} \epsilon_i \cdot p_j}{(ij)} \right) \Big|_{\text{multi-linear in } \epsilon_i}, \quad (4.2)$$

where ϵ_i are the polarizations and p_i the respective momentum, and $(ij) = z_i - z_j$. Since we are describing the scattering of gluons, in addition to the Koba-Nielsen factor [19], we also have a part encoding the information about the polarizations of the gluons, which is compactly represented in the exponential. Since gluon amplitudes are **linear** in each polarization, we are meant to keep only the term in the expansion of the exponential which is multilinear in all the polarizations.

This integral representation of the bosonic string amplitudes is fairly compact, however, it is less interesting for practical purposes such as computing the amplitudes. As it is usually the case for stringy integrals, the integrals in (4.2) do not converge and so if one wants to evaluate it for some physical kinematics, one has to first resort to analytic continuation to properly define it (we come back to this in section 4.8.)

In addition, expanding the exponential we can see that to each term proportional to $\epsilon_i \cdot \epsilon_j$ we get a factor of $(ij)^2$ in the denominator. The presence of such terms tells us that the integral has double poles when $(ij) \rightarrow 0$. Of course, such double poles are not physical and can be eliminated using integration by parts (IBPs).

Even forgetting about the convergence issues, one key difference between the (4.2) and the tachyon integral, (2.21), is that in the first, (4.2), we have a sum of different stringy integrals, each multiplied by a factor of $p_i \cdot \epsilon_j$, $\epsilon_i \cdot \epsilon_j$, while in the latter, (2.21), there is a single integral that generates everything. So a natural question is whether there is a

different starting point, that still describes gluons, but in which the amplitude, like in the scalar case, is represented as single term integral – this can be achieved exactly by **scaffolding the gluons in a scalar problem**.

To reach the $2n$ -scalar problem, define these scalars as the remaining degrees of freedom after fixing some configuration for the polarizations:

Concretely, we consider the scattering to happen in a sufficiently high-dimensional space, with \tilde{D} dimensions, so that we can achieve the following kinematical configuration:

$$\begin{aligned} p_i \cdot \epsilon_j &= 0, \quad \forall (i, j) \in (1, \dots, 2n), \\ \epsilon_i \cdot \epsilon_j &= \begin{cases} 1 & \text{if } (i, j) \in \{(1, 2); (3, 4); (5, 6); \dots; (2n-1, 2n)\}, \\ 0 & \text{otherwise.} \end{cases} \end{aligned} \quad (4.3)$$

This kinematics can be achieved by demanding that the momentum, p_i live in the first D dimensions of spacetime, and the polarizations live in the extra dimensions, of this big dimensional, \tilde{D} spacetime:

$$p_i = \begin{pmatrix} | \\ | \\ p_i^\mu \\ | \\ 0 \\ 0 \\ \vdots \\ 0 \\ 0 \\ 0 \end{pmatrix} \begin{array}{c} \uparrow \\ D \\ \downarrow \\ \uparrow \\ \text{Extra} \\ \text{dims.} \\ \downarrow \end{array}; \quad \epsilon_{2j/2j-1} = \begin{pmatrix} 0 \\ \vdots \\ 0 \\ 0 \\ \vdots \\ 1 \\ \vdots \\ 0 \end{pmatrix} \begin{array}{c} \uparrow \\ D \\ \downarrow \\ \leftarrow j \text{ th} \end{array}. \quad (4.4)$$

By making this kinematical choice, we fixed all the polarizations, and all the data left in the problem are the momenta. Therefore we are left only with scalar degrees of freedom, whose kinematics is described by the Mandelstam invariants, $p_i \cdot p_j$ living in D spacetime dimensions – these are exactly $2n$ **scaffolding scalars**.

Plugging this kinematical choice in the bosonic string integral (4.2), most of the terms in the exponential vanish, and the big sum collapses into a single term:

$$\mathcal{A}_{2n}(1, 2, \dots, 2n) \xrightarrow{2n\text{-scalar}} \int \frac{d^{2n} z_i}{\text{SL}(2, \mathbb{R})} \prod_{i, j \in (1, 2, \dots, 2n)} (ij)^{2\alpha' p_i \cdot p_j} \frac{1}{(12)^2 (34)^2 (56)^2 \dots (2n-1, 2n)^2}. \quad (4.5)$$

Recalling the definition of the u variables in terms of (ij) (2.22), we can rewrite (4.5) in terms of u 's as follows:

$$\begin{aligned} \mathcal{A}_{2n}(1, 2, \dots, 2n)[X_{i,j}] &= \int \frac{d^n z_i / \text{SL}(2, \mathbb{R})}{(12)(23)(34) \dots (2n, 1)} \prod_{i,j} u_{ij}^{\alpha' X_{i,j}} \frac{(23)(45)(67) \dots (2n, 1)}{(12)(34)(56) \dots (2n-1, 2n)} \\ &= \underbrace{\int \frac{d^n z_i / \text{SL}(2, \mathbb{R})}{(12)(23)(34) \dots (2n, 1)} \prod_{i,j} u_{ij}^{\alpha' X_{i,j}}}_{\text{Integrand of (2.24)}} \left(\frac{\prod_{(i,j) \in \text{even}} u_{i,j}}{\prod_{(i,j) \in \text{odd}} u_{i,j}} \right). \end{aligned} \quad (4.6)$$

This is exactly the form of equation (4.1) – the integrand of (2.24), times the extra multiplicative factor of the ratio of the product of all the $u_{i,j}$ for i and j even and the product of all the $u_{i,j}$ for i and j odd.

So, from this perspective, we learn that the external scaffolding scalars we are scattering are secretly **gluons in higher dimensions**, where we are expanding around a kinematic point where the gluons effectively become colored scalars. Exactly because of the gluon 3-point interaction, we have that these colored scalars interact with gluons through a cubic vertex whose Feynman rule is, once again, the expected one in figure 11. Note that, however, since we picked $\epsilon_i \cdot \epsilon_j = 0$, except for $(i, j) = (2k - 1, 2k)$, this cubic interaction is only present between **adjacent** pairs of scalars, $(2k - 1, 2k)$. This means that for a $2n$ -scalar process we have n -different species, $\{A_1, A_2, \dots, A_n\}$, of these colored scalars and the scattering process we are describing is $(1^{A_1}, 2^{A_1}, 3^{A_2}, 4^{A_2}, \dots, (2n - 1)^{A_n}, (2n)^{A_n})$. Such $2n$ -scalar bosonic string amplitudes were also studied in [29, 30], where a systematic IBP algorithm was developed and the field-theory limit produces $2n$ -scalar amplitudes of Yang-Mills-scalar theory [31] naturally given in CHY formulas [32, 33].

Therefore, to extract the gluon amplitude from (4.1) all we need to do is compute the scaffolding residue: $X_{2k-1, 2k+1} \rightarrow 0$. In this kinematical locus, each pair of adjacent scalars, $(2k - 1, 2k)$, produces an on-shell gluon, uncovering the n -point gluon amplitude. Of course, the answer will be in terms of the scalar Mandelstam invariants, $X_{i,j}$, and so to recover the usual expression for the amplitude in terms of polarizations we can use directly the dictionary presented in section 3.4.

4.2 The scaffolding residue

Let us now proceed and see in detail how to extract the scaffolding residue from the $2n$ -scalar amplitude (4.1). Following the procedure laid out in section 2, each a positive parametrization, $u_{i,j}[y]$, is associated with a triangulation of the disk with $2n$ marked points on the boundary, \mathcal{T} . As pointed out before, the final answer is **independent** of this choice, but it is simpler to access the singularities of a particular diagram by choosing the parametrization associated with its dual triangulation. Therefore, since we want to access the residue $X_{2i-1, 2i+1} \rightarrow 0$, it is helpful to choose a triangulation that includes the scaffolding chords – we call such triangulations as **scaffolding triangulation** (see figure 16).

4.2.1 The $2n$ -scalar form in the scaffolding triangulation

For such a choice of triangulation, the ratio of $u_{i,j}$ in the $2n$ -scalar form (4.1) reduces to something very simple. Recall from section 2.6.3, that the product of all the y_C can be written in terms of u 's as described in eq. (2.20).

Now something especially nice happens in the case of a scaffolding triangulation: by drawing the curves on the fat graph we can see that all the $X_{e,e}$ will be such that $P_{X_{e,e}} = -1$ and $X_{o,o}$ will be such that $P_{X_{o,o}} = +1$, while all the remaining will be zero⁵. Therefore, as long as we are working in the scaffolding triangulation we have:

⁵Note that this is **independent** of the internal details of the triangulation, and so it is true for any surface, which means it holds both tree-level as well as loop-level

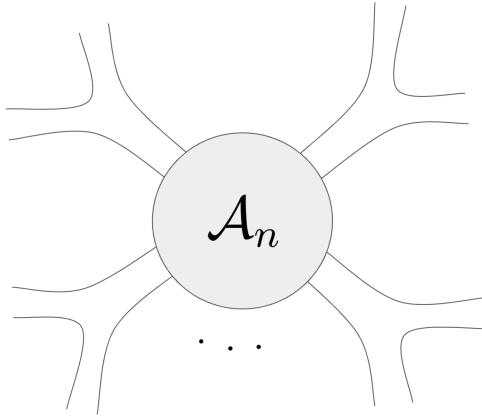


Figure 16: Scaffolding triangulation: including all the $X_{2i-1,2i+1}$ propagators.

$$\prod_{\mathcal{C}} y_{\mathcal{C}} = \prod_s y_s \prod_i y_i = \left(\frac{\prod_{(i,j) \in \text{odd}} u_{i,j}}{\prod_{(i,j) \in \text{even}} u_{i,j}} \right), \quad (4.7)$$

where y_s stands for the y 's corresponding to propagators in the scaffolding, $X_{2k-1,2k+1}$, while y_i are those associated with propagators of the internal gluon problem, $X_{o,o}$.

Therefore picking a positive parametrization of the stringy integral corresponding to a scaffolding triangulation, \mathcal{T}_s , (4.6) reduces to:

$$\begin{aligned} \mathcal{A}_{2n}(1, 2, \dots, 2n)[X_{i,j}] &= \int_0^\infty \prod_s \frac{dy_s}{y_s} \times \prod_i \frac{dy_i}{y_i} \prod_{i,j} u_{i,j}^{X_{i,j}}[y_s, y_i] \left(\frac{1}{\prod_s y_s \prod_i y_i} \right) \\ &= \int_0^\infty \underbrace{\prod_s \frac{dy_s}{y_s^2} \prod_i \frac{dy_i}{y_i^2} \prod_{i,j} u_{i,j}^{X_{i,j}}[y_s, y_i]}_{\Omega_{2n}}, \end{aligned} \quad (4.8)$$

where we have set $\alpha' = 1$. Note that this is exactly the scalar integral (2.24), but where instead of having a $d \log(y) = dy/y$ form, we have dy/y^2 . We call this non-dlog form that we are integrating the $2n$ -scalar form, Ω_{2n} .

4.2.2 Extracting the residue

Since we have picked the scaffolding chords to be part of the triangulation, we can factor out of the Koba-Nielsen factor a piece that looks like the $\prod_s y_s^{X_s}$, with X_s denoting the scaffolding chords, $X_{2k-1,2k+1}$. Therefore the integral over the scaffolding y_s reduces schematically to:

$$\int_0^\infty \prod_s \frac{dy_s}{y_s^2} y_s^{X_s} \times \mathcal{F}[y_s, y_i, X_{i,j}], \quad (4.9)$$

where \mathcal{F} represents some function of the remaining variables which is regular and non-zero when the y_s and X_s go to zero.

Looking at the integral we can see that if we set one of the scaffolding variables X_{s_i} to zero, then the integral over y_{s_i} is divergent for y_{s_i} near 0. Therefore, for $X_{s_i} \rightarrow 0$, the integral is dominated by the region y_{s_i} near 0. Focusing on this region, we can rewrite \mathcal{F} using the appropriate Taylor expansion:

$$\int_0^\infty \prod_{s \neq s_i} \frac{dy_s}{y_s^2} y_s^{X_s} \times \int_0^\epsilon \frac{dy_{s_i}}{y_{s_i}^2} y_{s_i}^{X_{s_i}} \left(\mathcal{F}[y_{s_i} = 0, y_s, y_i, X_{i,j}] + y_{s_i} \frac{d\mathcal{F}[y_s, y_i, X_{i,j}]}{dy_{s_i}} \Big|_{y_{s_i}=0} + \dots \right), \quad (4.10)$$

where the integration in y_{s_i} is from 0 to ϵ , and ϵ is some number arbitrarily close to zero, but non-zero.

One can now perform the integral, term by term in the expansion, using analytic continuation:

$$\int_0^\epsilon \frac{dy}{y} y^A = \frac{\epsilon^A}{A}, \quad (4.11)$$

which gives:

$$\int_0^\infty \prod_{s \neq s_i} \frac{dy_s}{y_s^2} y_s^{X_s} \times \left(\frac{\epsilon^{X_{s_i}-1}}{X_{s_i}-1} \mathcal{F}[y_{s_i} = 0, y_s, y_i, X_{i,j}] + \frac{\epsilon^{X_{s_i}}}{X_{s_i}} \cdot \frac{d\mathcal{F}[y_s, y_i, X_{i,j}]}{dy_{s_i}} \Big|_{y_{s_i}=0} + \dots \right). \quad (4.12)$$

From here we can read off directly the residue on $X_{s_i} = 0$ to be

$$\begin{aligned} \text{Res}_{X_{s_i}=0}(\mathcal{A}_{2n}(1, 2, \dots, 2n)) &= \int_0^\infty \prod_i \frac{dy_i}{y_i^2} \int_0^\infty \prod_{s \neq s_i} \frac{dy_s}{y_s^2} y_s^{X_s} \times \left(\frac{d\mathcal{F}[y_s, y_i, X_{i,j}]}{dy_{s_i}} \Big|_{y_{s_i}=0} \right) \\ &= \int_0^\infty \text{Res}_{y_{s_i}=0}(\Omega_{2n}). \end{aligned} \quad (4.13)$$

Repeating this procedure for all the scaffolding variables y_s , we obtain:

$$\mathcal{A}_n^{\text{gluon}} = \int_0^\infty \text{Res}_{y_{s_1}=0} \left(\text{Res}_{y_{s_2}=0} \left(\dots \left(\text{Res}_{y_{s_n}=0} \Omega_{2n} \right) \dots \right) \right), \quad (4.14)$$

and we conclude that this consecutive residue is simply given by the part of $\mathcal{F}[y_s, y_i, X_{i,j}]$ which is **linear in all the scaffolding** y 's, $\{y_{s_1}, \dots, y_{s_n}\}$.

4.3 Scaffolding residue \Rightarrow Gauge invariant and multi-linear amplitude

Let's now understand how the scaffolding residue of the 2n-scalar amplitude, automatically gives something of the form of (3.17), *i.e.* an object which is automatically gauge-invariant and multilinear in the corresponding polarizations. Without loss of generality, let us focus on what happens after taking the residue corresponding to putting gluon 1 on-shell, *i.e.* $X_{1,3} \rightarrow 0$, which is given by the residue of Ω_{2n} at $y_{1,3} = 0$:

$$\text{Res}_{y_{1,3}=0} \Omega_{2n}(1, 2, \dots, 2n)[X_{i,j}] = \prod_{s \neq (1,3)} \frac{dy_s}{y_s^2} \prod_i \frac{dy_i}{y_i^2} \sum_{(IJ)} \left(X_{I,J} \frac{\partial \log(u_{IJ})}{\partial y_{1,3}} \prod_{(km) \neq (IJ)} u_{km}^{X_{k,m}}[y] \right) \Big|_{y_{1,3}=0}. \quad (4.15)$$

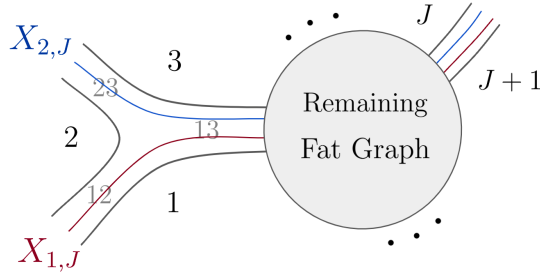


Figure 17: Curves $X_{1,J}$ and $X_{2,J}$.

However, not all the $u_{i,j}$ depend on $y_{1,3}$. In fact, only the u 's corresponding to curves that go through road 13, can depend on $y_{1,3}$. Therefore the only curves for which this derivative is non-zero are curves $X_{1,j}$ and $X_{2,j}$ (see figure 17):

$$\text{Res}_{y_{1,3}=0} \Omega_{2n}[X_{i,j}] = \prod_{s \neq (1,3)} \frac{dy_s}{y_s^2} \prod_i \frac{dy_i}{y_i^2} \sum_J \left(X_{1,J} \frac{\partial \log(u_{1J})}{\partial y_{1,3}} \prod_{(km) \neq (1J)} u_{km}^{X_{k,m}}[y] \right. \\ \left. + X_{2,J} \frac{\partial \log(u_{2J})}{\partial y_{1,3}} \prod_{(km) \neq (2J)} u_{km}^{X_{k,m}}[y] \right) \Bigg|_{y_{1,3}=0} \quad (4.16)$$

Now we claim that $\partial_{y_{1,3}} \log(u_{1J}) = -\partial_{y_{1,3}} \log(u_{2J})$. This follows immediately from one of the fundamental facts about the u variables we summarized in our surfaceology review. We can consider the smaller surface obtained simply by cutting just before the forking into (1,2). Let's consider the curve $[1J]$ on the smaller surface that starts on the road (13) and exits at J ; we use square brackets to remind us this is a curve on the smaller surface. This manifestly does not depend on $y_{1,3}$ which is a boundary in the smaller surface. This curve can be extended to a curve on the full surface in two ways, into (1J) and (2J). So we have that $U_{[1,J]} = u_{1,J}u_{2,J}$ is independent of $y_{1,3}$ and hence $\partial_{y_{1,3}} u_{1,J} = -\partial_{y_{1,3}} u_{2,J}$ as desired. We can also see this very simply directly, from the matrix formula for the u variables. Let's consider the words corresponding to curves $X_{2,J}$ and $X_{1,J}$. From figure 17, we see that these curves agree everywhere except for the last intersection, at the end of road 13. So we can write their u -variables as follows:

$$\underline{1J} : M_{\text{remaining}} \times M_L(y_{1,3}) = \begin{bmatrix} A & B \\ C & D \end{bmatrix} \times \begin{bmatrix} y_{1,3} & y_{1,3} \\ 0 & 1 \end{bmatrix} = \begin{bmatrix} Ay_{1,3} & Ay_{1,3} + B \\ Cy_{1,3} & Cy_{1,3} + D \end{bmatrix} \\ \Rightarrow u_{1J} = \frac{C(Ay_{1,3} + B)}{A(Cy_{1,3} + D)}, \\ \underline{2J} : M_{\text{remaining}} \times M_R(y_{1,3}) = \begin{bmatrix} A & B \\ C & D \end{bmatrix} \times \begin{bmatrix} y_{1,3} & 0 \\ 1 & 1 \end{bmatrix} = \begin{bmatrix} Ay_{1,3} + B & B \\ Cy_{1,3} + D & D \end{bmatrix} \\ \Rightarrow u_{2J} = \frac{B(Cy_{1,3} + D)}{D(Ay_{1,3} + B)}, \quad (4.17)$$

where A, B, C and D are functions of the remaining y 's. Even without knowing the details

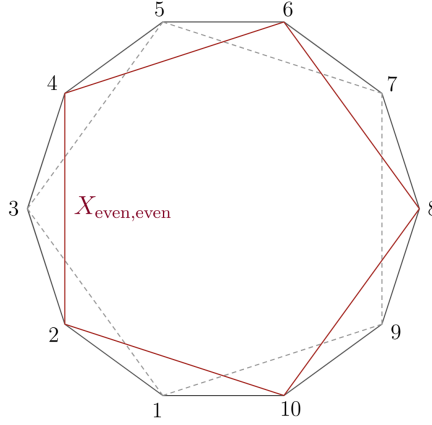


Figure 18: Triangulation containing $\{X_{2i,2i+2}\}$.

of the rest of the curves, we can check that the product $u_{1,J}u_{2,J}$ does **not** depend on $y_{1,3}$. Thus we have $d \log u_{1J} = -d \log u_{2J}$. This relation allows us to write the residue as:

$$\text{Res}_{y_{1,3}=0} \Omega_{2n}[X_{i,j}] = \sum_J (X_{2,J} - X_{1,J}) \underbrace{\prod_{s \neq (1,3)} \frac{dy_s}{y_s^2} \prod_i \frac{dy_i}{y_i^2} \times \frac{\partial \log(u_{2J})}{\partial y_{1,3}} \prod_{(km) \neq (1J), (2J)} u_{km}^{X_{k,m}}[y]}_{Q_{2,J}}, \quad (4.18)$$

which is exactly of the form required by gauge-invariance and multi-linearity (3.6). From (3.6), we should also be able to express this residue as a sum of terms proportional to $(X_{2,J} - X_{3,J})$. This is not as obvious and, to prove that this is the case, it is useful to triangulate the surface in a different way – using a triangulation containing $X_{2i,2i+2}$, with $i \in \{1, \dots, n\}$ (see figure 18).

In this case, the u 's are functions of different y 's, that we denote by \tilde{y} . In this parametrization, the residue corresponding to the original scaffolding residue, *i.e.* $X_{1,3} = X_{3,5} = \dots = X_{1,2n-1} = 0$, is obtained by taking the residue of Ω_{2n} at $y_{2i,2i+2} \rightarrow \infty$. Now in this new triangulation, by exactly the same argument presented for the original triangulation, we have that $\frac{\partial \log(u_{3,J})}{\partial \tilde{y}_{2,4}} = -\frac{\partial \log(u_{2,J})}{\partial \tilde{y}_{2,4}}$, therefore we also have:

$$\text{Res}_{\tilde{y}_{2,4}=\infty} \Omega_{2n}[X_{i,j}] = \sum_J (X_{2,J} - X_{3,J}) \underbrace{\prod_{s \neq (2,4)} \frac{d\tilde{y}_s}{\tilde{y}_s^2} \prod_i \frac{d\tilde{y}_i}{\tilde{y}_i^2} \times \frac{\partial \log(u_{2J})}{\partial \tilde{y}_{2,4}} \prod_{(km) \neq (2J), (3J)} u_{km}^{X_{k,m}}[\tilde{y}]}_{\tilde{Q}_{2,J}}. \quad (4.19)$$

Repeating the same argument, one can show that such a form holds for any triple of indices $(2i-1, 2i, 2i+1)$, and thus for each gluon in the problem. Just in the same way as before, (after taking the remaining scaffolding residues) we have $\int \tilde{Q}_{2,J} = \int Q_{2,J} = \partial_{X_{2,J}} \mathcal{A}_n$. Hence, we have proved that taking the scaffolding residue automatically gives us something that is manifestly **gauge invariant** as well as **multi-linear** in all polarizations.

4.4 Tree-level factorization

Our goal now is to understand what factorization looks like in this scalar language. As we know, for the usual way we write the amplitudes directly in terms of the polarizations of the gluons, when we extract the residue of the amplitude on a pole, $X_{a,b} = 0$, we obtain the gluing of the two lower point amplitudes, \mathcal{A}_L and \mathcal{A}_R :

$$\mathcal{A}_{\text{glued}} = \mathcal{A}_L^\mu \left(-\eta_{\mu,\nu} + \frac{p_\mu q_\nu + p_\nu q_\mu}{p \cdot q} \right) \mathcal{A}_R^\nu = -\mathcal{A}_L^\mu \eta_{\mu,\nu} \mathcal{A}_R^\nu, \quad (4.20)$$

where the term between brackets is doing the polarization sum for the intermediate gluon, I, I' we are producing. We define

$$\mathcal{A}_L^\mu = \partial_{\epsilon_{I,\mu}} \mathcal{A}_L \quad , \quad \mathcal{A}_R^\nu = \partial_{\epsilon_{I',\nu}} \mathcal{A}_R, \quad (4.21)$$

and $p_\mu = p_{I,\mu} = -p_{I',\mu}$ and q^μ is some reference vector for which $q \cdot p \neq 0$. Note that the final answer does not depend on the arbitrary choice of q^μ . In the second equality, we use the fact that $M_L^\mu p_{I,\mu} = M_R^\nu p_{I',\nu} = 0$, as required by gauge invariance.

We now want to phrase this rule for summing over polarizations (“gluing” rule) in terms of the scalar variables of the scaffolded problem. To do so, we think of gluons, I and I' as being scaffolded by a pair of scalars, such that in the momentum polygon this interaction is associated with a triangle whose vertices are (a, b, x) and (a, b, x') , respectively (see figure 19). Therefore, the polarizations of I and I' are, respectively, encoded in the scalar variables, X_x^μ , and $X_{x'}^\nu$. Now using our scalar definition of gauge-invariance and multi-linearity of \mathcal{A}_L and \mathcal{A}_R in gluons, I and I' , respectively, we have:

$$\begin{aligned} \mathcal{A}_L^\mu &= \partial_{X_x^\mu} \mathcal{A}_L = \frac{\partial}{\partial X_x^\mu} \left(\sum_j (X_{x,j} - X_{b,j}) \mathcal{Q}_{x,j} \right) = 2 \left(\sum_j (X_x^\mu - X_j^\mu) \frac{\partial \mathcal{A}_L}{\partial X_{x,j}} \right), \\ \mathcal{A}_R^\nu &= \partial_{X_{x'}^\nu} \mathcal{A}_R = \frac{\partial}{\partial X_{x'}^\nu} \left(\sum_J (X_{x',J} - X_{a,J}) \mathcal{Q}_{x',J} \right) = 2 \left(\sum_J (X_{x'}^\nu - X_J^\nu) \frac{\partial \mathcal{A}_R}{\partial X_{x',J}} \right). \end{aligned} \quad (4.22)$$

Therefore contracting with the flat metric, we obtain:

$$\mathcal{A}_{\text{glued}} = -4 \sum_{j,J} (X_x^\mu - X_j^\mu) (X_{x',\mu} - X_{J,\mu}) \frac{\partial \mathcal{A}_L}{\partial X_{x,j}} \frac{\partial \mathcal{A}_R}{\partial X_{x',J}}, \quad (4.23)$$

using a gauge transformation and a rescaling, we can choose $X_x^\mu = X_b^\mu$ and $X_{x'}^\nu = X_a^\nu$ which yields:

$$\begin{aligned} \mathcal{A}_{\text{glued}} &\propto \sum_{j,J} (X_b^\mu - X_j^\mu) (X_{a,\mu} - X_{J,\mu}) \partial_{X_{x,j}} \mathcal{A}_L \partial_{X_{x',J}} \mathcal{A}_R \\ &\propto \sum_{j,J} (-X_{b,J} - X_{a,j} + X_{j,J}) \partial_{X_{x,j}} \mathcal{A}_L \partial_{X_{x',J}} \mathcal{A}_R. \end{aligned} \quad (4.24)$$

To check factorization we want to extract the massless residues and interpret the result in terms of lower point gluon amplitudes. Let’s study the residue corresponding to having $X_{a,b}$ on-shell, so $X_{a,b} = 0$. Choosing an appropriate scaffolding triangulation that contains $X_{a,b}$, this residue is given by the coefficient multiplying $y_{a,b}$ in the expansion of $\prod u_X^X$. Similarly to what was argued in 4.3, the only u ’s that depend on $y_{a,b}$ are those that

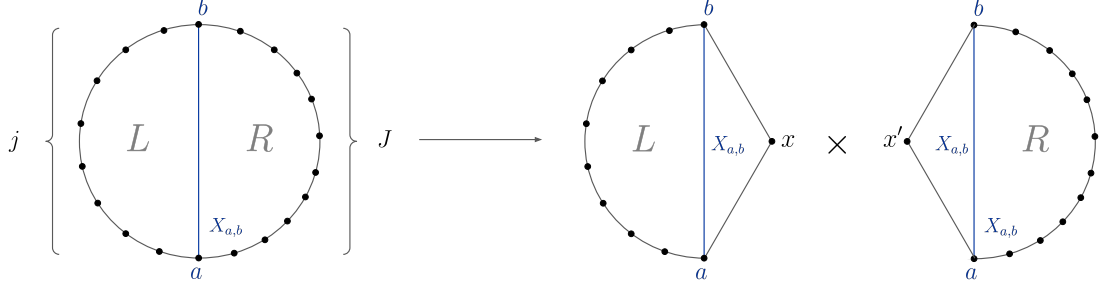


Figure 19: Tree-level factorization.

correspond to curves that intersect $X_{a,b}$ as laminations, i.e. all the curves that go through road ab in the fat graph. There are three types of such curves: $X_{j,J}$, $X_{a,J}$ and $X_{j,b}$, with $j \in \{a+1, \dots, b-1\}$ and $J \in \{b+1, \dots, a-1\}$. So expanding the Koba-Nielsen factor up to linear order in $y_{a,b}$ yields:

$$\prod_X u_X^X = 1 + y_{a,b} \left[\sum_{j,J} X_{j,J} \frac{\partial \log(u_{j,J})}{\partial y_{a,b}} + \sum_j X_{j,b} \frac{\partial \log(u_{j,b})}{\partial y_{a,b}} + \sum_J X_{a,J} \frac{\partial \log(u_{a,J})}{\partial y_{a,b}} \right] \Big|_{y_{a,b}=0} + \mathcal{O}(y_{a,b}^2). \quad (4.25)$$

Now we note that any triangulation containing road ab will look schematically like figure 20, and therefore, similarly to what we proved in 4.3, we have:

$$\prod_j u_{j,J} \times u_{a,J} \equiv \mathcal{U}_{ab,J}^{\text{right}}, \quad (4.26)$$

$$\prod_J u_{j,J} \times u_{j,b} \equiv \mathcal{U}_{j,ab}^{\text{left}}, \quad (4.27)$$

where $\mathcal{U}_{ab,J}^{\text{right}}$ and $\mathcal{U}_{j,ab}^{\text{left}}$ are the u 's of the smaller surfaces on the right/left of ab respectively, and thus **do not depend** on $y_{a,b}$. Therefore we have:

$$\begin{aligned} \frac{\partial \log(u_{a,J})}{\partial y_{a,b}} &= - \sum_j \frac{\partial \log(u_{j,J})}{\partial y_{a,b}}, \\ \frac{\partial \log(u_{j,b})}{\partial y_{a,b}} &= - \sum_J \frac{\partial \log(u_{j,J})}{\partial y_{a,b}}. \end{aligned} \quad (4.28)$$

Plugging these relations into (4.25), we get:

$$\prod_X u_X^X = 1 + y_{a,b} \sum_{j,J} (X_{j,J} - X_{j,b} - X_{a,J}) \frac{\partial \log(u_{j,J})}{\partial y_{a,b}} \Big|_{y_{a,b}=0} + \mathcal{O}(y_{a,b}^2). \quad (4.29)$$

Finally, we can get $\frac{\partial \log(u_{j,J})}{\partial y_{a,b}} \Big|_{y_{a,b}=0}$ using the u -equations:

$$u_{j,J} + u_{a,b} \prod_{X_L \in \mathcal{L}_j} u_{X_L} \prod_{X_R \in \mathcal{R}_J} u_{X_R} \prod_{X \in \mathcal{I}} u_X = 1, \quad (4.30)$$

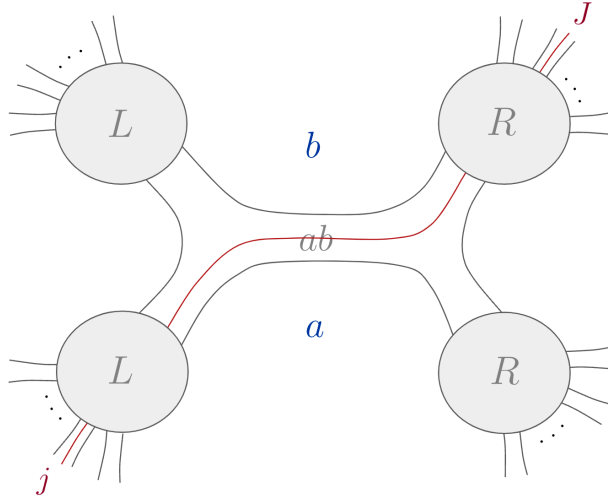


Figure 20: Fat graph around road ab .

where R_J and L_j stand for the set of curves that intersects $X_{j,J}$ but that live on the right/left on $X_{a,b}$, respectively, and so do **not** intersect $X_{a,b}$; \mathcal{I} stands for the set of curves that are simultaneously incompatible with $X_{a,b}$ and $X_{j,J}$. Since $u_{a,b} = 0$, when $y_{a,b} = 0$, we have:

$$\left. \frac{\partial \log(u_{j,J})}{\partial y_{a,b}} \right|_{y_{a,b}=0} = - \left. \frac{\partial u_{a,b}}{\partial y_{a,b}} \right|_{y_{a,b}=0} \prod_{X_L \in L_j} \tilde{u}_{X_L} \prod_{X_R \in R_J} \tilde{u}_{X_R}, \quad (4.31)$$

where $\tilde{u}_X = u_X|_{y_{a,b}=0}$, are the u 's of the smaller right and left surfaces, obtained when cut through curve $X_{a,b}$. In addition, we don't have any u_X for $X \in \mathcal{I}$ since these all go to 1 when $u_{a,b} \rightarrow 0$.

We now need to compute $\partial_{y_{a,b}} u_{a,b}|_{y_{a,b}=0}$. It is easy to see that this expression nicely factorizes in precisely the way needed to ensure factorization of the amplitude. Since (a,b) is road present in our triangulation, the word for (a,b) is a "V", with a series of right turns ending on (a,b) then a series of left turns thereafter, of the form $\alpha R a_1 \cdots a_l R y_{a,b} L b_1 L \cdots b_r L \beta$ where α, β are boundaries and the a 's and b 's denote the roads on the left and right of (a,b) . Then from the matrix product formula for $u_{a,b}$ it is very easy to see that

$$u_{a,b} = y_{a,b} F_L F_R + O(y_{a,b}^2), \quad (4.32)$$

where

$$F_L = (1 + a_l + a_l a_{l-1} + \cdots + a_l a_{l-1} \cdots a_1), \quad F_R = (1 + b_r + b_r b_{r-1} + \cdots + b_r b_{r-1} \cdots b_1). \quad (4.33)$$

So we have that $\partial_{y_{a,b}} u_{a,b}|_{y_{a,b}=0} = F_L F_R$ nicely factorizes. But each of these factors F_L, F_R is also directly interpreted as the coefficient of the leading term in $y_{a,b}$ for (a,b) curve on each of the obvious smaller L, R surfaces. The reason is simply that on each of the L, R surfaces, the $(a,b)^{L,R}$ curves is still a road in the triangulation, the word is still a V , but e.g. on the L surface, the word for $(a,b)^L$ immediately runs into a boundary after

turning left on (a, b) , similarly for $(a, b)^R$. Thus $\partial_{y_{a,b}} u_{a,b}^L|_{y_{a,b}=0} = F_L$, $\partial_{y_{a,b}} u_{a,b}^R|_{y_{a,b}=0} = F_R$. Thus we have that

$$\frac{\partial u_{a,b}}{\partial y_{a,b}}|_{y_{a,b}=0} = \frac{\partial u_{a,b}^L}{\partial y_{a,b}}|_{y_{a,b}=0} \times \frac{\partial u_{a,b}^R}{\partial y_{a,b}}|_{y_{a,b}=0}. \quad (4.34)$$

So then we have that the residue of the amplitude at $X_{a,b} = 0$ is:

$$\text{Res}_{X_{a,b}=0} \mathcal{A}_n = - \sum_{j,J} (X_{j,J} - X_{j,b} - X_{a,J}) \underbrace{\frac{\partial u_{a,b}^L}{\partial y_{a,b}}|_{y_{a,b}=0} \prod_{X_L \in \mathcal{L}_j} \tilde{u}_{X_L}}_{Q_j^L} \cdot \underbrace{\frac{\partial u_{a,b}^R}{\partial y_{a,b}}|_{y_{a,b}=0} \prod_{X_R \in \mathcal{R}_j} \tilde{u}_{X_R}}_{Q_j^R}. \quad (4.35)$$

But Q_j^L and Q_j^R are precisely the objects that show up in the lower-point amplitudes when we take the scaffolding residue on $y_{a,b}$! Consider two lower-point amplitudes: $\mathcal{A}_L(a, a+1, \dots, b-1, b, x)$ and $\mathcal{A}_R(b, b+1, \dots, a-1, a, x')$. As we saw in our discussion of gauge invariance and multilinearity above, when we take the scaffolding residue as $X_{a,b} \rightarrow 0$ we have $\mathcal{A}_L = \sum_j (X_{x,j} - X_{b,j}) \partial_{y_{a,b}} u_{x,j}|_{y_{a,b}=0}$ and similarly for \mathcal{A}_R . But by precisely the same steps above, by looking at the u equation for $u_{x,j}/u_{x',J}$ and differentiating with respect to $y_{a,b}$, we find that

$$\begin{aligned} \text{Res}_{X_{a,b}=0} \mathcal{A}_L(a, \dots, b, x) &= \sum_j (X_{x,j} - X_{b,j}) Q_{x,j}^L, \\ \text{Res}_{X_{a,b}=0} \mathcal{A}_R(b, \dots, a, x') &= \sum_J (X_{x',J} - X_{a,J}) Q_{x',J}^R, \end{aligned} \quad (4.36)$$

where the $Q_{x,j}^L, Q_{x',J}^R$ are precisely the factors that appeared in the residue of the full amplitude on the $X_{a,b} \rightarrow 0$ pole above, *i.e.* $Q_{x,j}^L \equiv Q_j^L$ and $Q_{x',J}^R \equiv Q_J^R$. Since $Q_j^L = \partial_{X_{x,j}} \mathcal{A}_L$ and similarly for Q_J^R , we finally have that

$$\text{Res}_{X_{a,b}=0} \mathcal{A}_n = - \sum_{j,J} (X_{j,J} - X_{j,b} - X_{a,J}) \partial_{X_{x,j}} \mathcal{A}_L \partial_{X_{x',J}} \mathcal{A}_R, \quad (4.37)$$

which is precisely the statement of factorization on the $X_{a,b} \rightarrow 0$ pole. Note that in this argument no use was made of the “left” and “right” surfaces being trees; we have proven general “tree exchange” factorizations for general loop amplitudes on the left and right.

4.5 Computing scaffolding residues for general n

In this section, we present explicit formulas for scaffolding residues for all n . We will see that the result becomes exactly the n -gluon bosonic string amplitude written in our new scalar language, whose integrand is a sum of products of surprisingly simple building blocks we call V 's and W 's, corresponding to first- and second-derivatives with respect to the scaffolding y 's. We will also see that the V 's and W 's can be expressed purely in terms of products of u variables of the inner n -gon problem in a nice graphical way. Our purpose here is to show how the bosonic string gluons amplitude naturally falls out of taking the scaffolding residue in the world of u and y variables; in an appendix A we show how to see this directly in terms of the conventional worldsheet z variables.

Of course, the consistent factorization of the scaffolded bosonic string amplitude at tree-level guarantees that taking the scaffolding residue will correctly land on the gluon amplitude, but we are performing this computation here for two reasons. First, in order to illustrate how the residues can be taken and subsequently interpreted directly in terms of integrands involving the u variables on the smaller n -gon surface. We expect this exercise will be useful for higher loops, where our picture for gluon amplitudes differs significantly (and is much simpler) than the string amplitude. Second, the final expressions written in terms of X and u variables have a very pretty direct combinatorial characterization, which is not manifested in the conventional bosonic string gluon amplitudes written in terms of polarization vectors and momenta.

We begin again by considering a scaffolding triangulation, denoting by $y_{s_k} \equiv y_{2k-1,2k+1}$ the y 's associated with the ‘‘outer’’ scaffolding propagators $X_{2k-1,2k+1}$, and y_i for the ones corresponding to the ‘‘inner’’ propagators of the gluon problem. For example, for $n = 4$, we have denoted $y_{s_1} = y_{1,3}, y_{s_2} = y_{3,5}, y_{s_3} = y_{5,7}, y_{s_4} = y_{1,7}$ and $y_1 = y_{1,5}$ or $y_1 = y_{3,7}$.

As we’ve discussed already taking the scaffolding residue amounts to extracting the coefficient of $y_1 \cdots y_n$ of the factor $\prod u^{\alpha' X}$, which is a function of y_{n+1}, \dots, y_{2n-3} and the X variables in the exponents. As we have seen in sec. 4.3, only $u_{1,j}$ and $u_{2,j}$ depend on y_1 since these are the only two chords that pass the road 13; they differ only by taking different turns after hitting (13) and the product $u_{1,j}u_{2,j}$ is independent of y_1 . Thus, the derivative with respect to y_1 brings down a factor

$$V_1 := \alpha' \sum_j (X_{2,j} - X_{1,j}) \left. \frac{\partial u_{2,j}}{\partial y_1} \right|_{y_1=0}, \quad (4.38)$$

where the sum is over $j = 1, \dots, 2n$, but the terms with $j = 1, 2, 3$ vanish ($X_{1,3} = 0$), and we have used the fact that $u_{2,j} = 1$ on the support of $y_1 = 0$ and so we omit it in the denominator.

Similarly only $u_{2a-1,j}, u_{2a,j}$ depend on y_a and their product is independent of it, thus we define for $a = 1, 2, \dots, n$

$$V_a := \alpha' \sum_j (X_{2a,j} - X_{2a-1,j}) \left. \frac{\partial u_{2a,j}}{\partial y_a} \right|_{y_a=0}, \quad (4.39)$$

and the simplest term of the residue contains the product of n such factors $V_1 V_2 \cdots V_n$, which is at order α'^n .

More complicated terms appear when the derivative with respect to y_b hits on V_a from previous steps. However, the higher-than-second-order derivative with respect to y_1, \dots, y_n of any u variable must vanish, since any chord has exactly one entrance and exit. Moreover, exactly four u variables, namely $u_{2a-1,2b-1}, u_{2a-1,2b}, u_{2a,2b-1}$ and $u_{2a,2b}$ have non-vanishing second derivatives with respect to y_a, y_b . Thus, in the summation over j of $\partial V_a / \partial y_b$, only two terms with $j = 2b$ and $j = 2b - 1$ are non-vanishing:

$$\alpha' \left. \frac{\partial V_a}{\partial y_b} \right|_{y_b=0} = (X_{2a,2b} - X_{2a-1,2b}) \frac{\partial^2 u_{2a,2b}}{\partial y_a \partial y_b} + \alpha' (X_{2a,2b-1} - X_{2a-1,2b-1}) \frac{\partial^2 u_{2a,2b-1}}{\partial y_a \partial y_b}, \quad (4.40)$$

where we have suppressed the conditions $y_a = y_b = 0$. Note that similarly for $\partial V_b / \partial y_a$ we have only two terms with $j = 2a$ and $2a - 1$ non-vanishing. An explicit computation shows

that these two derivatives are very nicely equal to each other, so we can write the result in a more symmetric way and define

$$W_{a,b} := \alpha' c_{2a-1,2b-1} \left. \frac{\partial^2 u_{2a,2b}}{\partial y_a \partial y_b} \right|_{y_a=y_b=0}, \quad (4.41)$$

where we have used $X_{2a,2b} + X_{2a-1,2b-1} - X_{2a-1,2b} - X_{2a,2b-1} = c_{2a-1,2b-1}$. Putting everything together, we have a pretty formula for the scaffolding residue

$$\int \prod_{a=n+1}^{2n-3} \frac{dy_a}{y_a^2} \left(\sum_{r=0}^{\lfloor n/2 \rfloor + 1} \sum_{\{i,j\},\{k\}} \prod_a^r W_{i_a,j_a} \prod_b^{n-2r} V_{k_b} \right) \prod_{(ij)} u_{i,j}^{\alpha' X_{i,j}}, \quad (4.42)$$

where we have the dy/y^2 form for the remaining $n-3$ variables within the n -gon, and the n -point Koba-Nielsen factor $\prod u^X$; inside the bracket, we have a summation over all partitions of $\{1, 2, \dots, n\}$ into r pairs $\{i_a, j_a\}$ and $n-2r$ singlets k_b , each given by the product of W 's and V 's. For example, the $n=3$ case reads $V_1 V_2 V_3 + W_{1,2} V_3 + W_{2,3} V_1 + W_{1,3} V_2$, and for $n=4$ we have

$$V_1 V_2 V_3 V_4 + (W_{1,2} V_3 V_4 + \text{perm.}) + (W_{1,2} W_{3,4} + \text{perm.}), \quad (4.43)$$

with 6 terms of the form WV and 3 terms of the form WW . Note that in the $\alpha' \rightarrow 0$ limit, only some of these terms contribute to the lowest-order, or the pure Yang-Mills amplitude. For example, for $n=3$ only VW terms contribute and for $n=4$ only WW and WV terms contribute, while V^n terms only contribute to amplitude with pure higher-dimensional operators such as F^3 and F^4 .

We remark that we can already learn many interesting facts about bosonic string gluon amplitudes and their field-theory limit (Yang-Mills plus higher-dimensional operators starting with F^3) from these expressions. For example, if we are interested in helicity amplitudes in $D=4$, there is a prescription to directly translate V and W into spinor-helicity expressions, which lead to formulas for n -gluon string and field-theory amplitudes in spinor-helicity variables [34]. Soft theorems for gluons can be derived using (4.42) which take the form of ‘‘double-soft theorems’’ for scaffolded scalars [35, 36]. We also discover hidden properties of gluon amplitudes, for instance, the field-theory amplitudes admit an interesting expansion associated with a sum over all facets of the associahedron [34].

4.5.1 Triangulation-independent formula

One apparent drawback of our result (4.42) is that it seems to depend on the triangulation, namely both the form dy/y^2 and those first and second derivatives in V and W depend on the triangulation of the n -gon. Here we will show that by absorbing some y factors into V and W we can make both of them triangulation independent. Such a rewriting also makes it manifest that the new V and W can be expressed in terms of products of u 's, which have nice graphical interpretations.

To begin with, note that in the scaffolding triangulation, each $u_{2a-1,2a+1}$ is proportional to y_a , and we define

$$u_{2a-1,2a+1} \equiv y_a \hat{u}_{2a-1,2a+1}, \quad (4.44)$$

and it is crucial to use the u -equations

$$u_{2a,j} + u_{2a-1,2a+1} \prod_{i \in D_j} u_i = 1, \quad (4.45)$$

where subset D_j includes the curves intersecting with $(2a, j)$ except $(2a-1, 2a+1)$. In the limit $y_a \rightarrow 0$, we expand u -equations (4.45) as

$$u_{2a,j}|_{y_a=0} = 1, \quad (4.46)$$

as well as

$$\frac{\partial u_{2a,j}}{\partial y_a} \Big|_{y_a=0} = -\hat{u}_{2a-1,2a+1} \prod_{i \in D_j} u_i|_{y_a=0}, \quad (4.47)$$

where we have expressed the first derivative in terms of \hat{u} and product of those u 's crossing $(2a-1, 2a+1)$. Similarly from the u -equation of $u_{2a,2b}$, we can derive that the second derivative is given by

$$\frac{\partial^2 u_{2a,2b}}{\partial y_a \partial y_b} = -\hat{u}_{2a-1,2a+1} \hat{u}_{2b-1,2b+1} \prod_{i \in E} u_i|_{y_a=0, y_b=0}, \quad (4.48)$$

where subset E includes curves intersecting with $(2a, 2b)$ except for $(2a-1, 2a+1)$ and $(2b-1, 2b+1)$.

Now it becomes obvious that for any term of the summation in (4.42), there is a common factor $\prod_{a=1}^n \hat{u}_{2a-1,2a+1}$ from the \hat{u} 's in each V and W 's, which cancels the ratio $(\prod_{(i,j) \in \text{even}} u_{i,j} / (\prod_{(i,j) \in \text{odd}} u_{i,j}))|_{y_a=0}$ to give:

$$\prod_{a=1}^n \hat{u}_{2a-1,2a+1} \left(\frac{\prod_{(i,j) \in \text{even}} u_{i,j}}{\prod_{(i,j) \in \text{odd}} u_{i,j}} \right) \Big|_{y_a=0} = \prod_{i,j \in n\text{-gon}} \frac{1}{u_{i,j}}, \quad (4.49)$$

This gives us a triangulation-independent formula for the scaffolding residue, which contains the invariant $(n-3)$ -form dy/y and the Koba-Nielsen factor $\prod u^{X-1}$:

$$\int_0^\infty \prod_a \frac{dy_a}{y_a} \left(\sum_{r=0}^{\lfloor n/2 \rfloor + 1} \sum_{\{i,j\}, \{k\}} \prod_a^r W'_{i_a, j_a} \prod_b^{n-2r} V'_{k_b} \right) \prod_{(i,j)} u_{i,j}^{\alpha' X_{i,j} - 1}, \quad (4.50)$$

where we have redefined V and W to be

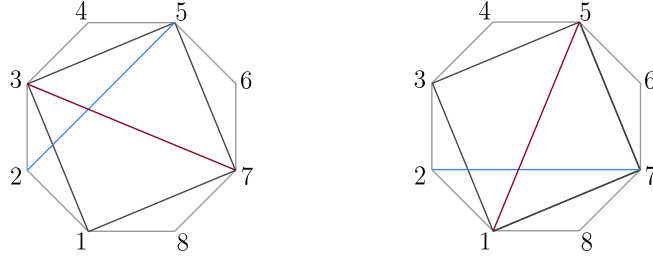
$$V'_a = -\alpha' \sum_j (X_{2a,j} - X_{2a-1,j}) \prod_{i \in D_j} u_i|_{y_a=0}, \quad W'_{a,b} = -\alpha' c_{2a-1,2b-1} \prod_{i \in E} u_i|_{y_a=0, y_b=0}, \quad (4.51)$$

which are written in terms of a product of u 's without referring to any specific triangulation.

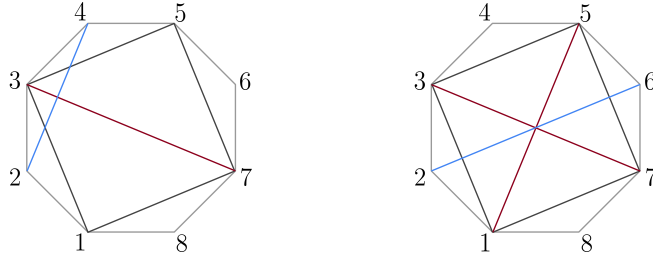
The product of the u 's appearing in the definitions of V'_a and $W'_{a,b}$ have a very simple graphical interpretation. For the coefficient of $(X_{2a,j} - X_{2a-1,j})$ in V'_a we simply take the product over all the u 's in the inner n -gon that intersects $(2a, j)$. For $W'_{a,b}$ we similarly have the product over all the u 's of the inner n -gon that intersect $(2a, 2b)$.

For example, the $n = 3$ amplitude is given by $V'_1 V'_2 V'_3 + V'_1 W'_{2,3} + \text{perm.}$ with

$$V'_1 = -\alpha' X_{2,5}, \quad W'_{1,2} = -\alpha' c_{1,3}, \quad (4.52)$$



$$V'_1 = -\alpha'(X_{2,5} - X_{1,5})u_{3,7} - \alpha'(X_{2,7} - 0)u_{1,5}$$



$$W'_{1,2} = -\alpha'c_{1,3}u_{3,7} \quad W'_{1,3} = -\alpha'c_{1,5}u_{1,5}u_{3,7}$$

Figure 21: V' and W' in terms u 's for $n = 4$.

and cyclic images *e.g.* $V_2 = -\alpha'X_{1,4}$. In this case, there is no integral left in (4.50) and we reproduce the familiar result (4.64).

For $n = 4$ case, we have the following V' and W' , where the product of u 's are shown in Fig. 21:

$$V'_1 = -\alpha'(u_{3,7}(X_{2,5} - X_{1,5}) + u_{1,5}X_{2,7}), \quad W'_{1,2} = -\alpha'c_{1,3}u_{3,7}, \quad W'_{1,3} = -\alpha'c_{1,5}u_{1,5}u_{3,7}, \quad (4.53)$$

as well as their cyclic images. Similar to (4.43), we have $3 + 6 + 1$ terms of the form $W'W'$, $W'V'V'$ and $V'V'V'V'$ respectively, and (4.50) becomes:

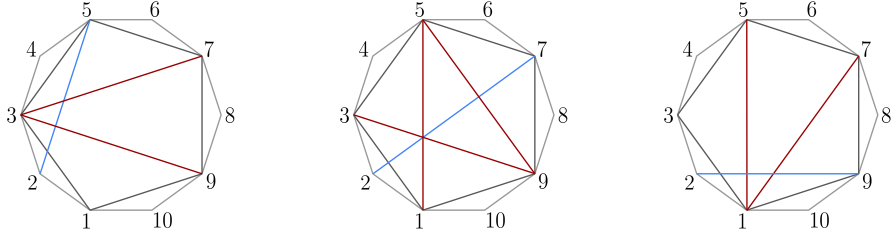
$$\int_0^\infty \frac{dy}{y} ((W'_{1,2}W'_{3,4} + \text{perms.}) + (W'_{1,2}V'_3V'_4 + \text{perm.}) + V'_1V'_2V'_3V'_4) u_{1,5}^{\alpha'X_{1,5}-1} u_{3,7}^{\alpha'X_{3,7}-1}, \quad (4.54)$$

where only one integration variable is left, which can be chosen as $y = y_{1,5}$ or $y_{3,7}$ depending on the inner triangulation. For the former we have $u_{1,5} = y_{1,5}/(1 + y_{1,5})$ and $u_{3,7} = 1 - u_{1,5} = 1/(1 + y_{1,5})$, and the other way around for the latter.

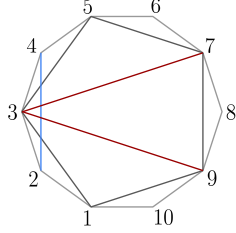
Finally, we present these building blocks for $n = 5$ amplitude which can be nicely summarized in figure 22. All cyclically inequivalent ones are:

$$V'_1 = -\alpha'(u_{3,7}u_{3,9}(X_{2,5} - X_{1,5}) + u_{1,5}u_{3,9}u_{5,9}(X_{2,7} - X_{1,7}) + u_{1,5}u_{1,7}X_{2,9}), \quad (4.55)$$

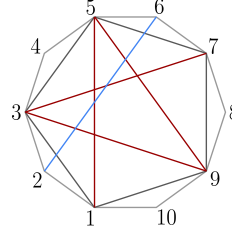
$$W'_{1,2} = -\alpha'c_{1,3}u_{3,7}u_{3,9}, \quad W'_{1,3} = -\alpha'c_{1,5}u_{1,5}u_{3,7}u_{3,9}u_{5,9}. \quad (4.56)$$



$$V'_1 = -\alpha' (X_{2,5} - X_{1,5}) u_{3,7} u_{3,9} - \alpha' (X_{2,7} - X_{1,7}) u_{1,5} u_{3,9} u_{5,9} - \alpha' (X_{2,9} - 0) u_{1,5} u_{1,7}$$



$$W'_{1,2} = -\alpha' c_{1,3} u_{3,7} u_{3,9}$$



$$W'_{1,3} = -\alpha' c_{1,5} u_{1,5} u_{3,7} u_{3,9} u_{5,9}$$

Figure 22: V' and W' in terms u 's for $n = 5$.

The $n = 5$ string amplitude is a two-fold integral as in (4.50), where in the summation we have $V'_1 \dots V'_5$, 10 permutations of $V'_1 V'_2 V'_3 W'_{4,5}$, and 15 permutations of $V'_1 W'_{2,3} W'_{4,5}$.

4.6 Consistency check: From $4n$ -scalars to $2n$ -scalars

Now that we have an explicit form for the gluon amplitude obtained after taking the scaffolding residue, we can perform a nice consistency check. Suppose we did not know the bosonic string answer, and so we did not know a priori that the scalars we are scattering can be thought of as higher-dimensional polarizations of gluons. How could we discover this fact inherently within our world?

One way of doing this is to start with a $4n$ -scalar string amplitude. In this case, taking the scaffolding residue leads to a $2n$ -gluon string amplitude; if we then choose the special polarizations in (4.3), the result must simplify dramatically to land on the $2n$ -scalar string amplitude again!

We will now see that very nicely this is indeed the case. Let us consider the $4n$ -scalar scattering labelled by $\{1, 1', 2, 2', \dots, 2n, 2n'\}$, which results in the $2n$ -gluon scattering by taking the scaffolding residues $\{X_{1,2}, X_{2,3}, \dots, X_{2n,1}\}$. Recalling the dimensional reduction that turns the gluons into the $2n$ -scalars, eq. (4.3), we see that this is equivalent to take the derivative $\partial_{\epsilon_1 \cdot \epsilon_2} \partial_{\epsilon_3 \cdot \epsilon_4} \dots \partial_{\epsilon_{2n-1} \cdot \epsilon_{2n}}$ on the conventional string correlator. On the other hand, in the $4n$ -scalar kinematic configuration, we have:

$$\epsilon_i^\mu \propto (1 - \alpha)(X_{i+1} - X_{i'})^\mu - \alpha(X_{i'} - X_i)^\mu, \quad (4.57)$$

$$q_i^\mu \propto (X_{i+1} - X_i)^\mu. \quad (4.58)$$

$$W'_{1,2} = -\alpha' c_{1,2} u_{2,4} u_{2,5} u_{2,6} \quad W'_{3,4} = -\alpha' c_{3,4} u_{1,4} u_{2,4} u_{4,6} \quad W'_{5,6} = -\alpha' c_{5,6} u_{2,6} u_{3,6} u_{4,6}$$

Figure 23: W' 's that contribute to the derivative from 6-scaffolding-gluon to 6-scalar.

Importantly, as we have mentioned before, the dependence on $X_{i',j'}$ only appears in $\epsilon_i \cdot \epsilon_j$. Therefore, the above derivative on Lorentz product of ϵ is equivalent to the following derivative in our kinematic configuration:

$$\partial_{\epsilon_1 \cdot \epsilon_2} \partial_{\epsilon_3 \cdot \epsilon_4} \dots \partial_{\epsilon_{2n-1} \cdot \epsilon_{2n}} \sim (-2)^n \partial_{X_{1',2'}} \partial_{X_{3',4'}} \dots \partial_{X_{2n-1',2n'}}, \quad (4.59)$$

where in the RHS we have included the normalization factor. Now recall the X 's dependence in the building blocks of our ‘‘stringy correlator’’: V'_i depends on $X_{i',j}$, $X_{i,j}$ for some j (with no prime), $W'_{i,j}$ depends on $c_{i,j} = X_{i,j} + X_{i',j'} - X_{i',j} - X_{i,j'}$. Therefore, it is clear that the derivative (4.59) resulting on only one term:

$$\begin{aligned} W'_{1,2} W'_{3,4} \dots W'_{2n-1,2n} &\rightarrow (-1)^n (-2)^n \prod_{i \in \text{even}} \prod_{j \neq i-1, i, i+1} u_{i,j} \\ &= 2^n \prod_{(i,j) \in \text{even}} u_{i,j}^2 \prod_{k \in \text{even}, l \in \text{odd}} u_{k,l}, \end{aligned} \quad (4.60)$$

where all the indices in the subscript only involve labels with no prime. For example, consider $(4n = 12)$ -scalar to $(2n = 6)$ -scalar, the one term that contributes to the derivative reads (see Fig. 23):

$$W'_{1,2} W'_{3,4} W'_{5,6} \rightarrow 8 u_{2,4}^2 u_{2,6}^2 u_{4,6}^2 u_{2,5} u_{1,4} u_{3,6}, \quad (4.61)$$

where we have set $\alpha' = 1$. Recall in (4.50) we have an overall factor $1/(\prod_{(i,j)} u_{i,j})$, therefore the dimensional reduction transforms the $2n$ -scaffolding-gluon to the $2n$ -scalar correctly with the factor $2^n \prod_{(i,j) \in \text{even}} u_{i,j} / \prod_{(i,j) \in \text{odd}} u_{i,j}$, which in the above example reads $8(u_{2,4} u_{2,6} u_{4,6}) / (u_{1,3} u_{1,5} u_{3,5})$ as expected.

4.7 Examples

We end our tree-level discussion by presenting some explicit examples of how to use (4.1) to extract gluon amplitudes. For simplicity, we will be focusing on the 3- and 4-point amplitudes. In section 4.8, we make some comments on how to systematically extract the field theory gluon amplitude at higher points.

4.7.1 3-point example

To obtain the 3-point gluon interaction we start with the 6-scalar amplitude. Picking the scaffolding triangulation $\{X_{1,3}, X_{3,5}, X_{1,5}\}$ we obtain

$$\mathcal{A}_6 = \int_0^\infty \frac{dy_{1,3} dy_{3,5} dy_{1,5}}{y_{1,3}^2 y_{3,5}^2 y_{1,5}^2} \prod_{i,j} u_{ij}^{\alpha' X_{i,j}} \left(\frac{u_{2,4} u_{2,6} u_{4,6}}{u_{1,3} u_{3,5} u_{5,7}} \right). \quad (4.62)$$

Plugging in the explicit parametrization, $u_{i,j}(y_{1,3}, y_{3,5}, y_{1,5})$, yields:

$$\begin{aligned} \mathcal{A}_6 = \int_0^\infty \frac{dy_{1,3} dy_{3,5} dy_{1,5}}{y_{1,3}^2 y_{3,5}^2 y_{1,5}^2} & y_{1,3}^{\alpha' X_{1,3}} y_{3,5}^{\alpha' X_{3,5}} y_{1,5}^{\alpha' X_{1,5}} (1 + y_{1,3})^{-\alpha' c_{1,4}} (1 + y_{1,5})^{-\alpha' c_{2,5}} (1 + y_{3,5})^{-\alpha' c_{3,6}} \\ & \times (1 + y_{1,3} + y_{1,3} y_{3,5})^{-\alpha' c_{1,3}} (1 + y_{1,5} + y_{1,5} y_{1,3})^{-\alpha' c_{1,5}} (1 + y_{3,5} + y_{3,5} y_{1,5})^{-\alpha' c_{3,5}}. \end{aligned} \quad (4.63)$$

As discussed in 4.2.2, taking the scaffolding residue amounts to setting $X_{1,3} = X_{3,5} = X_{1,5} = 0$, and collecting the piece of the integrand that is linear in $y_{1,3}, y_{3,5}$ and $y_{1,5}$. In this case, after taking this residue there are no integrations left and we get:

$$\begin{aligned} A_3^{\text{gluon}} &= \alpha'^2 (c_{1,3} c_{1,5} + c_{1,3} c_{2,5} + c_{1,3} c_{3,5} + c_{1,4} c_{3,5} + c_{1,5} c_{3,5} + c_{1,5} c_{3,6}) + \\ & - \alpha'^3 (X_{1,4} X_{2,5} X_{3,6}) \\ &= \alpha'^2 (-(X_{2,5} - X_{2,6}) X_{1,4} - (X_{3,6} - X_{4,6}) X_{2,5} - (X_{1,4} - X_{2,4}) X_{3,6}) \\ & - \alpha'^3 (X_{1,4} X_{2,5} X_{3,6}). \end{aligned} \quad (4.64)$$

The leading piece in α' is exactly the Yang-Mills amplitude, and we can check it precisely matches (3.27). The sub-leading term corresponds to the F^3 vertex, which has higher units.

Before proceeding, let's use this simple example to highlight two non-trivial features of this scaffolded gluon amplitude: First, since we extract the answer via this scaffolding residue, the amplitude can be written as a function of **solely non-planar variables**, $c_{i,j} = -p_i \cdot p_j$, with i and j non-adjacent. This is a non-trivial general fact that will be explored further in [34]. Second, as we have mentioned already, in this scalar language the amplitude takes a unique form, there is no gauge-redundancy ambiguity in how it is expressed.

4.7.2 4-point example: string and field-theory amplitudes

For $n = 4$, after taking the scaffolding residue we are left with one integration – which we can trivially perform – so we now present explicitly the integrated 4-gluon string amplitude. To do this, we use the result we get after taking the scaffolding residue in terms of V 's and W 's presented in (4.54), but now we explicitly evaluate the last integration.

Let us define

$$I(a, b) := \frac{\Gamma(X_{1,5} + a) \Gamma(X_{3,7} + b)}{\Gamma(X_{1,5} + X_{3,7} + a + b)}, \quad (4.65)$$

with integer shifts a, b . The first term reads

$$\int_0^\infty \frac{dy_{1,5}}{y_{1,5}} u_{1,5}^{X_{1,5}-1} u_{3,7}^{X_{3,7}-1} W'_{1,2} W'_{3,4} = c_{1,3} c_{5,7} I(1, -1). \quad (4.66)$$

The second term, *i.e.* the integral of $W'_{2,3}W'_{1,4}$ is given by the cyclic rotation for the 4-gon: $X_{i,j} \rightarrow X_{i+2,j+2}$, which acts on $I(a,b)$ as $I(a,b) \rightarrow I(b,a)$. The third term reads:

$$\int_0^\infty \frac{dy_{1,5}}{y_{1,5}} u_{1,5}^{X_{1,5}-1} u_{3,7}^{X_{3,7}-1} W'_{1,3} W'_{2,4} = c_{1,3} c_{3,7} I(1,1). \quad (4.67)$$

For combinations of the type $W'V'V'$, we have

$$\begin{aligned} & \int_0^\infty \frac{dy_{1,5}}{y_{1,5}} u_{1,5}^{X_{1,5}-1} u_{3,7}^{X_{3,7}-1} W'_{1,2} V'_3 V'_4 \\ &= \frac{c_{1,3} I(1,0)}{(X_{1,5}-1) X_{1,5}} ((X_{1,5}-1)(X_{1,5}(X_{3,6}-X_{3,7})+X_{1,6}X_{3,7})(X_{3,7}-X_{3,8}) \\ & \quad + X_{3,7}(X_{3,6}-X_{1,6}(X_{3,7}+1)+X_{1,5}(-X_{3,6}+X_{3,7}+1))X_{5,8}), \end{aligned} \quad (4.68)$$

and three more terms with $W'_{2,3}V'_4V'_1$, $W'_{3,4}V'_1V'_2$, and $W'_{1,4}V'_2V'_3$ are obtained from cyclic rotations (proportional to $I_{0,1}$, $I_{1,0}$ and $I_{0,1}$). Similarly, for $W'_{1,3}V'_2V'_4$ we have

$$\begin{aligned} & \int_0^\infty \frac{dy_{1,5}}{y_{1,5}} u_{1,5}^{X_{1,5}-1} u_{3,7}^{X_{3,7}-1} W'_{1,3} V'_2 V'_4 \\ &= \frac{c_{1,5} I(1,1)}{X_{1,5} X_{3,7}} (X_{1,5}(X_{3,7}-X_{3,8})((X_{1,4}-X_{1,5}-1)X_{3,7}+(X_{1,5}+1)X_{4,7}) \\ & \quad - X_{3,7}(X_{1,4}(X_{3,7}+1)+X_{1,5}(X_{4,7}-X_{3,7}))X_{5,8}), \end{aligned} \quad (4.69)$$

and another term with $W'_{2,4}V'_1V'_3$ by cyclic rotation. The last case, the integral with $V'_1V'_2V'_3V'_4$, is given by

$$P_0 I(-1,3) + P_1 I(0,2) + P_2 I(1,1) + P_3 I(2,0) + P_4 I(3,-1), \quad (4.70)$$

where we have degree-4 polynomials in X 's, P_i with $i = 0, 1, \dots, 4$, as follows

$$P_0 = X_{1,4} X_{5,8} (X_{2,5} - X_{1,5}) (X_{1,6} - X_{1,5}), \quad (4.71)$$

$$\begin{aligned} P_1 = & X_{1,4} (X_{1,6} - X_{1,5}) (X_{2,5} - X_{1,5}) (X_{3,8} - X_{3,7}) + X_{1,4} (X_{1,6} - X_{1,5}) X_{2,7} X_{5,8} \\ & + X_{1,4} (X_{2,5} - X_{1,5}) X_{3,6} X_{5,8} + (X_{1,6} - X_{1,5}) (X_{2,5} - X_{1,5}) (X_{4,7} - X_{3,7}) X_{5,8}, \end{aligned} \quad (4.72)$$

$$\begin{aligned} P_2 = & X_{1,4} (X_{1,6} - X_{1,5}) X_{2,7} (X_{3,8} - X_{3,7}) + X_{1,4} (X_{2,5} - X_{1,5}) X_{3,6} (X_{3,8} - X_{3,7}) \\ & + (X_{1,6} - X_{1,5}) (X_{2,5} - X_{1,5}) (X_{4,7} - X_{3,7}) (X_{3,8} - X_{3,7}) + X_{1,4} X_{2,7} X_{3,6} X_{5,8} \\ & + (X_{1,6} - X_{1,5}) X_{2,7} (X_{4,7} - X_{3,7}) X_{5,8} + (X_{2,5} - X_{1,5}) X_{3,6} (X_{4,7} - X_{3,7}) X_{5,8}; \end{aligned} \quad (4.73)$$

and P_3 and P_4 are obtained from P_1 and P_0 by cyclic rotation, respectively. Adding these contributions we obtain the explicit result of $n = 4$ string amplitude.

Finally, we present the 4-point Yang-Mills amplitude, which is given by the $\alpha' \rightarrow 0$ limit of the full stringy result. Just as we saw at 3-points case, we find that the result takes a suggestive ‘‘c-expansion’’ form:

$$A_4^{\text{YM}} = \alpha'^2 \left(\frac{N_{1,5}(\{c_{i,j}\})}{X_{1,5}} + \frac{N_{3,7}(\{c_{i,j}\})}{X_{3,7}} + c_{1,5} c_{3,7} \right), \quad (4.74)$$

where we have two poles, $X_{1,5}$ and $X_{3,7}$, with numerators $N_{1,5}$ and $N_{3,7} = N_{1,5}|_{i \rightarrow i+2}$, as well as a “contact term” $c_{1,5}c_{3,7}$. Both the contact term and these two numerators can be expressed solely in terms of $c_{i,j}$'s. This is not at all guaranteed a priori but reflects a general phenomenon we will explore for all n in forthcoming work [34]. The numerator $N_{1,5}$ is given by:

$$\begin{aligned}
N_{1,5} = & -c_{1,5}c_{3,7}^2 - c_{1,3}c_{1,5}c_{3,7} - c_{1,5}c_{1,7}c_{3,7} - c_{1,3}c_{2,5}c_{3,7} - c_{1,5}c_{2,7}c_{3,7} - c_{1,3}c_{3,5}c_{3,7} \\
& - c_{1,5}c_{3,6}c_{3,7} - c_{1,5}c_{3,8}c_{3,7} - c_{1,5}c_{4,7}c_{3,7} - c_{1,3}c_{5,7}c_{3,7} - c_{1,4}c_{5,7}c_{3,7} - c_{1,5}c_{5,7}c_{3,7} \\
& - c_{1,3}c_{5,8}c_{3,7} - c_{1,4}c_{5,8}c_{3,7} - c_{1,7}c_{5,8}c_{3,7} - c_{1,3}c_{1,5}c_{1,7} - c_{1,3}c_{1,7}c_{2,5} - c_{1,3}c_{1,5}c_{2,7} \\
& - c_{1,4}c_{1,7}c_{3,5} - c_{1,5}c_{1,7}c_{3,5} - c_{1,3}c_{2,7}c_{3,5} - c_{1,4}c_{2,7}c_{3,5} - c_{1,5}c_{2,7}c_{3,5} - c_{1,5}c_{1,7}c_{3,6} \\
& - c_{1,5}c_{2,7}c_{3,8} - c_{1,3}c_{1,5}c_{4,7} - c_{1,3}c_{2,5}c_{4,7} - c_{1,3}c_{3,5}c_{4,7} - c_{1,4}c_{3,5}c_{4,7} - c_{1,5}c_{3,5}c_{4,7} \\
& - c_{1,3}c_{1,5}c_{5,7} - c_{1,3}c_{1,6}c_{5,7} - c_{1,3}c_{1,7}c_{5,7} - c_{1,3}c_{2,5}c_{5,7} - c_{1,3}c_{2,6}c_{5,7} - c_{1,3}c_{2,7}c_{5,7} \quad (4.75) \\
& - c_{1,5}c_{3,5}c_{5,7} - c_{1,6}c_{3,5}c_{5,7} - c_{1,7}c_{3,5}c_{5,7} - c_{1,3}c_{3,6}c_{5,7} - c_{1,4}c_{3,6}c_{5,7} - c_{1,5}c_{3,6}c_{5,7} \\
& - c_{1,5}c_{3,8}c_{5,7} - c_{1,6}c_{3,8}c_{5,7} - c_{1,7}c_{3,8}c_{5,7} - c_{1,3}c_{1,7}c_{5,8} - c_{1,3}c_{2,7}c_{5,8} - c_{1,7}c_{3,5}c_{5,8} \\
& - c_{1,5}c_{3,5}c_{3,7} - c_{1,7}c_{5,7}c_{3,7} - c_{1,3}c_{1,7}c_{3,5} - c_{1,5}c_{1,7}c_{3,8} - c_{1,5}c_{3,8}c_{4,7} - c_{1,4}c_{3,5}c_{5,7} \\
& - c_{1,4}c_{3,5}c_{3,7} - c_{1,6}c_{5,7}c_{3,7} - c_{1,3}c_{2,5}c_{2,7} - c_{1,5}c_{2,7}c_{3,6} - c_{1,5}c_{3,6}c_{4,7} - c_{1,3}c_{3,5}c_{5,7} \\
& - c_{1,7}c_{3,6}c_{5,7} - c_{1,7}c_{3,8}c_{5,8} - c_{1,6}c_{3,6}c_{5,7} - c_{1,7}c_{3,6}c_{5,8}.
\end{aligned}$$

This reduces to the “leading singularity” given in (6.9) upon sending $X_{1,5} \rightarrow 0$. It is possible to simplify this formula somewhat by introducing the notation $c_{A,B} = \sum_{k \in A, l \in B} c_{k,l}$, so that e.g. $c_{12,34} = c_{1,3} + c_{1,4} + c_{2,3} + c_{2,4}$. Then we have

$$\begin{aligned}
N_{1,5} = & -c_{3,5678} (c_{1,67}c_{5,7} + c_{1,5}c_{12345,7} + c_{1,7}c_{5,8}) - c_{1,4} (c_{12345,7}c_{3,5} + c_{3,67}c_{5,7} + c_{3,7}c_{5,8}) \\
& - c_{1,3} (c_{123,5}c_{1234,7} + c_{123,567}c_{5,7} + c_{123,7}c_{5,8}). \quad (4.76)
\end{aligned}$$

Note that already the 4-point gluon amplitude looks more complicated than we are used to from the familiar Parke-Taylor formulas in four dimensions. This reflects the basic fact that D -dimensional gluon amplitudes simply are richer than in four dimensions, and that we are non-redundantly describing all possible gluon polarizations in a single expression.

4.8 Further comments

Simplicity of residue extraction A fascinating general phenomenon has been encountered repeatedly in “surfaceology” for amplitudes, which also appears in the context of the computation of scaffolding residues we began with in this section that we would like to highlight here.

After taking the scaffolding residue, we end up (as with the bosonic string gluon expression) with a sum over exponentially many terms. What then is the point of beginning with the “one-term” expression for the $2n$ scalar problem, if the final gluon expression looks exponentially complicated in any case? Of course the scalar starting point is much more compact and crucially allows us to see the deep connection between scalar, pions, and gluons. But does it have a practical, computational advantage of any sort?

Naively the answer would seem to be “no”, but remarkably, while the analytic expression for the residue indeed has exponentially many terms, the actual computation of the residue can be done in polynomial time! This is a famous occurrence in various branches of mathematics and physics. For instance, the analytic expression for the determinant of an $n \times n$ matrix has $n!$ terms but can be trivially computed in n^3 time using Gaussian elimination. Similarly, if we look at the 10-th Newton polynomial of 10^3 variables $\sum x_{i_1} \cdots x_{i_{10}}$ where the i 's range from $1, \dots, 10^3$, there are roughly 10^{30} terms in the sum, but for any numerical values of the x_i we can get the answer in a nanosecond on a computer, simply by looking at to the coefficient of t^{10} in the expansion of $(1 + tx_1)(1 + tx_2) \cdots (1 + tx_{1000})$.

The same thing occurs for the computation of our residue: the “one-term” starting point from the $2n$ scalar problem allows us to compute a result naively needing exponentially many terms in polynomial time. As mentioned this is a special case of a general fact we have encountered repeatedly in the connection between amplitudes and the combinatorial geometry of surfaces. At the most basic level, the u_X variables and their tropicalizations to the “headlight functions” α_X generate the exponentially many cones associated with Feynman diagrams from polynomially many expressions involving polynomially many terms. Extensions of the tropical formalism for computing amplitudes for very general Lagrangians [37] see the same feature for generating numerator factors. It would be fascinating to better understand the origins of this huge reduction in apparent complexity for the sorts of polynomial expressions we encounter in scattering amplitudes.

Integration Contour for Gluons Our integral form for the $2n$ scalar scaffolded amplitude is given as an integral over positive $y_i > 0$, but of a form $\prod_i dy_i/y_i^2$ with power-law singularities as $y_i \rightarrow 0$. As such even in the field theory limit, where the X_{ij} close to zero, the integral is not well defined on this naive contour and the result must be appropriately analytically continued from the domain where the X 's are positive enough to make the integral converge. Given that these amplitudes arise from a simple kinematic shift of the $\text{Tr } \phi^3$, this can be rephrased as the familiar fact discussed in our review of stringy $\text{Tr } \phi^3$ integrals, that the integral form of the Koba-Nielsen formula only converges when the $X_{i,j} > 0$, and continuing to the physically interesting region where we see resonances and the amplitude has poles, where $X_{i,j} < 0$, is accomplished by analytic continuation. As discussed there and at greater length in [27], the u/y variables make it easy to define an explicit contour on which the integral converges for *any* $X_{i,j}$. For the purposes of this paper, this is enough to concretely specify a contour on which our scaffolded gluon amplitudes can be concretely evaluated.

Field Theory Limit For Gluons Extracting the field theory limit of our scalar-scaffolded gluon amplitude is more challenging than for $\text{Tr } \phi^3$ theory. As we discussed earlier, the dy/y singularity makes it easy to extract the low-energy limit of the amplitudes for $\alpha' X \ll 1$, localizing to logarithmic divergences as $|\log y| \rightarrow \infty$. This procedure does not work immediately for our scaffolded gluons, where the dy/y^2 form has power-law divergences and the integral must be defined by analytic continuation, even at tree-level. In [34] will report on an elementary and direct way of extracting the field theory limit, via a “cone-by-cone” analysis of the singular behavior of the integrand. This will be analyzed systematically

at tree and loop level in [34], but we can illustrate with the simplest but still non-trivial example of the four-point amplitude.

We begin by arbitrarily dividing the integral over y into two regions, for y between $(0,1)$ and $(1, \infty)$. Then we have

$$\mathcal{A}_4^{\text{gluon}} = \left(\int_0^1 + \int_1^\infty \right) \frac{dy_{1,3}}{y_{1,3}^2} y_{1,3}^{X_{1,3}} (1 + y_{1,3})^{-c_{1,3}}, \quad (4.77)$$

where $c_{1,3} = X_{1,3} + X_{2,4}$ is a “mesh constant” in the language of [6, 12].

We will now extract the leading singular behavior from each piece in a standard way. For $y \in (0, 1)$, we can expand

$$\begin{aligned} \int_0^1 \frac{dy_{1,3}}{y_{1,3}^2} y_{1,3}^{X_{1,3}} \left(1 + (-c_{1,3})y_{1,3} + \frac{(-c_{1,3})(-c_{1,3}-1)}{2} y_{1,3}^2 + \dots \right) &= \\ = \frac{1}{X_{1,3}-1} - \frac{c_{1,3}}{X_{1,3}} + \frac{(-c_{1,3})(-c_{1,3}-1)}{2} + \dots = -1 + \dots - \frac{c_{1,3}}{X_{1,3}} + \dots, \end{aligned} \quad (4.78)$$

where in the second line we have kept the leading terms at low energies, which here scale as X^0 as opposed to X^{-1} we are familiar with for the $\text{Tr } \phi^3$ amplitude. Note that in performing this integral we are assuming that $X_{1,3} > 1$ for convergence, and indeed the leading singular term $1/(X_{1,3}-1)$ has a pole at $X_{1,3} = 1$, but we are then free to analytically continue and expand in $X_{1,3}$ around zero. Doing this converts the naive power-law divergence we would get from the $dy_{1,3}/y_{1,3}^2$ behavior near $y_{1,3} \rightarrow 0$, to simply the constant term -1 . Performing a similar analysis for $y_{1,3} \in (1, \infty)$, we find that the leading behavior simply gives us $(+1)$:

$$\begin{aligned} \int_1^\infty \frac{dy_{1,3}}{y_{1,3}^2} y_{1,3}^{X_{1,3}} (1 + y_{1,3})^{-X_{1,3}-X_{2,4}} &= \int_1^\infty \frac{dy_{1,3}}{y_{1,3}^2} \left(\frac{1}{y_{1,3}} \right)^{X_{2,4}} \left(1 + \frac{-c_{1,3}}{y_{1,3}} + \frac{(-c_{1,3})(-c_{1,3}-1)}{2y_{1,3}^2} + \dots \right) \\ &= 1 + \dots. \end{aligned} \quad (4.79)$$

This $(+1)$ cancels the (-1) remnant from the naive power divergence in the first regions, leaving us with

$$\mathcal{A}_4^{\text{gluon}} \rightarrow \frac{-c_{1,3}}{X_{1,3}}. \quad (4.80)$$

The cancellation of the “ -1 ” and “ 1 ” pieces from the two regions reflects the basic fact used repeatedly in the zeros analysis of [12] that the classic “scale-less integral” $\int_0^\infty dy/y y^\alpha = 0$.

The same strategy works in general. It is more convenient to set the $y_i = e^{-t_i}$ and work in t space, which is divided into cones corresponding to the different degenerations of the surface/diagrams. In each cone, there is a leading behavior at infinity, that can be nicely controlled by understanding the “ g -vector fan”, which we can factor out and then expand around. The resulting functions of the kinematic variables X can then in turn be expanded about $X = 0$, keeping the leading low-energy behavior.

5 Loop-level Gluon Amplitudes

Having just learned how to describe tree-level gluon scattering amplitudes using scalar-scaffolding, we now turn to making our proposal for gluon amplitudes at loop level. At tree-level, we had the luxury of being able to easily compare with the corresponding expressions in the bosonic string, but at loop-level we will be proceeding more adventurously.

At tree level, we understood that the simple kinematic shift—which is equivalent to inserting the magic monomials in u 's ($\prod u_{e,e}/\prod u_{o,o}$), which is equal to the product of all $\prod_i y_i$ in the scaffolding triangulation—is responsible for transmuting the “boring” amplitudes of $\text{Tr } \phi^3$ theory into ones that enjoy the gauge invariance, multilinearity and factorization of gluon amplitudes.

But in fact, as mentioned in our review of surfaceology, this monomial has exactly the same property for *any* surface. This motivates an extension of our proposal to any surface and hence all loop orders/orders in the 't Hooft expansion.

Our goal in this section is to present this all-loop generalization, discussing a number of novelties that arise along the way: we will see that the product over curves \mathcal{C} must include open curves with up to one self-intersection per loop, as well as a product over closed curves Δ with exponents u_{Δ}^{1-D} where D is the number of spacetime dimensions. The treatment of self-intersecting curves marks a major difference from the conventional bosonic string theory. For $\text{Tr } \phi^3$ theory matching (bosonic) string theory at loop-level from the curve-integral formalism asks us to consider the product over *all* curves [14], including those with arbitrarily high intersection numbers. Meanwhile, if we want a “stringy” integral that reduces to $\text{Tr } \phi^3$ at low energies it suffices to only keep non-self-intersecting curves, which are the only ones dually interpretable as propagators in Feynman diagrams. It is intriguing that in order to describe gluons we must make the curve integral “slightly more stringy” by including curves with a finite number of self-intersections, but still distinct from the infinite number of curves needed to describe the “real bosonic string” in this language.

5.1 Loop scaffolding form

In the tree-level case, we derived the scaffolding form Ω_{2n} starting from the bosonic string $2n$ gluon amplitude and choosing a kinematic configuration in which the gluons become effectively scalars – $2n$ scalars. Following the same procedure at loop-level is much less trivial, as bosonic string loop amplitudes are significantly more complicated.

Instead, we will follow a different strategy that once more relies on how the tree-level amplitudes are formulated in terms of the surface problem. As we saw in the previous section, the resulting scaffolding form, in terms of u 's, was simply that of the bosonic string $\text{Tr } \phi^3$ amplitude, times the factor corresponding to the ratio of u 's, (4.6). In particular, choosing the scaffolding triangulation, we can simplify this to the bosonic string $\text{Tr } \phi^3$ amplitude where instead of a logarithmic form in the y 's, we have a dy/y^2 form (4.8).

In order to generalize this scaffolding form to the loop level, we consider exactly the same integrand but instead of being defined on the disk, it is now defined on the punctured

disk. So we start with (2.26) and replace the integration measure:

$$\mathcal{A}_{2n}^{1\text{-loop}}(1, 2, \dots, 2n) = \int_0^\infty \prod_i \frac{dy_i}{y_i^2} \prod_C u_C^{\alpha' X_C} \times \prod_{C' \in \text{s.i.}} u_{C'}^{\alpha' X_{C'}} \times u_\Delta^\Delta. \quad (5.1)$$

This is our candidate for the loop stringy integral. The version for higher loops is exactly the same except that at higher loops there are more closed curves, so instead we have a product over u_{Δ_i} .

As pointed out previously, since there are an infinite number of self-intersecting curves, this integrand contains an infinite number of terms. In the case of $\text{Tr } \phi^3$, we can truncate this infinite product, since all self-intersection curves had no impact on the field-theory limit: their u variables can never go to zero since they occur in both terms of the u equations, and hence they don't affect the leading singularities that dominate the field theory limit. We now want to understand how this generalizes to gluons, *i.e.* what is the minimal set of curves we need to include in the integrand that gives us gluons at low energies.

Another feature of gluon loop amplitudes is the dependence on the spacetime dimension, D . If tree amplitudes are written either in terms of dot products of momenta and polarization vectors, or in our scalar scaffolding language, they are D independent. However, loop amplitudes/integrands are certainly D dependent, mechanically arising from the trace of the metric $\eta^{\mu\nu}\eta_{\mu\nu} = D$. However, from (5.1) we do not see any explicit dependence on D , so where is the spacetime dimension dependence coming from?

5.1.1 Δ

At the outset of our discussion we mentioned that in order to describe gluons at loop level, we have to consider closed curves that naturally live on the surface. In the planar limit, these are closed curves surrounding punctures. These are not needed for “stringy” $\text{Tr } \phi^3$ integrals, at least if we only want to match the low-energy field theory limit (they are needed for the full bosonic string amplitude), but together with the self-intersecting curves we will mention in a moment, they will be important to describe gluons.

By homology closed curves should have zero momentum, but we will give the corresponding u_Δ variables an exponent Δ . We will see that in order to describe gluons in D spacetime dimensions we must take

$$\Delta = 1 - D. \quad (5.2)$$

Note again the importance of using the scalar scaffolding picture, which allows our description of momentum kinematics to be dimension agnostic, and now allows us to introduce the dependence on spacetime dimension D as a continuous parameter we can choose at will.

5.1.2 Self-Intersecting Curves

As we mentioned previously, in the case of $\text{Tr } \phi^3$ the contribution from self-intersecting curves does not affect the low energy limit. For gluons, however, the minimal set of curves

we need includes curves that self-intersect at most once (around each puncture, in case we are considering a higher loop process). Thus the proposal for the gluon loop integrand is:

$$\mathcal{A}_{2n}^{\text{m-loop}}(1, 2, \dots, 2n) = \int_0^\infty \underbrace{\prod_i \frac{dy_i}{y_i^2} \prod_C u_C^{\alpha' X_C} \times \prod_{C' \in \# \text{ s.i.}=1} u_{C'}^{\alpha' X_{C'}} \times \prod_{k \in \{1, \dots, m\}} u_{\Delta_k}^{\Delta_k}}_{\Omega_{2n}^{\text{m-loop}}}, \quad (5.3)$$

where Δ_k denotes the closed curve going around puncture k .

Before proceeding, let's highlight the following: at tree-level, the $2n$ -scaffolding form was derived directly from the bosonic string answer, and thus the low energy limit had to be gluons. For the loop integrand (5.1), this is **not** the case, so there is no guarantee a priori that we are describing gluons, and in particular that (5.3) is the correct truncation.

One encouraging feature is that the object we get after taking the scaffolding residue satisfies a notion of gauge-invariance/multi-linearity, just like in the tree-level case. We will explore this notion in section 5.2.

Another check on this object is to compute the loop-leading singularities and check that they agree with gluon-leading singularities. Some nontrivial examples of this matching are presented in 6.3. These computations make manifest how the self-intersecting curves are important at low energies.

However to prove the full consistency of this formulation what one has to do is show that starting with (5.3) and going on the cut of the loop propagator, we land on the tree-level answer (4.8) of the corresponding cut surface. This turns out to be quite non-trivial, but we present the full proof of this matching in section 7. As a byproduct, we will understand why we need to keep all the curves up to self-intersection one.

5.2 Surface gauge invariance

It is well known that the notion of gauge invariance for loop integrands is afflicted with difficulties associated with the presence of the tadpole (as well as massless external bubble) propagators. But we have already seen, at tree level, that simple properties of the u 's directly hand us a certain linear expansion of the amplitude in terms of the scaffolding kinematic variables, that automatically encodes gauge invariance and multilinearity. We will now see how this extends to loop level, to determine the general form of "gluon amplitudes" predicted by the binary geometry of the surface. As we will see these will give a natural home for incorporating tadpoles/massless external bubbles with no ambiguities, and we will use this to **define** what we mean by gauge invariance and multilinearity. To avoid this mouthful of a phrase in what follows we will refer to this simply as "surface gauge invariance".

To do this let us focus on gluon 1, and look at the scaffolding residue, $y_{1,3} \rightarrow 0$. Similarly to the tree-level example, the u 's that depend on $y_{1,3}$ are: $u_{1,J}$ and $u_{2,J}$, and then on top of these we have the tadpoles, $u_{1,1}$ and $u_{2,2}$, the loop variables, u_{Y_1} and u_{Y_2} , as well as $u_{2,1}$ which is the curve that goes around the puncture. However, since we set $X_{i,j} = X_{j,i}$, we have that $X_{2,1} = 0$ (corresponding to the massless scaffolded scalars) so $u_{2,1}$ does not appear in the integrand.

For the same reasons as we saw in the tree-level case, we have that:

$$\frac{\partial \log u_{1,j}}{\partial y_{1,3}} = -\frac{\partial \log u_{2,j}}{\partial y_{1,3}}, \quad (5.4)$$

and similarly for the loop variables:

$$\frac{\partial \log u_{Y_1}}{\partial y_{1,3}} = -\frac{\partial \log u_{Y_2}}{\partial y_{1,3}}. \quad (5.5)$$

So after taking the scaffolding residue in $X_{1,3}$, we get:

$$\begin{aligned} \text{Res}_{y_{1,3}=0} \Omega_{2n}^{\text{loop}}[X_{i,j}] &= \sum_J (X_{2,J} - X_{1,J}) \underbrace{\prod_{s \neq (1,3)} \frac{dy_s}{y_s^2} \prod_i \frac{dy_i}{y_i^2} \times \frac{\partial \log(u_{2J})}{\partial y_{1,3}} \prod_{(km) \neq (1J), (2J)} u_{km}^{X_{k,m}}[y]}_{\mathcal{Q}_J} \Big|_{y_{1,3}=0} \\ &+ (Y_2 - Y_1) \underbrace{\prod_{s \neq (1,3)} \frac{dy_s}{y_s^2} \prod_i \frac{dy_i}{y_i^2} \times \frac{\partial \log(u_{Y_2})}{\partial y_{1,3}} \prod_{(km) \neq Y_1, Y_2} u_{km}^{X_{k,m}}[y]}_{\mathcal{Q}_0} \Big|_{y_{1,3}=0} \\ &+ X_{1,1} \underbrace{\prod_{s \neq (1,3)} \frac{dy_s}{y_s^2} \prod_i \frac{dy_i}{y_i^2} \times \frac{\partial \log(u_{1,1})}{\partial y_{1,3}} \prod_{(km) \neq (11)} u_{km}^{X_{k,m}}[y]}_{\mathcal{Q}_{1,1}} \Big|_{y_{1,3}=0} \\ &+ X_{2,2} \underbrace{\prod_{s \neq (1,3)} \frac{dy_s}{y_s^2} \prod_i \frac{dy_i}{y_i^2} \times \frac{\partial \log(u_{2,2})}{\partial y_{1,3}} \prod_{(km) \neq (11)} u_{km}^{X_{k,m}}[y]}_{\mathcal{Q}_{2,2}} \Big|_{y_{1,3}=0}. \end{aligned} \quad (5.6)$$

Note the sum over J above includes all curves leaving out of roads (1,2) and (2,3); at loop level these include the roads going around punctures in all possible ways, so at 1-loop we have *e.g.* both $(X_{2,J} - X_{1,J})$ and $(X_{J,2} - X_{J,1})$ terms in the sum.

Usually, we set the tadpole variables, $X_{1,1}, X_{2,2}$ as well as massless external gluon bubbles $X_{3,1}$ to zero. However, from the surface perspective, there is nothing forcing us to set these variables to zero. This leads to the generalized notion of gauge invariance at the level of loop integrand, which takes the form of a particular expansion demanded for the residue giving the gluon amplitude:

$$\text{Res}_{y_{1,3}=0} \Omega_{2n}^{\text{loop}}[X_{i,j}] = \sum_J (X_{2,J} - X_{1,J}) \mathcal{Q}_J + (Y_2 - Y_1) \mathcal{Q}_0 + X_{1,1} \mathcal{Q}_{1,1} + X_{2,2} \mathcal{Q}_{2,2}, \quad (5.7)$$

where we have that \mathcal{Q}_J is independent of $X_{2,J}$ and \mathcal{Q}_0 is independent of Y_2 . Note importantly that $\mathcal{Q}_{1,1}, \mathcal{Q}_{2,2}$ **can** still depend on $X_{1,1}, X_{2,2}$, and indeed can (and do) have poles $1/X_{1,1}, 1/X_{2,2}$. This is the reflection of the familiar difficulty in defining non-supersymmetric Yang-Mills integrands where the tadpoles/massless external bubbles are set to zero by fiat, and this is also why we cannot simply set *e.g.* the $X_{i,i}$ variables to zero. But the expansion of equation 5.7 is completely well-defined, and our curve integral for gluons gives a well-defined integrand with its own notion of gauge invariance and multilinearity. Of

course this notion differs from what is standard in ordinary gauge theory, but the difference arises precisely from terms with tadpole/massless external gluon bubble poles, that multiply scale-less integrands integrating to zero. We will make further comments about this well-defined integrand after we see a concrete example below.

5.3 Example: 1-loop 2-point

In this section, we present the case of the 2-point 1-loop gluon amplitude. We obtain it by starting with a 4-scalar 1-loop process described by (5.3), taking the scaffolding residue, reducing us to the 2-point 1-loop stringy gluon integrand from which we ultimately extract the low-energy limit to obtain the field theory integrand.

We choose the underlying triangulation to be the bubble triangulation for the gluon problem, *i.e.* $\{X_{1,3}, X_{3,1}, Y_1, Y_3\}$, where $X_{1,3}$ and $X_{3,1}$ are the scaffolding chords and Y_1, Y_3 are the loop propagators of the gluon amplitude. Keeping only curves with self-intersection at most one as prescribed, we get that the stringy gluon integrand is:

$$\mathcal{A}_2^{\text{gluon}} = \int \frac{dy_1 dy_3}{y_1^2 y_3^2} \text{Res}_{y_{1,3}=y_{3,1}=0} \left(\frac{1}{y_{1,3}^2 y_{3,1}^2} u_{2,4}^{X_{2,4}} u_{4,2}^{X_{2,4}} \prod_{i=1,\dots,4} u_{i,i}^{X_{i,i}} u_{Y_i}^{Y_i} \times u_{\Delta}^{\Delta} \right. \\ \left. u_{2,4}^{\text{S.I. } X_{2,4}} u_{4,2}^{\text{S.I. } X_{4,2}} \prod_{i=1,\dots,4} u_{i,i}^{\text{S.I. } X_{i,i}} \right), \quad (5.8)$$

where we have set: $X_{i,j} = X_{j,i}$, $X_{i,i+1} = 0$ and $X_{1,3} = X_{3,1} = 0$. Now since we picked the triangulation corresponding to the bubble diagram for the gluon problem, containing chords $\{Y_1, Y_3\}$, the singularity corresponding to this diagram is located near $y_1, y_3 \rightarrow 0$. There are two other diagrams, corresponding to the tadpole diagrams with chords, $\{Y_1, X_{1,1}\}$ and $\{Y_3, X_{3,3}\}$, whose singularities are located in different boundaries of the integration domain. To extract the field theory limit of (5.8), we proceed as outlined in section 4.8, fully explained in [34], and extract the contribution to the integrand from each of these 3 regions. We find the following three contributions:

1. Cone $\{Y_1, Y_3\}$ – bubble diagram:

$$\frac{X_{1,1}X_{3,3} + X_{2,4}(X_{3,3} + X_{1,1}) + (1 + \Delta)(-Y_1Y_3 + Y_2Y_3 + Y_1Y_4 - Y_2Y_4) + \Delta X_{2,4}(Y_3 + Y_1)}{Y_1Y_3}. \quad (5.9)$$

2. Cone $\{Y_1, X_{1,1}\}$ – tadpole with Y_1 :

$$\frac{(1 + \Delta)(-2X_{1,1}X_{2,4} + X_{2,4}Y_1 - X_{1,1}Y_3 - X_{2,4}Y_3 + X_{1,1}Y_4)}{Y_1X_{1,1}}. \quad (5.10)$$

3. Cone $\{Y_3, X_{3,3}\}$ – tadpole with Y_3 :

$$\frac{(1 + \Delta)(-2X_{3,3}X_{2,4} - X_{2,4}Y_1 - X_{3,3}Y_1 - X_{3,3}Y_2 + X_{2,4}Y_3)}{Y_3X_{3,3}}. \quad (5.11)$$

The full field theory integrand is then given by the sum of these three pieces. We can as usual translate from our scalar description of the kinematics to standard presentations depending on dot products of momenta and polarization vectors if we like. The polarization vectors are still given by (3.21); we can make the gauge choice $\alpha = 1$ so that

$$\epsilon_i^\mu \propto -(X_{2i} - X_{2i-1})^\mu. \quad (5.12)$$

In addition, we have the freedom to choose the loop momentum so that $Y_1 = l^2$. Then the X, Y variables are expressed in terms of the usual Lorentz invariants as

$$Y_1 = l^2, \quad Y_2 = Y_1 - 2\epsilon_1 \cdot l, \quad Y_3 = l^2 + 2q_1 \cdot l, \quad Y_4 = Y_3 - 2\epsilon_2 \cdot l, \quad X_{2,4} = -2\epsilon_1 \cdot \epsilon_2. \quad (5.13)$$

Note that we do *not* put $X_{1,1}, X_{3,3} = 0$ at the level of the integrand; we will make further comments on this point in a moment. We obviously have similar expressions for higher points and loops, once we specify some choice for polarizations and loop momenta. Of course, the integrated result is independent of such choices, and post-integration we are also free to put tadpoles to zero.

5.3.1 Gauge Invariance check

In the previous section, we explained how this surface definition of the integrand gives us a generalized notion of gauge invariance for the loop integrand. Now that we have derived an explicit example of the one-loop two-point integrand we can check that the form predicted in (5.6) holds in this case.

Let us present the explicit check of this form for gluon 1 (the same holds for gluon 2 by cyclic invariance). According to (5.6), we should be able to write the integrand as: $\mathcal{A}_2^{\text{gluon}} = X_{2,4} \mathcal{Q}_{2,4} + (Y_2 - Y_1) \mathcal{Q}_{Y_2} + X_{1,1} \mathcal{Q}_{X_{1,1}}$, where $\mathcal{Q}_{2,4}$ and \mathcal{Q}_{Y_2} are independent of $X_{2,4}$ and Y_2 , respectively. Indeed one can explicitly check this is the case with

$$\begin{aligned} \mathcal{Q}_{2,4} &= \frac{(1 + \Delta)(-X_{1,1} + Y_1 - Y_3)}{Y_1 X_{1,1}} + \frac{X_{1,1} + X_{3,3} - Y_1 - Y_3}{Y_1 Y_3} + \frac{(1 + \Delta)(-X_{3,3} - Y_1 - Y_3)}{Y_3 X_{3,3}}, \\ \mathcal{Q}_{Y_2} &= \frac{(1 + \Delta)}{Y_3} + \frac{(1 + \Delta)(Y_3 - Y_4)}{Y_1 Y_3}, \\ \mathcal{Q}_{X_{1,1}} &= \frac{X_{3,3}}{Y_1 Y_3} - \frac{(1 + \Delta)(Y_3 - Y_4)}{X_{1,1} Y_1}. \end{aligned} \quad (5.14)$$

5.4 A well-defined Yang-Mills integrand

It is interesting to compare the integrand we have obtained in this way with the conventional Yang-Mills bubble integrand. Here we run into the familiar difficulty that we do not have a well-defined conventional Yang-Mills integrand, precisely due to the existence of the tadpole/massless external bubble terms and the infamous “1/0” problem associated with them, as well as massless external bubbles. We are usually instructed to throw out the tadpoles/massless external bubbles, on the grounds that they are “scale-less integrals that integrate to zero”, but clearly something nice about the integrand must be lost in doing so, and indeed it now fails to be gauge invariant.

By contrast, the bubble integrand we have just produced is perfectly well defined. We encounter the familiar $1/0$ difficulties if we were to set the tadpole $X_{1,1} \rightarrow 0$, but nothing forces us to do this, and at finite $X_{1,1}$ we have an object that is both well-defined and is consistent with its own internal-to-the-world-of-surfaces notion of gauge invariance. If we were to set $X_{1,1} \rightarrow 0$, we can only get singularities in terms with $1/X_{1,1}$ poles. These are of course precisely tadpole factorizations, and therefore must obviously multiply scale-less integrals that integrate to zero. So, we get to have our integrand cake and eat our amplitude too: we have a well-defined integrand at finite values of tadpole/massless external bubble variables, when these are set to zero as naively needed to match normal kinematics we do encounter divergences which are however guaranteed to be proportional to objects that integrate to zero.

We can also check that our integrand has the correct cuts to match field theory gluing. The most straightforward check is the usual unitarity double-cut. But it also has the correct single-cuts, which again needs a proper discussion of $X_{1,1} \neq 0$ for the “forward limit” term. We will discuss at length in our discussion of the loop-cut/forward limit connection, even at finite α' , in the penultimate section of this paper.

The elementary mechanism by which tadpoles/massless external bubbles are naturally dealt with suggests a recursive procedure for computing integrands for Yang-Mills theory [17] in any number of dimensions, in the planar limit where integrands are well-defined. We have computed integrands determined by this recursion through a number of one- and two-loop examples, which have passed all obvious consistency checks [17]. Optimistically an all-loop recursion for non-supersymmetric Yang-Mills theory in the planar limit may be at hand, as a counterpart to the very different recursion for planar $\mathcal{N} = 4$ SYM [38].

6 Leading Singularities

We have given an integral representation for scalar-scaffolded gluon scattering amplitudes. In principle, with a correct contour prescription for integrating over the y variables, we have a “curve integral” representation for these amplitudes. Just as for $\text{Tr } \phi^3$ theory, at loop level we can also integrate over the loop momenta as Gaussian integrals, to represent the integrated amplitudes as an integral over y space. We can also attempt to understand the field theory limit directly, which as we have indicated a number of times, is more interesting than the trivial tropicalization seen in $\text{Tr } \phi^3$ theory, due to the non-logarithmic character of the dy/y^2 measure.

We will take up both these lines of investigation in future works, defining the contour for the amplitude [27] as well as understanding a number of aspects of the field theory limit [34]. In this section we will instead content ourselves with performing the most basic but fundamental check that we are correctly describing gluon amplitudes at multi-loop level: we will show that our curve integral form correctly produces the leading singularities of gluon amplitudes in a number of non-trivial examples, from trees through to two loops.

Unlike the computation of the full amplitude/integrand, which needs care in defining the contour in y space, computing leading singularities is much simpler. We are interested in computing a leading singularity corresponding to gluing together three-particle ampli-

tudes according to any particular trivalent diagram. Now, if we choose the underlying triangulation of the surface to be dual to the diagram of the leading singularity, it is easy to see that the residue on the pole setting all the $X \rightarrow 0$ for the glued internal lines, is computed simply by setting all these X 's to zero in the y integrand and simply computing the **residue** of the integrand around all the $y \rightarrow 0$. Since the form is a dy/y^2 form, this residue ultimately gives us simply the part of the expansion of the product of the u_X^X for small y , that is linear in all the y 's, and so we need the expansion of each u_X around $y \rightarrow 0$ up to first order in all the y_i .

Note that leading singularities for the $\text{Tr } \phi^3$ theory are completely trivial—they are all equal to 1, since all we are doing in that case is taking residues of the dy/y form at $y = 0$ which sets the remaining $u \rightarrow 1$. This reflects the obvious fact that the $\text{Tr } \phi^3$ theory has only poles and no numerators. The leading singularities are (essentially by definition!) a clean probe of the “purely numerator” part of gluon amplitudes, and we see directly that this is associated with the dy/y^2 form. This already also alerts us to the possibility that curves with small self-intersection numbers can be important. Even though their u 's can never go to zero, expanding around 1 they can have terms first-order in y . It is intuitive that curves with higher self-intersection will begin with higher powers of y and so up to linear order we will only need curves with low self-intersection number. Indeed in a moment we will prove that curves with two or more self-intersections around a given puncture begin at quadratic order or higher in some y variable and hence never contribute to leading singularities. But we also see that curves with up to one self-intersection around each loop puncture will indeed be needed to correctly match leading singularities.

6.1 Linearized u 's

The computation of leading singularities needs an expansion for the u 's up to first order in the y 's. Quite beautifully, there is a direct expression for u_X to first order in the y 's that we can simply read off by looking at the pattern of intersections of the curve X and the base triangulation of the surface, which will greatly simplify our analysis. We are borrowing here from [18] where this and more general results will be explained and derived. Let us start by picking the underlying triangulation, corresponding to the leading singularity we are interested in. Now consider some curve, $X_{a,b}$, not in the triangulation, and its respective u variable, $u_{X_{a,b}}$ (see figure 24).

Let's denote by $\mathcal{I}_{a,b}$ the set of curves in the triangulation that $X_{a,b}$ intersects. Next, we look at each marked point a and b , and check whether there are triangulation chords ending on these points. Let us say that this is the case for point a , and list these chords together with chord $X_{a,b}$ and twist them clockwise to obtain the respective laminations. Then let us list all these chords in clockwise order: $\{X_{p_1}, \dots, X_{a,b}, X_{p^*}, \dots, X_{p_k}\}$ (see figure 24). We do the same for vertex b and we get a set $\{X_{q_1}, \dots, X_{a,b}, X_{q^*}, \dots, X_{q_l}\}$. Then the

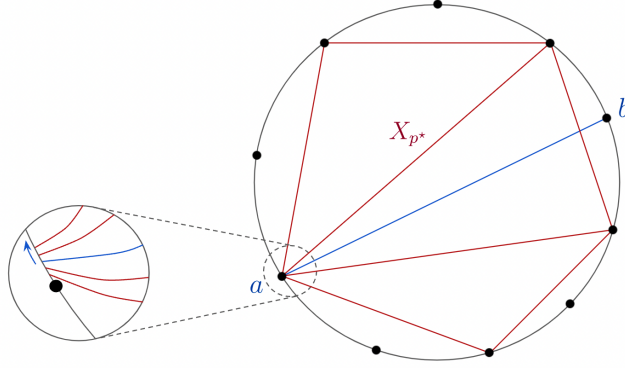


Figure 24: Linearized u 's.

linearized $u_{a,b}$ is:

$$\begin{aligned}
u_{a,b}^{X_{a,b}} = & 1 - X_{a,b} \left[\prod_{\mathcal{C} \in \mathcal{I}_{a,b}} y_{\mathcal{C}}^{\text{Int}[\{\mathcal{C}, X_{a,b}\}]} - \prod_{\mathcal{C} \in \mathcal{I}_{a,b}} y_{\mathcal{C}}^{\text{Int}[\{\mathcal{C}, X_{a,b}\}]} \left(y_{p^*} + y_{p^*} y_{p^*+1} + \cdots + y_{p^*} y_{p^*+1} \cdots y_{p_k} \right) \right. \\
& - \prod_{\mathcal{C} \in \mathcal{I}_{a,b}} y_{\mathcal{C}}^{\text{Int}[\{\mathcal{C}, X_{a,b}\}]} \left(y_{q^*} + y_{q^*} y_{q^*+1} + \cdots + y_{q^*} y_{q^*+1} \cdots y_{q_l} \right) \\
& \left. + \prod_{\mathcal{C} \in \mathcal{I}_{a,b}} y_{\mathcal{C}}^{\text{Int}[\{\mathcal{C}, X_{a,b}\}]} \left(y_{p^*} + y_{p^*} y_{p^*+1} + \cdots + y_{p^*} y_{p^*+1} \cdots y_{p_k} \right) \left(y_{q^*} + y_{q^*} y_{q^*+1} + \cdots + y_{q^*} y_{q^*+1} \cdots y_{q_l} \right) \right] \\
& + \mathcal{O}^2(y).
\end{aligned} \tag{6.1}$$

This makes manifest that any curve that intersects one of the triangulation chords more than once will **not** contribute to the leading singularity, as it will be automatically quadratic in that y . Thus as alluded to above, any curve that self-intersects twice or more going around any loop puncture will not contribute to leading singularities. But curves with up to one self-intersection per puncture can (and will) be relevant.

Let us now give a specific example for the case of a loop-level amplitude. We consider a 3-point 1-loop gluon amplitude, which is a 6-point 1-loop scalar amplitude. We are interested in the leading singularity in which one of the legs has a bubble (see figure 25), which corresponds to the triangulation of the punctured disk with chords $\{X_{1,3}, X_{3,5}, X_{5,1}, Y_1, Y_5\}$. Kinematically, $X_{1,5} = X_{5,1}$ but they are different curves on the surface, as we can see in figure 25. We want to find the linearized expression of u_{Y_3} in terms of $\{y_{1,3}, y_{3,5}, y_{5,1}, y_1, y_5\}$. As a chord, Y_3 only intersects $X_{1,5}$. However, as a lamination, on the side of marked point 3, it intersects $X_{3,5}$; while on the puncture end, it intersects first Y_1 and then Y_5 . Strictly speaking, as a lamination, Y_3 intersects Y_1 and Y_5 an infinite number of times, but since we are only interested in the expansion up to linear order, we can truncate it at intersection 1. This means that the linearized u_{Y_3} is simply:

$$(u_{Y_3})^{Y_3} = 1 - Y_3 [y_{1,5} - y_{1,5} y_{3,5} - y_{1,5} (y_1 + y_1 y_5) + y_{1,5} y_{3,5} (y_1 + y_1 y_5)]. \tag{6.2}$$

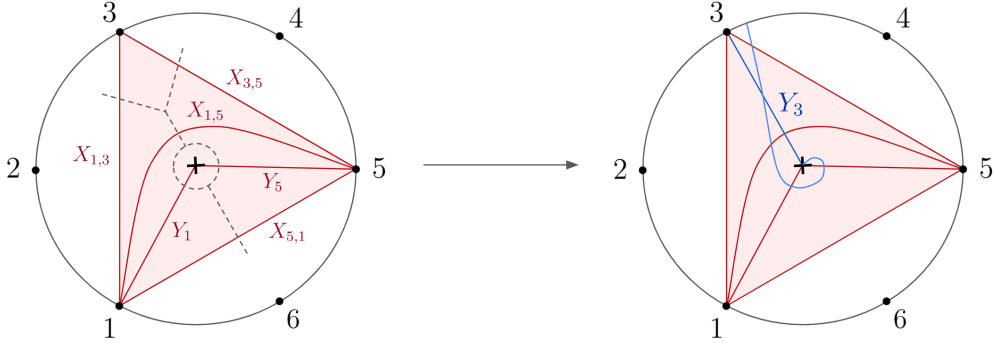


Figure 25: Bubble triangulation and curve for linearized u_{Y_3} .

6.2 Tree level

Let us study tree-level leading singularities in detail. It suffices to present explicit examples for 3- and 4-point cases, and the general rules for computing any tree-level leading singularities will become clear. The $n = 3$ case is trivial in that after scaffolding no more residues are needed thus the only leading singularity corresponds to the amplitudes obtained in 3.5. However, we still go through it to illustrate how the same result can be obtained from the linearized u 's discussed above. Recall that we simply take $2n = 6$ integral and take scaffolding residues in $\{X_{1,3}, X_{3,5}, X_{1,5}\}$ which already forms a triangulation. The linearized u 's we need are simply

$$u_{1,4}^{X_{1,4}} = 1 - X_{1,4}(y_{3,5} - y_{1,3}y_{3,5}), \quad (6.3)$$

$$u_{2,4}^{X_{2,4}} = 1 - X_{2,4} y_{1,3}y_{3,5}, \quad (6.4)$$

and their cyclic images $u_{2,5}, u_{3,6}$, and $u_{4,6}, u_{2,6}$ respectively. Note that for our purpose we have sent $X_{1,3}, X_{3,5}, X_{1,5} \rightarrow 0$ in these expressions. From here it is easy to read off the terms that are linear in all y 's at the leading α' order, which gives the 3-point Yang-Mills amplitude or leading singularity:

$$X_{1,4}X_{2,6} - X_{1,4}X_{2,5} + \text{cyclic}, \quad (6.5)$$

and of course in agreement with (3.27). In addition, there is one more term that contributes to the next order in α' , $-X_{1,4}X_{2,5}X_{3,6}$, which is exactly the F^3 amplitude or leading singularity.

Moving on to 4 points and we consider the “ s -channel” leading singularity given by the triangulation $\{X_{1,3}, X_{3,5}, X_{5,7}, X_{1,7}$ and $X_{1,5}\}$ (see first of figure 26). We need to take residue in corresponding y 's, which corresponds to taking the coefficient of $y_{1,3}y_{3,5}y_{5,7}y_{1,7}$ of $\prod u^X$. Again it is straightforward to obtain the linearized u 's from the rules above, for example (see figure 26):

$$u_{1,4}^{X_{1,4}} = 1 - X_{1,4}(y_{3,5} - y_{1,3}y_{3,5}), \quad (6.6)$$

$$u_{1,6}^{X_{1,6}} = 1 - X_{1,6}(y_{5,7} - y_{1,5}y_{5,7} - y_{1,3}y_{1,5}y_{5,7}), \quad (6.7)$$

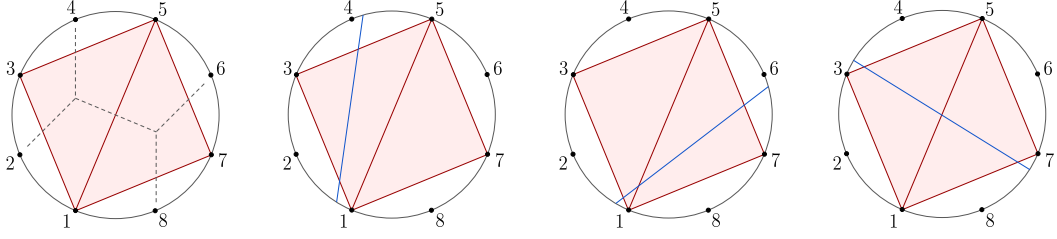


Figure 26: Dual diagram and linearized u 's for 4-point leading singularity.

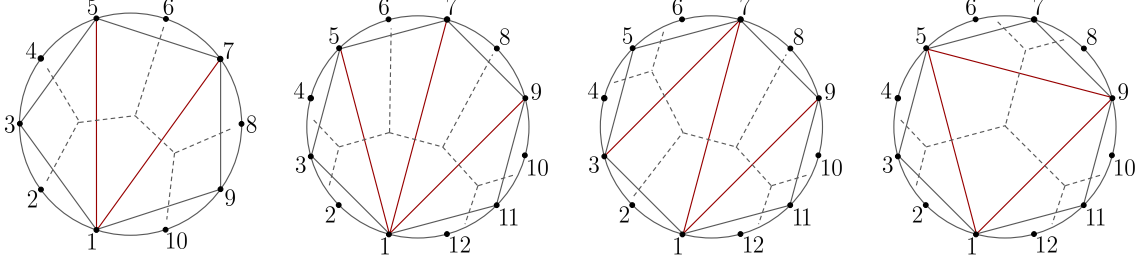


Figure 27: Dual diagrams for 5- and 6-point leading singularities.

$$u_{3,7}^{X_{3,7}} = 1 - X_{3,7}y_{1,5}(-1 + y_{1,7})(-1 + y_{3,5}). \quad (6.8)$$

Now the leading singularity obtained from the coefficient above contains three different orders, α'^k for $k = 3, 4, 5$, which correspond to gluing 2 three-point amplitudes with 0, 1 or 2 of them being F^3 vertices, respectively. The leading pure YM contribution reads

$$\begin{aligned} & c_{5,8} (X_{1,4} (X_{2,7} - X_{2,5}) + X_{2,5} X_{4,7}) - c_{1,4} (c_{5,8} X_{3,7} - X_{3,6} X_{5,8} + X_{1,6} (X_{5,8} - X_{3,8})) \\ & - X_{1,4} X_{1,6} (X_{2,8} - X_{5,8}) - X_{1,4} X_{2,6} X_{5,8} + X_{2,5} (X_{1,4} - X_{4,6}) X_{5,8} + X_{1,6} X_{2,5} (X_{1,4} - X_{4,8} + X_{5,8}), \end{aligned} \quad (6.9)$$

where we have kept the expression directly from the computation, which is written in terms of both c 's and X 's. The sub-leading contribution with one F^3 insertion reads

$$\begin{aligned} & X_{1,4} X_{1,6} X_{2,5} X_{3,8} + X_{1,4} X_{1,6} X_{2,7} X_{5,8} + X_{1,6} X_{2,4} X_{5,8} X_{3,7} \\ & - X_{1,4} X_{1,6} X_{2,5} X_{3,7} - X_{1,4} X_{1,6} X_{2,5} X_{5,8} - X_{1,4} X_{2,5} X_{5,8} X_{3,7} + (X_{i,j} \rightarrow X_{i+4,j+4}). \end{aligned} \quad (6.10)$$

Finally, the pure F^3 term is simply $-X_{1,4} X_{1,6} X_{2,5} X_{3,7} X_{5,8}$. Remarkably, the pure F^3 contribution contains only one term in both cases we have considered above. In fact, this is true for any pure F^3 leading singularity, or equivalently the highest α' order, to all loops! For now, let us discuss tree-level pure F^3 leading singularities for any triangulation to all n . According to (6.1), each X is multiplied with at least one y , thus the highest α' order is given by a single term, namely the product of all X 's (with a minus sign) that intersects only one of those initial X 's. For example, for $n = 5$ with scaffolding triangulation $\{X_{1,3}, X_{3,5}, \dots, X_{9,1}\}$ and inner triangulation $\{X_{1,5}, X_{1,7}\}$ (see the first graph in figure 27), the term with only F^3 vertices is

$$\text{LS}_{5;X_{15}=X_{17}=0}^{F^3} = -X_{1,4} X_{1,6} X_{1,8} X_{2,5} X_{3,7} X_{5,9} X_{7,10}. \quad (6.11)$$

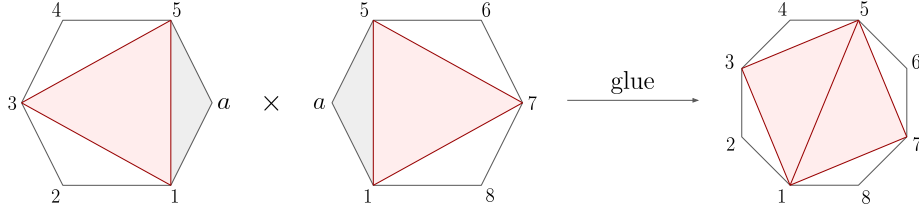


Figure 28: Gluing of 3-point amplitudes.

For $n = 6$ with inner triangulations $a = \{X_{1,5}, X_{1,7}, X_{1,9}\}$, $b = \{X_{3,7}, X_{1,7}, X_{1,9}\}$ and $c = \{X_{1,5}, X_{5,9}, X_{1,9}\}$ as presented in figure 27, the LS are

$$\begin{aligned}
\text{LS}_{6;a}^{F^3} &= -X_{1,4}X_{1,6}X_{1,8}X_{1,10}X_{2,5}X_{3,7}X_{5,9}X_{7,11}X_{9,12}, \\
\text{LS}_{6;b}^{F^3} &= -X_{1,5}X_{1,8}X_{1,10}X_{2,7}X_{3,6}X_{3,9}X_{4,7}X_{7,11}X_{9,12}, \\
\text{LS}_{6;c}^{F^3} &= -X_{1,4}X_{1,7}X_{1,10}X_{2,5}X_{3,9}X_{5,8}X_{5,11}X_{6,9}X_{9,12}.
\end{aligned} \tag{6.12}$$

In general, the highest-order contribution of any n -point LS is given by a product of $2n-3$ X 's, which is consistent with the fact that it is obtained from gluing $n-2$ F^3 vertices. For lower order terms, we replace $k = 1, 2, \dots, n-2$ of F^3 vertices by three-point Yang-Mills ones, which have mass dimension of X^{2n-3-k} , thus for the lowest order, *i.e.* pure YM LS, the mass dimension is the expected X^{n-1}). Since YM 3-point amplitude has more terms than F^3 , the number of terms grows for lower order terms.

Now it is a remarkable fact that any such $(2n-3)$ -fold residue, computed by extracting the coefficient of $\prod y$ in the expansion, agrees with gluing $n-2$ three-point amplitudes (which is the sum of both the YM and F^3 pieces) together! Of course, at tree-level this is guaranteed by the fact that the formula is computing n -gluon tree amplitude in the bosonic string which must contain all such LS. However, even without such a direct relation with bosonic string at loop level, as we will see shortly residues of loop-level stringy formulas continue to give correct loop-level LS!

Already at tree-level, these residues are compared with the actual leading singularities obtained from gluing three-point amplitudes using the factorization rule (4.35). For example, the four-point LS is given by the gluing of two three-point amplitudes, which is illustrated in figure 28.

$$\begin{aligned}
\text{LS}_L^{\text{YM}}(1, 2, 3, 4, 5, a) &= \sum_{j=2}^4 (X_{j,a} - X_{j,5}) Q_j^L = g_{2,a}(-X_{1,4}) + g_{3,a}(c_{1,4}) + g_{4,a}(-X_{2,5}), \\
\text{LS}_R^{\text{YM}}(a, 5, 6, 7, 8, 1) &= \sum_{J=6}^8 (X_{a,J} - X_{1,J}) Q_J^R = g_{a,6}(-X_{5,8}) + g_{a,7}(c_{5,8}) + g_{a,8}(-X_{1,6}),
\end{aligned} \tag{6.13}$$

where $\text{LS}_{L/R}^{\text{YM}}$ denotes three-point YM amplitude/LS on the left/right side, and $g_{j,a} = (X_{j,a} - X_{j,5})$, $g_{a,J} = (X_{a,J} - X_{1,J})$. The gluing rule directly formulated in X variables is given by the factorization (4.35):

$$\sum_{j,J} (X_{j,a} - X_{j,5}) Q_j^L (X_{a,J} - X_{1,J}) Q_J^R \rightarrow - \sum_{j,J} (X_{j,J} - X_{j,5} - X_{1,J}) Q_j^L Q_J^R, \tag{6.14}$$

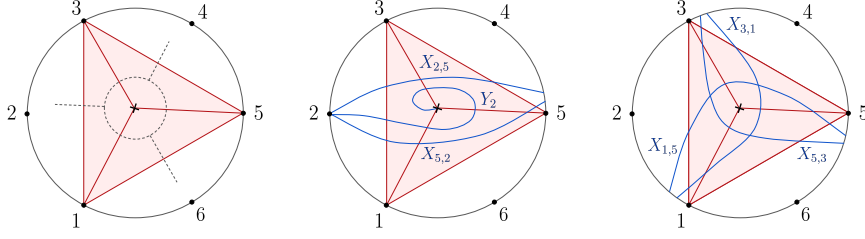


Figure 29: Dual diagram and linearized u 's for 1-loop triangle leading singularity.

which is equal to $g_{j,a}g_{a,J} \rightarrow g_{j,J} \equiv (X_{j,5} + X_{1,J} - X_{j,J})$.

$$\begin{aligned}
\text{LS}_4^{\text{YM}} &= \text{LS}_L^{\text{YM}}(1, \dots, 5, a) \otimes \text{LS}_R^{\text{YM}}(a, 5, \dots, 1) \\
&= g_{2,6}(X_{1,4}X_{5,8}) + g_{3,6}(-c_{1,4}X_{5,8}) + g_{4,6}(X_{2,5}X_{5,8}) \\
&\quad + g_{2,7}(-X_{1,4}c_{5,8}) + g_{3,7}(c_{1,4}c_{5,8}) + g_{4,7}(-X_{2,5}c_{5,8}) \\
&\quad + g_{2,8}(X_{1,4}X_{1,6}) + g_{3,8}(-c_{1,4}X_{1,6}) + g_{4,8}(X_{2,5}X_{1,6}),
\end{aligned} \tag{6.15}$$

where of course the gluing result LS_4^{YM} agrees with the residue (6.9), and \otimes denotes the gluing rule $g_{j,a}g_{a,J} \rightarrow g_{j,J}$.

Recall the 3-point F^3 amplitude obtained in section 3.5 (for both L and R):

$$\begin{aligned}
\text{LS}_L^{F^3}(1, 2, 3, 4, 5, a) &= g_{3,a}X_{1,4}X_{2,5}, \\
\text{LS}_R^{F^3}(a, 5, 6, 7, 8, 1) &= g_{a,7}X_{1,6}X_{5,8}.
\end{aligned} \tag{6.16}$$

We can glue F^3 amplitude with YM amplitude to give the 4-point LS $\text{LS}_4^{\text{YM}+F^3}$, and $\text{LS}_4^{F^3}$ with two F^3 vertices:

$$\begin{aligned}
\text{LS}_4^{\text{YM}+F^3} &= \text{LS}_L^{F^3}(1, \dots, 5, a) \otimes \text{LS}_R^{\text{YM}}(a, 5, \dots, 1) + \text{LS}_L^{\text{YM}}(1, \dots, 5, a) \otimes \text{LS}_R^{F^3}(a, 5, \dots, 1) \\
&= (g_{2,7}(-X_{1,4}) + g_{3,7}(c_{1,4}) + g_{4,7}(-X_{2,5}))X_{1,6}X_{5,8} \\
&\quad + (g_{3,6}(-X_{5,8}) + g_{3,7}(c_{5,8}) + g_{3,8}(-X_{1,6}))X_{1,4}X_{2,5},
\end{aligned}$$

$$\begin{aligned}
\text{LS}_4^{F^3} &= \text{LS}_L^{F^3}(1, \dots, 5, a) \otimes \text{LS}_R^{F^3}(a, 5, \dots, 1) \\
&= g_{3,7}X_{1,6}X_{5,8}X_{1,4}X_{2,5} = -X_{1,4}X_{1,6}X_{2,5}X_{3,7}X_{5,8}.
\end{aligned} \tag{6.17}$$

It is straightforward to see that the gluing of F^3 vertices is particularly simple, always giving one term for any n and agrees with the residue discussed above.

6.3 Loop level

Now we present examples at loop level. Starting with one-loop three-point triangle with triangulation $\{X_{1,3}, X_{3,5}, X_{5,1}, Y_1, Y_3, Y_5\}$, the linearized u 's are, for example, (see figure 29)

$$u_{2,5}^{X_{2,5}} = 1 - X_{2,5}y_{1,3}y_3(1 - y_{3,5}), \tag{6.18}$$

$$u_{5,2}^{X_{5,2}} = 1 - X_{5,2}y_{1,3}y_1(1 - y_5 - y_5y_{3,5}), \tag{6.19}$$

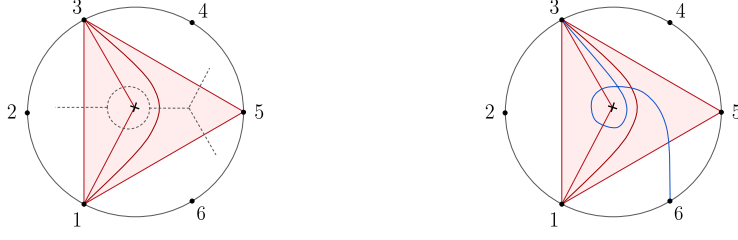


Figure 30: Dual diagram for 1-loop massless bubble and self-intersecting curve needed for the leading singularity computation.

$$(u_{Y_2})^{Y_2} = 1 - Y_2 y_{1,3} (1 - y_1 - y_1 y_5 - y_1 y_3 y_5). \quad (6.20)$$

The remaining u 's that give non-vanishing contribution are cyclic of (6.18)-(6.20) and the one corresponds to the closed curve:

$$(u_\Delta)^\Delta = 1 - \Delta y_1 y_3 y_5. \quad (6.21)$$

Then we can directly obtain the result:

$$-2Y_6 X_{1,4} X_{2,5} - 2Y_2 X_{1,4} X_{3,6} - 2Y_4 X_{2,5} X_{3,6} + 2X_{1,4} X_{2,5} X_{3,6} - (\Delta + 1) Y_2 Y_4 Y_6. \quad (6.22)$$

It is worth noting that the complete result for this case contains no contribution from the F^3 vertices. In fact, if we include the u 's corresponding to the curves $\{X_{3,1}, X_{5,3}, X_{1,5}\}$ (See right of figure 29), we can compute the F^3 term $Y_2 Y_4 Y_6 X_{3,1} X_{5,3} X_{1,5}$ but it vanishes since we have set $\{X_{3,1}, X_{5,3}, X_{1,5}\} \rightarrow 0$ (on-shell). Similarly, all the terms with at least one F^3 vertex vanish.

For the 3-point massless bubble, as depicted in figure 30 (left), it is crucial to include the curve with a single self-intersection (see figure 30, right), whose corresponding linearized u reads:

$$(u_{3,6}^{\text{S.I.}})^{X_{3,6}} = 1 - X_{3,6} y_1 y_3 y_1 y_3 y_5. \quad (6.23)$$

Then one can compute the result which contains contributions with zero and one F^3 vertex to be

$$(1 + \Delta) Y_2 (Y_5 X_{1,4} - Y_6 X_{1,4} - Y_4 X_{3,6} + Y_5 X_{3,6} - Y_5 X_{4,6} + X_{3,6} X_{1,4} + Y_5 X_{3,6} X_{1,4}). \quad (6.24)$$

Again curves with higher self-intersection are irrelevant as they begin at quadratic or higher order and don't contribute to the leading singularity.

For the 4-point box, the result already contains 434 terms which we present in appendix B, however, the highest α' order is again given by a single term:

$$Y_2 Y_4 Y_6 Y_8 X_{1,5}^2 X_{3,7}^2. \quad (6.25)$$

In fact, using the rule we have previously introduced, we can obtain directly the contribution with only F^3 vertices for the 5- and 6-point penta- and hexa-gon:

$$\begin{aligned} \underline{\text{Pentagon}} &: -Y_2 Y_4 Y_6 Y_8 Y_{10} X_{1,5} X_{1,7} X_{3,7} X_{3,9} X_{5,9}, \\ \underline{\text{Hexagon}} &: Y_2 Y_4 Y_6 Y_8 Y_{10} Y_{12} X_{1,5} X_{1,9} X_{3,7} X_{3,11} X_{5,9} X_{7,11}. \end{aligned} \quad (6.26)$$

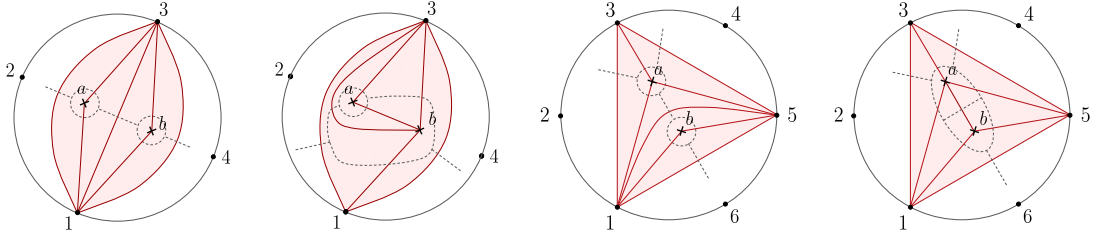


Figure 31: Dual diagrams of 2-loop 2- and 3-point leading singularities.

It is straightforward to generalize the computation to one-loop higher points, and in particular for n -gon LS, one can check that the result agrees with those written in terms of polarization and (external and loop) momenta [39].

Finally, let us present some examples for 2-loop 2- and 3-point. We attach the same Δ to all closed curves. For simplicity, we will focus on the leading a' order. Now for the gluing of two 1-loop 2-point bubble (first graph in figure 31), the result reads:

$$-(1 + \Delta)^2 Y_{a,2} Y_{b,4} Y_{a,b} + (a \leftrightarrow b), \quad (6.27)$$

where we have the second term since the integrand contains the contribution of the graph from symmetrization of loop punctures a, b . For the second graph in figure 31, the result is

$$2(1 + \Delta) X_{2,4} Y_{a,1}^2, \quad (6.28)$$

where the factor of 2 comes from the symmetrization ($1 \leftrightarrow 3, a \leftrightarrow b$) of the graph. For 3-point, the third graph reads:

$$(1 + \Delta) Y_{b,6} \left(-(1 + \Delta) Y_{a,2} Y_{a,4} Y_{a,b} + 2(X_{1,4} X_{2,5} Y_{b,3} - X_{1,4} X_{2,5} Y_{a,b} - X_{1,4} Y_{a,2} Y_{b,3} - X_{2,5} Y_{a,4} Y_{b,3}) \right), \quad (6.29)$$

and the final graph is:

$$Y_{b,3} \left(4X_{1,4} X_{2,5} Y_{a,6} - 4X_{1,4} Y_{a,2} Y_{a,6} - 4X_{2,5} Y_{a,4} Y_{a,6} - (1 + \Delta) Y_{b,6} (X_{1,4} Y_{a,2} + X_{2,5} Y_{a,4} - X_{1,4} Y_{b,2} + X_{1,4} Y_{b,3} - X_{2,4} Y_{b,3} + X_{2,5} Y_{b,3} - X_{2,5} Y_{b,4}) \right). \quad (6.30)$$

It is important to include the curves that can self-intersect up to once around either of the punctures. Of course the expression again matches what we get from explicit gluing.

7 Loop Cut and Matching with Tree-level Gluing

We finally turn to the most non-trivial check on our proposal. We will consider the residues of our curve integral at loop level, on a “single cut” setting a single loop propagator to zero. By consistency, this should match the “forward limit” of an amplitude with one loop lower. Now this match is usually fraught with subtlety in non-supersymmetric theories, due to the fact that both single-cuts and forward limits are naively infected with “1/0” divergences. But as we have already mentioned, the labeling of variables on surfaces gives

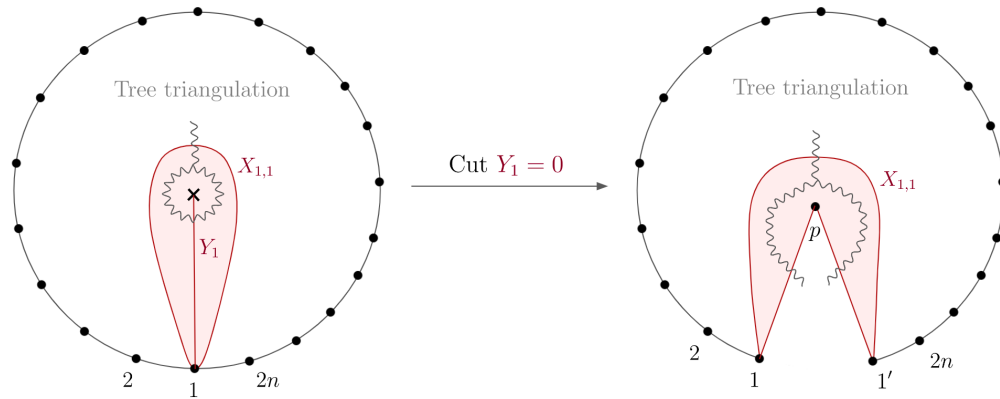


Figure 32: Tadpole Triangulation with Y_1 and $X_{1,1}$, and loop cut.

us a way out of this impasse, at least allowing a non-trivial comparison between “loop cut” and “forward limit” to be made.

In this section, we will focus on showing this connection at one loop. We will see that if we cut any loop propagator at one loop, it matches the tree-level amplitude in the forward limit, with the cut loop adding two color-adjacent particles, “glued” by summing over polarization states. This will hold not only in the field theory limit but even at finite α' .

We will do this by examining the single-cut and forward-limit integrands. We will see that due to a number of new properties of u variables we first encounter here—hardwired into their combinatorial definition—the two integrands beautifully match, up to a total derivative in the y variables.

While our proof of “loop-cut = forward limit” in this section is strictly valid at one loop, as we will see the character of the argument is quite “local” to the loop being cut, and one can expect the argument to be extendable to general surfaces.

Note also that correctly matching the single loop cut, together with our earlier proof of the correct “tree-like” factorization, automatically implies that all the leading singularities computed in the previous section must be correctly matched at one loop. An extension of the loop cut argument to all loop orders would similarly guarantee inter-alia the matching of all leading singularities, and the non-trivial matching of two-loop leading singularities in the previous section bolsters the belief that the loop-cut matching should work at all loops.

7.1 Set up

On the loop side, we will be considering a $2n$ -scalar 1-loop amplitude, from which we get the n -point 1-loop gluon amplitude. To define the corresponding surface, we will find it convenient to pick a particular “tadpole” triangulation, whose fat-graph includes the loop propagator Y_1 as well as the tadpole propagator $X_{1,1}$ (see figure 32). Taking the loop cut corresponds to extracting the residue when $Y_1 = 0$, which is easy to do in this triangulation

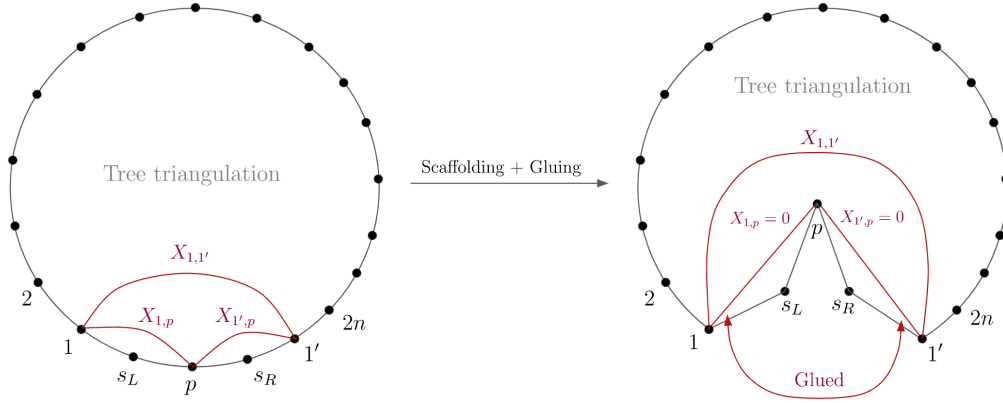


Figure 33: Tree triangulation and scaffolding residue.

since Y_1 is one of the chords in the triangulation. The resulting tree-level result corresponds to a $(2n+2)$ -point amplitude, with the two extra gluon legs glued. We call these extra two legs $1'$ and p (see figure 32). Regardless of $Y_1 = 0$ we still keep $X_{1,1}$ as the label of the curve on the cut surface.

To do the matching, we consider the tree-level amplitude of $2n+4$ scalars, where we label the particles as $(1, 2, \dots, 2n, 1', s_R, p, s_L)$ so that the matching with the loop computation becomes clearer. We make the gluons, $1'$ and p , on-shell by taking the scaffolding residue, $X_{1,p} = X_{1',p} = 0$. Therefore we pick a triangulation to define the surface that contains propagators $\{X_{1,p}, X_{1,p'}, X_{1,1'}\}$, the last propagator is chosen to replicate the triangulation picked in the loop cut part (see figure 33). The corresponding fat graphs associated with the 1-loop and tree-level triangulations are presented in figure 34.

7.2 Gluing in the forward limit

We will now describe the procedure for performing the polarization sum (“gluing”) for the two gluons in the forward limit opened up by cutting a loop. This will be a bit more interesting than the gluing we already encountered in our discussion of tree-level factorization, where we took two separate gauge-invariant objects $\mathcal{A}_L^\mu(p, \dots), \mathcal{A}_R^\nu(-p, \dots)$ and performed the polarization sum over the intermediate particle which finally yielded (thanks to the gauge-invariance of $\mathcal{A}_L, \mathcal{A}_R$) the trivial gluing rule $\mathcal{A}_L^\mu \mathcal{A}_R^\nu \eta_{\mu\nu}$. Now instead here we wish to start with a single n -point tree-level amplitude, and glue together two of its adjacent legs, say 1 and n . The polarization sum is:

$$\mathcal{A}_{\text{glued}} = \mathcal{A}_n^{\mu\nu} \left(-\eta_{\mu,\nu} + \frac{p_\mu q_\nu + p_\nu q_\mu}{p \cdot q} \right), \quad \text{with} \quad \mathcal{A}_n^{\mu\nu} = \partial_{\epsilon_{1,\mu}} \partial_{\epsilon_{n,\nu}} \mathcal{A}_n. \quad (7.1)$$

Now, there is a crucial difference with the tree-like gluing case. Gauge invariance does **not** imply that $\mathcal{A}_n^{\mu\nu} p_\mu$ vanishes, and in general for non-Abelian gauge theories we have

$$\mathcal{A}_n^{\mu\nu} p_\mu \neq 0. \quad (7.2)$$

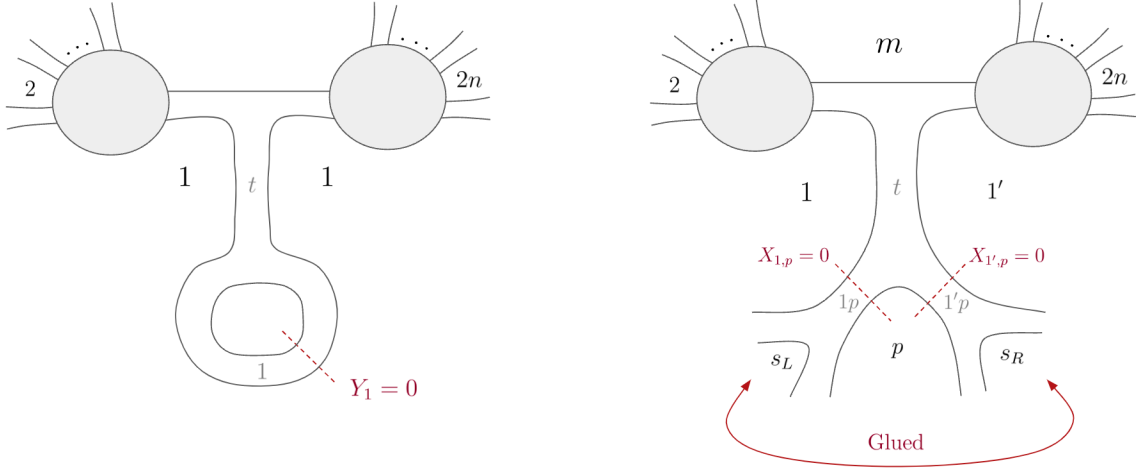


Figure 34: 1-loop fat graph (left) and tree-level fat graph (right).

This is famously related to the need to introduce ghost fields in the Lagrangian at loop level. However all is not lost, gauge invariance still constrains the form of this object, since we must have:

$$\mathcal{A}_n^{\mu\nu} p_\mu p_\nu = 0 \quad \Rightarrow \quad \mathcal{A}_n^{\mu\nu} p_\mu = \mathcal{N} p^\nu, \quad (7.3)$$

where \mathcal{N} is some function of the remaining kinematics and polarizations. Using this fact, the result after gluing can be written as:

$$\mathcal{A}_{\text{glued}} = \mathcal{A}_n^{\mu\nu} \left(-\eta_{\mu,\nu} + \frac{p_\mu q_\nu + p_\nu q_\mu}{p \cdot q} \right) = -\mathcal{A}_n^{\mu\nu} \eta_{\mu,\nu} + 2\mathcal{N}, \quad (7.4)$$

where the q^μ dependence dropped out again, as expected. Therefore, to perform the gluing in the forward limit, we need to determine \mathcal{N} .

Let us now rephrase some of these statements in scalar language using the $X_{i,j}$'s from the scaffolded gluon amplitude. Again, let us say we start with an n -point tree-level gluon amplitude, so $2n$ scalar amplitude, and we want to glue gluons 1 and n . Then the X 's associated with the polarizations of these gluons are, respectively, X_2^μ and X_{2n}^ν , so we have:

$$\mathcal{A}_n^{\mu\nu} = \frac{\partial^2 \mathcal{A}_n}{\partial X_2^\mu \partial X_{2n}^\nu}, \quad (7.5)$$

where \mathcal{A}_n stands for the amplitude obtained after taking the scaffolding residue in gluons 1 and n . Now, gauge invariance and multi-linearity in particles 1 and n , we know we can write:

$$\mathcal{A}_n = \sum_j (X_{2,j} - X_{1,j}) \mathcal{Q}_j^2 = \sum_j (X_{2n,j} - X_{1,j}) \mathcal{Q}_j^{2n}. \quad (7.6)$$

Now by linearity in the polarizations the \mathcal{Q}_j^2 cannot depend in $X_{2,k}$ for any k , and similarly for \mathcal{Q}_j^{2n} . Therefore we can rewrite (7.6) as:

$$\mathcal{A}_n = \sum_j (X_{2,j} - X_{1,j}) \frac{\partial \mathcal{A}_n}{\partial X_{2,j}} = \sum_j (X_{2n,j} - X_{1,j}) \frac{\partial \mathcal{A}_n}{\partial X_{2n,j}}. \quad (7.7)$$

Now plugging the second form of \mathcal{A}_n into the derivative with respect to $X_{2,j}$, we get:

$$\mathcal{A}_n = \sum_{j,k} (X_{2,j} - X_{1,j})(X_{2n,k} - X_{1,k}) \frac{\partial^2 \mathcal{A}_n}{\partial X_{2,j} \partial X_{2n,k}} + X_{2,2n} \frac{\partial \mathcal{A}_n}{\partial X_{2,2n}}. \quad (7.8)$$

From this expression we can read off $\mathcal{A}_n^{\mu\nu}$:

$$\mathcal{A}_n^{\mu\nu} = 4 \sum_{j,k} (X_2^\mu - X_j^\mu)(X_{2n}^\nu - X_k^\nu) \frac{\partial^2 \mathcal{A}_n}{\partial X_{2,j} \partial X_{2n,k}} - 2\eta^{\mu\nu} \frac{\partial \mathcal{A}_n}{\partial X_{2,2n}}. \quad (7.9)$$

Now doing a gauge transformation and a rescaling in gluon 2 and 2n, let us choose $X_2^\mu = X_1^\mu$ and $X_{2n}^\nu = X_1^\nu$. So we get the following representation of $\mathcal{A}_n^{\mu\nu}$:

$$\mathcal{A}_n^{\mu\nu} \propto 4 \sum_{j,k} (X_1^\mu - X_j^\mu)(X_1^\nu - X_k^\nu) \frac{\partial^2 \mathcal{A}_n}{\partial X_{2,j} \partial X_{2n,k}} - 2\eta^{\mu\nu} \frac{\partial \mathcal{A}_n}{\partial X_{2,2n}}. \quad (7.10)$$

Now this is a particularly nice representation because it is such that \mathcal{N} is zero:

$$\begin{aligned} \mathcal{A}_n^{\mu\nu} p_\mu &\propto \left[4 \sum_{j,k} (X_1^\mu - X_j^\mu)(X_1^\nu - X_k^\nu) \frac{\partial^2 \mathcal{A}_n}{\partial X_{2,j} \partial X_{2n,k}} - 2\eta^{\mu\nu} \frac{\partial \mathcal{A}_n}{\partial X_{2,2n}} \right] (X_3 - X_1)_\mu \\ &= 2 \sum_{j,k} (X_{3,j} - X_{1,j})(X_1^\nu - X_k^\nu) \frac{\partial^2 \mathcal{A}_n}{\partial X_{2,j} \partial X_{2n,k}} - 2(X_3^\nu - X_1^\nu) \frac{\partial \mathcal{A}_n}{\partial X_{2,2n}} \\ &= 2 \sum_k (X_1^\nu - X_k^\nu) \frac{\partial}{\partial X_{2n,k}} \left(\underbrace{\sum_j (X_{3,j} - X_{1,j}) \frac{\partial \mathcal{A}_n}{\partial X_{2,j}}}_{=0} \right) - 2(X_1^\nu - X_3^\nu) \frac{\partial \mathcal{A}_n}{\partial X_{2,2n}} \\ &\quad + 2(X_1^\nu - X_3^\nu) \frac{\partial \mathcal{A}_n}{\partial X_{2,2n}} \\ &= 0, \end{aligned} \quad (7.11)$$

where the sum over j vanishes because of gauge invariance. Therefore we found a representation of $\mathcal{A}_n^{\mu\nu}$ for which $\mathcal{N} = 0$, and so in which the gluing becomes simply:

$$\begin{aligned} \mathcal{A}_{\text{glued}} &\propto -\mathcal{A}_n^{\mu\nu} \eta_{\mu\nu} \propto 2 \sum_{j,k} (X_1^\mu - X_j^\mu)(X_{1\mu} - X_{k\mu}) \frac{\partial^2 \mathcal{A}_n}{\partial X_{2,j} \partial X_{2n,k}} - D \frac{\partial \mathcal{A}_n}{\partial X_{2,2n}} \\ &= \sum_{j,k} (X_{1,j} + X_{1,k} - X_{j,k}) \frac{\partial^2 \mathcal{A}_n}{\partial X_{2,j} \partial X_{2n,k}} - D \frac{\partial \mathcal{A}_n}{\partial X_{2,2n}}. \end{aligned} \quad (7.12)$$

This is finally our expression for gluing in the forward limit, written purely in terms of X variables.

Of course, this holds for gluing any gauge-invariant object in the forward limit, but we now turn to the specific representations we give for M in terms of integrals of forms of y variables, and translate this statement into a gluing rule for these forms. Let's start by defining the two forms we obtain by taking one scaffolding residue after the other:

$$\Omega_{s_{1,3}} = \text{Res}_{y_{1,3}=0} \Omega_{2n}^{\text{loop}}, \quad \Omega_S = \text{Res}_{y_{1,2n-1}=0} \Omega_{s_{1,3}}. \quad (7.13)$$

Then we have:

$$\begin{aligned}
\frac{\partial \mathcal{A}_n}{\partial X_{2,j}} &= \int \frac{\partial \Omega_S}{\partial X_{2,j}} = \int \text{Res}_{y_{1,2n-1}=0} \left(\frac{\partial \Omega_{s_{1,3}}}{\partial X_{2,j}} \right) \\
&= \int \text{Res}_{y_{1,2n-1}=0} \left(\prod_{s \neq (1,3)} \frac{dy_s}{y_s^2} \prod_i \frac{dy_i}{y_i^2} \times \frac{\partial \log(u_{2,j})}{\partial y_{1,3}} \prod_{(k,m) \neq \{(1,j), (2,j)\}} u_{k,m}^{X_{k,m}} [y] \Big|_{y_{1,3}=0} \right) \\
&= \int \prod_{\substack{s \neq \{(1,3), \\ (1,2n-1)\}}} \frac{dy_s}{y_s^2} \prod_i \frac{dy_i}{y_i^2} \left[\sum_k (X_{2n,k} - X_{2n-1,k}) \frac{\partial \log(u_{2,j})}{\partial y_{1,3}} \frac{\partial \log(u_{2n,k})}{\partial y_{1,2n-1}} \right. \\
&\quad \left. + \frac{\partial^2 \log(u_{2,2n})}{\partial y_{1,3} \partial y_{1,2n-1}} \right] \times \prod_{\substack{(k,m) \neq \{(1,j), (2,j), \\ (1,k), (2n-1,k)\}}} u_{k,m}^{X_{k,m}} [y] \Big|_{y_{1,3}=y_{1,2n-1}=0}, \tag{7.14}
\end{aligned}$$

which further taking a derivative on $X_{2n,k}$, gives

$$\begin{aligned}
\frac{\partial^2 \mathcal{A}_n}{\partial X_{2n,k} \partial X_{2,j}} &= \int \underbrace{\prod_{\substack{s \neq \{(1,3), \\ (1,2n-1)\}}} \frac{dy_s}{y_s^2} \prod_i \frac{dy_i}{y_i^2} \prod_{\substack{(k,m) \neq \{(1,j), (2,j), \\ (1,k), (2n-1,k)\}}} u_{k,m}^{X_{k,m}} [y]}_{(\tilde{\text{KN}})} \\
&\quad \times \left(\frac{\partial \log(u_{2,j})}{\partial y_{1,3}} \frac{\partial \log(u_{2n,k})}{\partial y_{1,2n-1}} \right) \Big|_{y_{1,3}=y_{1,2n-1}=0}, \tag{7.15}
\end{aligned}$$

so we can summarize the gluing rule as follows:

$$\mathcal{A}_{\text{Glued}} = \int \sum_{j,k} (X_{1,j} + X_{1,k} - X_{j,k}) \frac{\partial \log(u_{2,j})}{\partial y_{1,3}} \frac{\partial \log(u_{2n,k})}{\partial y_{1,2n-1}} \times (\tilde{\text{KN}}) - D \cdot \frac{\partial \Omega_S}{\partial X_{2,2n}}. \tag{7.16}$$

We finally translate this result using the variables of the loop-cut we want to compute, and find that the glued form is given by:

$$\begin{aligned}
\Omega_{\text{Glued}}^{2n} &= \prod_i \frac{dy_i}{y_i^2} \prod u_C^{X_C} \left[\sum_{\substack{j \in \{2, \dots, 1'\}, \\ k \in \{1, \dots, 2n\}}} (X_{p,j} + X_{p,k} - X_{j,k}) \frac{\partial \log u_{s_L,j}}{\partial y_{1,p}} \frac{\partial \log u_{s_R,k}}{\partial y_{1',p}} \right] \Big|_{y_{1,p}=y_{1',p}=0} \\
&\quad - D \cdot \frac{\partial \Omega_S}{\partial X_{s_L, s_R}}, \tag{7.17}
\end{aligned}$$

where y_i are now all remaining variables in the triangulation (other than the two scaffolding ones we extracted the residue) and C stands for the curves living in the smaller surface, obtained after taking the scaffolding residue. Ω_S is now the form resulting from taking both scaffolding residues that now correspond to $y_{1,p} = y_{1',p} = 0$.

Now it is particularly useful to reorganize this equation in the following way:

$$\begin{aligned}
\Omega_{\text{Glued}}^{2n} = & -D \cdot \underbrace{\frac{\partial \Omega_S}{\partial X_{s_L, s_R}}}_{(\dagger)} + \prod_i \frac{dy_i}{y_i^2} \prod u_C^{X_C} \left[\underbrace{- \sum_{j, k \in \{2, \dots, 2n\}} X_{j, k} \frac{\partial \log u_{s_L, j}}{\partial y_{1, p}} \frac{\partial \log u_{s_R, k}}{\partial y_{1', p}}}_{(\ddagger)} \right. \\
& + \underbrace{\sum_{j \in \{2, \dots, 2n\}} X_{p, j} \left(\frac{\partial \log u_{s_L, j}}{\partial y_{1, p}} \sum_{k \in \{1, \dots, 2n\}} \frac{\partial \log u_{s_R, k}}{\partial y_{1', p}} + \frac{\partial \log u_{s_R, j}}{\partial y_{1', p}} \sum_{k \in \{2, \dots, 1'\}} \frac{\partial \log u_{s_L, k}}{\partial y_{1, p}} \right)}_{(\ddagger\ddagger)} \\
& - \underbrace{\sum_{k \in \{2, \dots, 2n\}} X_{1', k} \left(\frac{\partial \log u_{s_L, 1'}}{\partial y_{1, p}} \frac{\partial \log u_{s_R, k}}{\partial y_{1', p}} + \frac{\partial \log u_{s_L, k}}{\partial y_{1, p}} \frac{\partial \log u_{s_R, 1'}}{\partial y_{1', p}} \right)}_{(\ddagger\ddagger\ddagger)} \\
& \left. - \underbrace{X_{1, 1'} \left(\frac{\partial \log u_{s_L, 1'}}{\partial y_{1, p}} \frac{\partial \log u_{s_R, 1'}}{\partial y_{1', p}} \right)}_{(\ddagger\ddagger\ddagger\ddagger)} \right] \Bigg|_{y_{1, p} = y_{1', p} = 0}, \tag{7.18}
\end{aligned}$$

where we are setting $X_{1, j} = X_{1', j}$. Our goal now is to show the different terms agree with the loop cut result, up to a possible total derivative. Let's look at what the loop-cut result looks like before proceeding.

7.3 Loop-cut

As explained before, in the loop integrand we include all the curves up to self-intersection one. So by taking the residue on Y_1 , we are effectively taking the residue of the integrand at $y_1 = 0$, which leads to:

$$\begin{aligned}
\text{Res}_{y_1=0} \Omega_{2n}^{\text{loop}} = & \prod_i \frac{dy_i}{y_i^2} \prod u_C^{X_C} \left[\sum_{j \in \{2, \dots, 2n\}} Y_j \frac{\partial \log u_{Y_j}}{\partial y_1} + \sum_{j < k \in \{2, \dots, 2n\}} X_{k, j} \frac{\partial \log u_{k, j}}{\partial y_1} \right. \\
& \left. + X_{1, 1} \frac{\partial \log u_{1, 1}}{\partial y_1} + \sum_{k \in \{2, \dots, 2n\}} X_{k, k} \frac{\partial \log u_{k, k}}{\partial y_1} - \Delta \right] \Bigg|_{y_{1, p} = y_{1', p} = 0}. \tag{7.19}
\end{aligned}$$

For the matching, we set $X_{k, k} = 0$ for all $k \neq 1$. So, using $\Delta = 1 - D$, we can rewrite

(7.19) as follows:

$$\begin{aligned}
\text{Res}_{y_1=0} \Omega_{2n}^{\text{loop}} = & D \cdot \underbrace{\prod_i \frac{dy_i}{y_i^2} \prod u_C^{X_C}}_{(*)} + \prod_i \frac{dy_i}{y_i^2} \prod u_C^{X_C} \left[\underbrace{\sum_{j < k \in \{2, \dots, 2n\}} X_{k,j} \left(\frac{\partial \log u_{j,k}^{S.I.}}{\partial y_1} + \frac{\partial \log u_{k,j}}{\partial y_1} \right)}_{(**)} \right. \\
& + \underbrace{\sum_{j \in \{2, \dots, 2n\}} Y_j \frac{\partial \log u_{Y_j}}{\partial y_1}}_{(***)} + \underbrace{\sum_{j \in \{3, \dots, 2n-1\}} X_{1,j} \left(\frac{\partial \log u_{j,1}}{\partial y_1} + \frac{\partial \log u_{1,j}^{S.I.}}{\partial y_1} + \frac{\partial \log u_{j,1}^{S.I.}}{\partial y_1} \right)}_{(****)} \\
& \left. + \underbrace{X_{1,1} \left(\frac{\partial \log u_{1,1}}{\partial y_1} + \frac{\partial \log u_{1,1}^{S.I.}}{\partial y_1} \right)}_{(*****)} - 1 \right] \Bigg|_{y_{1,p}=y_{1',p}=0}.
\end{aligned} \tag{7.20}$$

Now since $X_{k,j} = X_{j,k}$, from figures 32 and 33, we can see that these variables correspond to the ones present in (††) in the tree-level glue side. The only subtlety is that on the loop side, we have $X_{1,2n} = X_{1,2} = 0$ and these don't have to be zero on the tree side. However, setting these to zero on the tree side will not introduce any new poles, and therefore for the matching we set them to zero as well. In addition, from figures 32 and 33, we can also check that Y_j on the loop side maps to $X_{p,j}$ on the tree glue side. Finally, the choice of triangulation for the loop/tree problems makes it clear that $\prod_i \frac{dy_i}{y_i^2} \prod u_C^{X_C}$ is the same for both of them.

The approach we will follow is to analyze each term separately and understand whether they match directly or differ by a total derivative. The matching works quite intricately, and we devote the appendix C for more details, here we simply summarize the results.

Both (*) and (**) can be shown to match (†) and (††), respectively. The same is not true for the remaining three terms, however, the difference will be shown to be the following rather non-trivial total derivative:

$$-\frac{\partial}{\partial y_t} \left(\prod \frac{1}{y_i^2} \frac{\prod_{k \in \{1, \dots, m-1\}} u_{p,k} u_{1',k}}{u_{1,p} \prod_{j \in \{2, \dots, 2n\}} u_{p,j}^2} \prod_C u_C^{X_C} \right) \Bigg|_{y_{1,p}=y_{1',p}=0}. \tag{7.21}$$

It is very pleasing that the total derivative is with respect to the only variable we could possibly have “local” to the triangulation.

This establishes the consistency of our curve integral for scalar-scaffolded gluons, by showing that the loop-cut and the tree-level gluing agree up to a total derivative. We stress again that while this argument is strictly valid at 1-loop, its quite “local” character makes it likely that it can be extended to any number of loops.

8 Outlook

The first concrete example for reformulating the fundamental physics of scattering amplitudes in a new mathematical language, based on elementary but deep ideas in combinatorics and geometry, arose ten years ago in the content of the positive Grassmannian [11] and the amplituhedron [1] for planar $\mathcal{N} = 4$ SYM. The past decade has seen a succession of developments pushing away from this very special theory and closer to the physics of Yang-Mills theory in the real world [5, 7–9, 12, 13]. This program has been motivated by the belief that more magic—not less!—should reveal itself as we move from toy models towards describing the universe we actually live in.

We believe that with the results reported in this paper, we have entered a new phase in this adventure, in which combinatorial geometry in kinematic space is finally seen to directly describe major aspects of the world we see outside our windows. In one fell swoop, we have freed ourselves from the shackles of supersymmetry and integrability and “dlog forms”, along the way discovering a startling unity between non-supersymmetric gluons, pions, and the simplest theory of colored scalars.

As such there are a huge number of avenues for exploration, both in better understanding the conceptual origins and underpinnings of our proposal, as well as in seeking to propel us ever closer to describing all aspects of real-world physics from this new point of view. Instead of making a long list of these entirely obvious big questions, we close by mentioning a small number of directions of exploration immediately following from the developments here, which we hope to report on in the near future.

To begin with, we have left a number of important loose ends that need to be fully understood to precisely define our proposal at all orders in the topological expansion. We have emphasized that the dependence on dimensionality D arises through the product of the closed Δ curves wrapping around punctures, keeping one self-intersection per puncture. This is a perfectly well-defined proposal for the planar diagrams contributing to single-trace amplitudes, but starting with the torus corrections at two loops there are many kinds of closed Δ curves that can contribute, and the precise statement about the choice of Δ 's and exponents must be understood. Similarly, the precise statement about Δ 's for multi-trace amplitudes must be determined. We have checked that in the simplest case of 1-loop annulus corrections to double-trace amplitudes, where there is a unique closed Δ curve separating the two boundaries, the obvious choice of Δ with the same exponent $(1 - D)$ correctly matches leading singularities, so we expect a consistent choice is possible at all orders in the topological expansion. Also, our proof for the equality of the loop-cut and forward limit was strictly only for the one-loop cut \rightarrow tree-level forward limit. The character of the argument was however very “local” on the surface, and we expect that it can be extended to all orders— as supported by the successful checks of leading singularities at two loops— but it is important to establish this definitively.

Perhaps the most pressing question is learning how to effectively extract the low-energy, field-theory limit of the amplitudes from our stringy integrals. This is more challenging than the analogous problem for the $\text{Tr } \phi^3$ theory, where the dy/y singularity makes it easy to extract the low-energy limit of the amplitudes for $\alpha'X \ll 1$, localizing to logarithmic

divergences as $|\log y| \rightarrow \infty$. This can be easily computed by “tropicalizing” the u variables, giving a global Schwinger parametrization for the full amplitude directly in the field theory limit. This procedure does not work straightforwardly for our scaffolded gluons, where the dy/y^2 form has power-law divergences and the integral must be defined by analytic continuation, even at tree-level. In [34] we will report on an elementary and direct way of extracting the field theory limit, via a “cone-by-cone” analysis of the singular behavior of the integrand. This will already expose a number of surprising facts about gluon amplitudes. For instance, it will allow us to establish what we call the “mesh expansion” for tree amplitudes, in terms of interesting sums associated with *all* facets of the ABHY associahedron. Extremes of this expansion can be described very efficiently either by closed-form formulae at all multiplicity, or by novel “tropical” expressions. But we are still seeking an efficient “tropical” representation of the *full* gluon amplitudes, as a counterpart of the existing “tropical” formulae for $\text{Tr } \phi^3$ theory at all orders in the topological expansion.

We have emphasized that our surface picture for gluons provides a solution to a long-standing difficulty of making sense of “nice” integrands for non-supersymmetric Yang-Mills theories, by giving a natural way of treating the infamous “1/0” difficulties associated with tadpoles and massless external bubbles [16]. Quite apart from its conceptual importance especially at “stringy” level, the elementary mechanism by which tadpoles/massless external bubbles are naturally dealt with suggests a recursive procedure for computing integrands for Yang-Mills theory [17] in any number of dimensions, in the planar limit where integrands are well-defined. We have computed integrands determined by this recursion through a number of one- and two-loop examples, which have passed all obvious consistency checks [17]. Optimistically an all-loop recursion for non-supersymmetric Yang-Mills theory in the planar limit may be at hand, as a counterpart to the very different recursion based on BCFW recursion for planar $\mathcal{N} = 4$ SYM [38].

We have seen that the extremely simple and purely kinematical idea of thinking about particles with spin in the “scalar-scaffolding” language allows highly non-trivial hidden features of gluon amplitudes to be brought to light. As such it is clearly interesting to study more general spinning amplitudes in this language. Clearly tree-level gravity amplitudes can be described in exactly the same $2n$ scalar scaffolding language, with an obvious extension of the notions of multilinearity and gauge invariance. Their stringy integrands are again a single term, arising as usual from the mod-square of the scalar-scaffolded gluon integrand. Amplitudes for particles of any mass and spin, including the string resonances, can also be kinematically described using scalar scaffolding. The surprise for gluons is that the “dynamics” can be captured by a simple kinematic shift/monomial in the u variables. It would therefore be fascinating to look for an analog of our $(\prod u_{e,e}/\prod u_{o,o})$ factor that might describe the scattering of general string states.

Finally, while our new description for scalar-scaffolded gluons works in any number of dimensions, we know amplitudes in $D = 4$ spacetime dimensions are not only particularly important, but should have extra simplicity reflected in the Abelian nature of the little group and the natural decomposition of the amplitude into helicity sectors. In fact we expect the behavior of the amplitude *near* four dimensions to also be significant; for instance, it has long been appreciated that the enigmatic “rational terms” in loop amplitudes are

determined by “ ϵ/ϵ ” effects in dimensional regularization, and hence are sensitive to the behavior of the integrand close to four dimensions. There is a natural way to approach this physics, parametrizing the X kinematic data in $D = 4$ using momentum twistor variables and considering general perturbations $\epsilon\delta X$ as an expansion in ϵ .

This also gives a new avenue for trying to understand the lingering mystery of having an embarrassment of riches in describing the dynamics of gluons using combinatorial geometry. In four dimensions and with maximal supersymmetry, we have the story of the positive Grassmannian [11] and the amplituhedron [1], while now in general dimensions and with no supersymmetry, we have the scalar-scaffolded gluons arising from the combinatorics of surfaces. Obviously, in $D = 4$ these two stories must be connected. Perhaps the closest point where a technical connection can be made is at the level of leading singularities, where we have two different formulations as the residues of a master differential form, in the Grassmannian and the binary geometry of surfaces respectively. Of course, the two stories also differ crucially at the very outset, by the way they describe the scattering kinematics. In the positive Grassmannian and amplituhedron, the external data is labeled “one-particle at a time”, by specifying momentum(-twistor) variables for each particle, while in the scaffolding picture it is crucial that the data is specified in terms of variables X_{ij} encoding Lorentz-invariants labeled by *pairs* of points/particles. An understanding of the approach to $D = 4$ from the scalar-scaffolding story, encoding the kinematic data in momentum-twistor variables, should help bring the connection between these two fascinating worlds closer to light.

Acknowledgments

It is our pleasure to thank Hadleigh Frost, Sebastian Mizera, Pierre-Guy Plamondon, Giulio Salvatori, and Hugh Thomas for numerous inspiring discussions. The work of N.A.H. is supported by the DOE (Grant No. DE-SC0009988), by the Simons Collaboration on Celestial Holography, and further support was made possible by the Carl B. Feinberg cross-disciplinary program in innovation at the IAS. The work of C.F. is supported by FCT/Portugal (Grant No. 2023.01221.BD). The work of S.H. is supported in part by the National Natural Science Foundation of China under Grant No. 11935013, 12047503, 12247103, 12225510.

A Scaffolding residues using worldsheet variables of bosonic string

In sec. 4 we have given elegant and practical formulas for the n -gluon amplitudes obtained from scaffolding $2n$ -scalar amplitudes (which are special components of $2n$ -gluon amplitudes) in bosonic string theory; we have also shown a consistency check from $4n$ scalars to $2n$ gluons and then $2n$ scalars, which concludes the tree-level story.

However, we can also directly compute scaffolding residue of $2n$ -scalar amplitudes using worldsheet variables, which gives again the n -gluon correlator of bosonic-string integrand

as shown in (4.1). Our starting point is:

$$\mathcal{I}_{(12)\dots(2n-12n)} = \int \frac{d^{2n}z}{\text{SL}(2, \mathbb{R})} \frac{\prod_{i<j} z_{i,j}^{2p_i p_j}}{z_{12}^2 z_{34}^2 \dots z_{2n-1,2n}^2} = \int \frac{d^{2n}z}{\text{SL}(2, \mathbb{R})} \frac{\langle \prod_{a=1}^{2n} e^{ip_a \cdot X(z_a)} \rangle}{z_{12}^2 z_{34}^2 \dots z_{2n-1,2n}^2}, \quad (\text{A.1})$$

where we have rewritten the Koba-Nielsen factor in terms of the OPE of vertex operators.

It is important to make the special choice $\epsilon_i = p_{2i-1}$ (recall $q_i^\mu = p_{2i-1}^\mu + p_{2i}^\mu$): as we have discussed one can check that $\epsilon_a \cdot \epsilon_b \propto c_{2a-1,2b-1}$ in $W_{a,b}$, and for a given a , the collection of $\epsilon_a \cdot q_b$ for $b \neq a$ is equivalent to those $X_{2a,j} - X_{2a-1,j}$ for all j . Taking the scaffolding residues corresponds to taking the residues at $z_{i,i+1} = 0$ for odd i , in terms of the z variables. The residue $z_{12} = 0$ is given by taking the derivative of the vertex operator and setting $z_1 = z_2$:

$$\partial_{z_1} \left\langle \prod_{a=1}^{2n} e^{ip_a \cdot X(z_a)} \right\rangle \Big|_{z_1=z_2} = \left\langle ip_1 \cdot \partial_{z_2} X(z_2) e^{ip_1 \cdot X(z_2)} \prod_{a=3}^{2n} e^{ip_a \cdot X(z_a)} \right\rangle. \quad (\text{A.2})$$

Remember the special choice $\epsilon_a = p_{2a-1}$, and $q_a = p_{2a-1} + p_{2a} = p_{2a-1,2a}$, after scaffolding the $2n$ -scalar correlator becomes the n -gluon correlator

$$\left\langle \prod_{a=1}^n ip_{2a-1} \cdot \partial_{z_{2a}} X(z_{2a}) e^{ip_{2a-1,2a} \cdot X(z_{2a})} \right\rangle = \left\langle \prod_{a=1}^n i\epsilon_a \cdot \partial_{z_{2a}} X(z_{2a}) e^{iq_a \cdot X(z_{2a})} \right\rangle, \quad (\text{A.3})$$

with the relabelling the worldsheet coordinates $z_{2a} \rightarrow z_a$. Therefore, the $2n$ -scalar bosonic string amplitude becomes the n -gluon bosonic string amplitude by scaffolding:

$$\mathcal{I}_{(12)\dots(2n-12n)} \xrightarrow{\text{scaffolding}} \int \frac{\prod_{a=1}^n dz_a}{\text{vol SL}(2, \mathbb{R})} \left\langle \prod_{a=1}^n i\epsilon_a \cdot \partial_{z_a} X(z_a) e^{iq_a \cdot X(z_a)} \right\rangle. \quad (\text{A.4})$$

Having made connections with the more familiar worldsheet variables, we can also repeat such a derivation for closed-string and conclude that the n -graviton scattering amplitudes of bosonic string is again given by scaffolding residue of $2n$ -scalar amplitudes, which are “mod-square” closed-stringy integrals over “complex binary geometries” [10]. Obviously, such a “mod-square” $2n$ -scalar integral for closed-string is related to those for open-string via Kawai-Lewellen-Tye (KLT) relations [40]. In the field-theory limit, they become double copy relations [41] between gravity and gluon amplitudes, now written in this scalar-scaffolding language.

B Complete results for 1-loop 4-point box leading singularity

We present the complete result of 1-loop 4-point box leading singularity (with $Y_1 = Y_2 = Y_3 = Y_4 = 0$) which contains terms with mass dimension X^m for $m = 4, 5, 6, 7, 8$. These terms correspond to the pure Yang-Mills leading singularity and those with 1, 2, 3 and 4

insertions of F^3 vertices, respectively. The pure Yang-Mills leading singularity reads:

$$\begin{aligned}
& -\frac{(\Delta+1)}{4}Y_2Y_4Y_6Y_8 - 2Y_6Y_8X_{1,4}X_{2,5} + \frac{1}{4}X_{3,7}^2X_{1,5}^2 + \frac{1}{2}X_{2,7}X_{3,6}X_{1,5}^2 - X_{2,8}X_{3,6}X_{1,5}^2 - X_{2,7}X_{3,7}X_{1,5}^2 \\
& + X_{2,8}X_{3,7}X_{1,5}^2 + \frac{1}{2}X_{2,8}X_{4,6}X_{1,5}^2 - X_{1,6}X_{3,7}^2X_{1,5} + 2Y_6Y_8X_{2,4}X_{1,5} - Y_4Y_8X_{2,6}X_{1,5} + 2Y_4Y_8X_{2,7}X_{1,5} \\
& - Y_8X_{2,4}X_{3,6}X_{1,5} + Y_4X_{2,7}X_{3,6}X_{1,5} - X_{1,4}X_{2,7}X_{3,6}X_{1,5} - Y_4X_{2,8}X_{3,6}X_{1,5} + X_{1,4}X_{2,8}X_{3,6}X_{1,5} \\
& - Y_2Y_6X_{3,7}X_{1,5} + Y_6X_{2,4}X_{3,7}X_{1,5} + Y_8X_{2,4}X_{3,7}X_{1,5} - Y_4X_{2,6}X_{3,7}X_{1,5} + X_{1,4}X_{2,7}X_{3,7}X_{1,5} \\
& + X_{1,6}X_{2,7}X_{3,7}X_{1,5} - X_{1,4}X_{2,8}X_{3,7}X_{1,5} - X_{1,6}X_{2,8}X_{3,7}X_{1,5} + Y_4X_{2,6}X_{3,8}X_{1,5} - X_{2,5}X_{3,6}X_{3,8}X_{1,5} \\
& + X_{1,6}X_{3,7}X_{3,8}X_{1,5} + X_{1,4}X_{1,6}X_{3,7}^2 - X_{1,6}X_{2,4}X_{3,7}^2 + \frac{1}{2}X_{1,6}X_{2,5}X_{3,7}^2 + Y_4Y_8X_{1,6}X_{2,5} - 2Y_4Y_8X_{1,6}X_{2,7} \\
& + Y_8X_{1,4}X_{2,5}X_{3,6} + Y_4Y_8X_{2,7}X_{3,6} - Y_8X_{1,4}X_{2,7}X_{3,6} + 2Y_4Y_8X_{1,6}X_{3,7} - Y_8X_{1,6}X_{2,4}X_{3,7} \\
& - Y_6X_{1,4}X_{2,5}X_{3,7} - Y_8X_{1,4}X_{2,5}X_{3,7} + Y_4X_{1,6}X_{2,5}X_{3,7} - Y_4Y_8X_{2,6}X_{3,7} + Y_8X_{1,4}X_{2,6}X_{3,7} \\
& - X_{1,4}X_{1,6}X_{2,7}X_{3,7} - Y_4X_{1,6}X_{2,8}X_{3,7} + X_{1,4}X_{1,6}X_{2,8}X_{3,7} + Y_6X_{1,4}X_{2,5}X_{3,8} - Y_4X_{1,6}X_{2,5}X_{3,8} \\
& + X_{1,6}X_{2,4}X_{3,7}X_{3,8} - X_{1,6}X_{2,5}X_{3,7}X_{3,8} + \frac{1}{4}X_{1,6}X_{2,5}X_{3,8}X_{4,7} + \frac{1}{4}X_{1,4}X_{2,7}X_{3,6}X_{5,8} \\
& + (\text{cyclic}, i \rightarrow i+2, i+4, i+6),
\end{aligned} \tag{B.1}$$

which, by setting $\Delta = 1 - D$, agrees with the well-known D -dimensional result (*c.f.* [39]) once we translate it to polarizations and momenta.

Those with 1, 2 and 3 insertions of F^3 vertices are:

$$\begin{aligned}
& Y_2X_{3,7}^2X_{1,5}^2 - 2Y_4Y_6X_{2,7}X_{1,5}^2 + 2Y_4Y_6X_{2,8}X_{1,5}^2 + Y_4X_{2,7}X_{3,6}X_{1,5}^2 - Y_4X_{2,8}X_{3,6}X_{1,5}^2 + 2Y_4Y_6X_{3,7}X_{1,5}^2 \\
& - Y_4X_{2,7}X_{3,7}X_{1,5}^2 - Y_6X_{2,7}X_{3,7}X_{1,5}^2 - Y_8X_{2,7}X_{3,7}X_{1,5}^2 + Y_4X_{2,8}X_{3,7}X_{1,5}^2 + Y_6X_{2,8}X_{3,7}X_{1,5}^2 \\
& - Y_2X_{1,6}X_{3,7}^2X_{1,5} - Y_4X_{1,6}X_{3,7}^2X_{1,5} - Y_8X_{1,6}X_{3,7}^2X_{1,5} + 2Y_2Y_8X_{1,4}X_{3,6}X_{1,5} + Y_4Y_8X_{2,7}X_{3,6}X_{1,5} \\
& - Y_8X_{1,4}X_{2,7}X_{3,6}X_{1,5} - 2Y_2Y_8X_{1,4}X_{3,7}X_{1,5} - 2Y_2Y_8X_{1,6}X_{3,7}X_{1,5} + 2Y_6Y_8X_{2,4}X_{3,7}X_{1,5} \\
& - Y_4Y_8X_{2,6}X_{3,7}X_{1,5} + Y_6X_{1,4}X_{2,7}X_{3,7}X_{1,5} + Y_8X_{1,4}X_{2,7}X_{3,7}X_{1,5} + Y_4X_{1,6}X_{2,7}X_{3,7}X_{1,5} \\
& + Y_8X_{1,6}X_{2,7}X_{3,7}X_{1,5} - Y_6X_{1,4}X_{2,8}X_{3,7}X_{1,5} - Y_4X_{1,6}X_{2,8}X_{3,7}X_{1,5} + 2Y_4Y_6X_{2,5}X_{3,8}X_{1,5} \\
& - Y_4X_{2,5}X_{3,6}X_{3,8}X_{1,5} + Y_2X_{1,6}X_{3,7}X_{3,8}X_{1,5} + Y_4X_{1,6}X_{3,7}X_{3,8}X_{1,5} - 2Y_2Y_4X_{1,6}X_{3,7}^2 \\
& + Y_8X_{1,4}X_{1,6}X_{3,7}^2 - Y_8X_{1,6}X_{2,4}X_{3,7}^2 + Y_4X_{1,6}X_{2,5}X_{3,7}^2 + 2Y_2Y_8X_{1,4}X_{1,6}X_{3,7} + Y_2X_{1,4}X_{1,6}X_{3,7}^2 \\
& - 2Y_6Y_8X_{1,4}X_{2,5}X_{3,7} + Y_4Y_8X_{1,6}X_{2,5}X_{3,7} - Y_8X_{1,4}X_{1,6}X_{2,7}X_{3,7} - Y_4X_{1,6}X_{2,5}X_{3,7}X_{3,8} \\
& + (\text{cyclic}, i \rightarrow i+2, i+4, i+6);
\end{aligned} \tag{B.2}$$

$$\begin{aligned}
& Y_2 Y_4 X_{3,7}^2 X_{1,5}^2 + 2Y_2 Y_4 Y_6 Y_8 X_{1,5}^2 - 2Y_4 Y_6 Y_8 X_{2,7} X_{1,5}^2 + Y_2 Y_4 Y_6 Y_8 X_{3,7} X_{1,5} \\
& + 2Y_2 Y_4 Y_6 X_{3,7} X_{1,5}^2 + 2Y_2 Y_4 Y_8 X_{3,7} X_{1,5}^2 - Y_4 Y_6 X_{2,7} X_{3,7} X_{1,5}^2 - Y_4 Y_8 X_{2,7} X_{3,7} X_{1,5}^2 \\
& + Y_4 Y_6 X_{2,8} X_{3,7} X_{1,5}^2 - Y_2 Y_4 X_{1,6} X_{3,7}^2 X_{1,5} - Y_2 Y_8 X_{1,6} X_{3,7}^2 X_{1,5} - Y_4 Y_8 X_{1,6} X_{3,7}^2 X_{1,5} \\
& - 2Y_2 Y_6 Y_8 X_{1,4} X_{3,7} X_{1,5} - 2Y_2 Y_4 Y_8 X_{1,6} X_{3,7} X_{1,5} + Y_6 Y_8 X_{1,4} X_{2,7} X_{3,7} X_{1,5} \\
& + Y_2 Y_4 X_{1,6} X_{3,7} X_{3,8} X_{1,5} - 2Y_2 Y_4 Y_8 X_{1,6} X_{3,7}^2 + Y_2 Y_8 X_{1,4} X_{1,6} X_{3,7}^2 - Y_6 Y_8 X_{2,7} X_{3,7} X_{1,5}^2 \\
& + \frac{1}{2} Y_4 Y_8 X_{2,7} X_{3,6} X_{1,5}^2 + \frac{1}{2} Y_4 Y_8 X_{1,6} X_{2,5} X_{3,7}^2 + \frac{1}{2} Y_2 Y_6 X_{3,7}^2 X_{1,5}^2 \\
& + Y_4 Y_8 X_{1,6} X_{2,7} X_{3,7} X_{1,5} + (\text{cyclic}, i \rightarrow i+2, i+4, i+6);
\end{aligned} \tag{B.3}$$

$$\begin{aligned}
& Y_2 Y_4 Y_6 X_{3,7}^2 X_{1,5}^2 + 2Y_2 Y_4 Y_6 Y_8 X_{3,7} X_{1,5}^2 - Y_4 Y_6 Y_8 X_{2,7} X_{3,7} X_{1,5}^2 \\
& - Y_2 Y_4 Y_8 X_{1,6} X_{3,7}^2 X_{1,5} + (\text{cyclic}, i \rightarrow i+2, i+4, i+6).
\end{aligned} \tag{B.4}$$

Finally, the one term with 4 F^3 vertices reads:

$$Y_2 Y_4 Y_6 Y_8 X_{1,5}^2 X_{3,7}^2. \tag{B.5}$$

C Matching of the loop-cut with gluing of tree in the forward limit

In this appendix, we show the highly non-trivial matching of the loop-cut and the gluing of tree amplitude. We separate the matching of each term into different parts, and in the end, we show the difference is actually a total derivative.

C.1 Matching of the D -dependent part

We will start by showing that $(\dagger)=(*)$, *i.e.* that the D -dependent part of both answers agree.

To do this, we look at the tree-level side and understand how we can write $\partial_{X_{s_L, s_R}} \mathcal{A}$, in terms of u 's. After taking the scaffolding residue on s_L , we know we can write the answer as:

$$\begin{aligned}
\text{Res}_{y_{1,p}=0} \mathcal{A} &= \prod_i \frac{dy_i}{y_i^2} \sum_j (X_{s_L, j} - X_{p, j}) \frac{\partial \log(u_{s_L, j})}{\partial y_{1,p}} \times \prod_X u_X^X \Big|_{y_{1,p}=0} \\
&= \prod_i \frac{dy_i}{y_i^2} \sum_j (X_{s_L, j} - X_{p, j}) \frac{\partial u_{s_L, j}}{\partial y_{1,p}} \times \prod_X u_X^X \Big|_{y_{1,p}=0},
\end{aligned} \tag{C.1}$$

where in the last line we used the fact that $u_{s_L, j} \rightarrow 1$ when $y_{1,p} = 0$, which follows directly from the u -equations. Therefore, the part proportional to X_{s_L, s_R} after taking the residue in $y_{1', p}$, is simply:

$$\text{Res}_{y_{1', p}=0} (\text{Res}_{y_{1,p}=0} \mathcal{A}) = \prod_i \frac{dy_i}{y_i^2} \left(X_{s_L, s_R} \frac{\partial^2 u_{s_L, s_R}}{\partial y_{1', p} \partial y_{1,p}} \times \prod_X u_X^X \Big|_{y_{1,p}=y_{1', p}=0} + \dots \right). \tag{C.2}$$

Now using the word for curve X_{s_L, s_R} , we can write u_{s_L, s_R} in terms of $y_{1,p}$ and $y_{1', p}$:

$$u_{s_L, s_R} = \frac{1 + y_{1', p}}{1 + y_{1', p} + y_{1', p} y_{1,p}} \Rightarrow \frac{\partial^2 u_{s_L, s_R}}{\partial y_{1', p} \partial y_{1,p}} \Big|_{y_{1,p}=y_{1', p}=0} = -1. \tag{C.3}$$

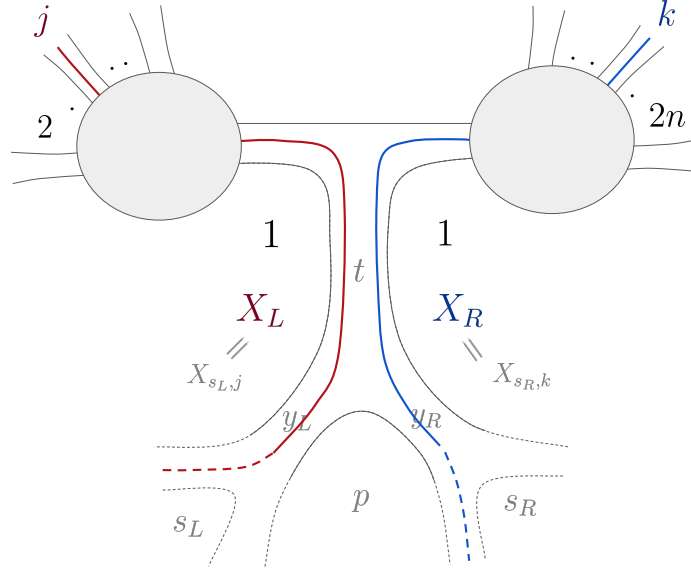


Figure 35: Curve $X_{k,j}$ after loop cut, and corresponding extension to the scaffolded surface (dashed).

Therefore we have:

$$-D \cdot \frac{\partial \mathcal{A}}{\partial X_{s_L, s_R}} = D \cdot \prod_i \frac{dy_i}{y_i^2} \prod_X u_X^X \Big|_{y_{1,p}=y_{1',p}=0}, \quad (\text{C.4})$$

which is exactly what we get on the loop-cut side. So indeed we have $(\dagger)=(*)$, and the D-dependent parts agree without any need for total derivative identities.

C.2 Matching of variables of tree triangulation

Let's proceed to the matching of $(\dagger\dagger)$ with $(**)$, *i.e.* the parts proportional to $X_{j,k}$. Let's start by looking at the loop-side. In this case, we have contributions from two curves, $X_{k,j}$ intersecting Y_1 and $X_{j,k}$ that self-intersects once. Let's now understand how we can write the derivatives $\partial_{y_1} \log u_{k,j}$ in terms of the u 's of the cut surface. Let's start by looking at $u_{k,j}$, using the matrix method to get this u -variable we have:

$$\begin{aligned} \underline{kj}: \quad M_1 M_R(y_1) M_2 &= \begin{bmatrix} x & y \\ z & w \end{bmatrix} \begin{bmatrix} y_1 & 0 \\ 1 & 1 \end{bmatrix} \begin{bmatrix} a & b \\ c & d \end{bmatrix} = \begin{bmatrix} cy + a(y + xy_1) & dy + b(y + xy_1) \\ cw + a(w + zy_1) & dw + b(w + zy_1) \end{bmatrix}. \\ \Rightarrow u_{k,j} &= \frac{(by + dy + bxy_1)(aw + cw + ay_1z)}{(ay + cy + axy_1)(bw + dw + by_1z)} \Rightarrow \frac{\partial \log u_{k,j}}{\partial y_1} \Big|_{y_1=0} = \frac{(bc - ad)(wx - yz)}{(a + c)(b + d)wy}, \end{aligned} \quad (\text{C.5})$$

where M_1 and M_2 are the matrices corresponding to the word to the left/right of y_1 , respectively. After cutting the loop surface, this curve breaks into two, one on the left and

one on the right, that we call X_L and X_R (see figure 35). Now we consider their extensions into the scaffolded surface which turns them into curves that are defined on the tree-level side (represented in dashed in figure 35). This way of extending X_R and X_L is exactly such that the corresponding u 's are

$$\begin{aligned}
\underline{u_{X_L}}: \quad M_1 M_R(y_L) &= \begin{bmatrix} y + xy_L & y \\ w + zy_L & w \end{bmatrix} \\
\Rightarrow u_{X_L} &= \frac{y(w + y_L z)}{w(y + xy_L)} \Rightarrow \left. \frac{\partial \log u_{X_L}}{\partial y_L} \right|_{y_L=0} = -\frac{(wx - yz)}{(wy)}. \\
\underline{u_{X_R}}: \quad M_L(1) M_R(y_R) M_2 &= \begin{bmatrix} c + a(1 + y_R) & d + b(1 + y_R) \\ a + c & b + d \end{bmatrix} \\
\Rightarrow u_{X_R} &= \frac{(a + c)(b + d + by_R)}{(b + d)(a + c + ay_R)} \Rightarrow \left. \frac{\partial \log u_{X_R}}{\partial y_R} \right|_{y_R=0} = \frac{(bc - ad)}{(a + c)(b + d)}.
\end{aligned} \tag{C.6}$$

Therefore we have:

$$\left. \frac{\partial \log u_{k,j}}{\partial y_1} \right|_{y_1=0} = - \left. \frac{\partial \log u_{X_R}}{\partial y_R} \right|_{y_R=0} \times \left. \frac{\partial \log u_{X_L}}{\partial y_L} \right|_{y_L=0}, \tag{C.7}$$

from figure 35, we can read off directly the extensions in the scaffolded problem, which gives us exactly the tree-level result:

$$\left. \frac{\partial \log u_{k,j}}{\partial y_1} \right|_{y_1=0} = - \frac{\partial \log u_{s_L,j}}{\partial y_{1,p}} \frac{\partial \log u_{s_R,k}}{\partial y_{1',p}}. \tag{C.8}$$

Proceeding exactly in the same way for the self-intersecting curve, we find:

$$\left. \frac{\partial \log u_{k,j}^{SI}}{\partial y_1} \right|_{y_1=0} = - \frac{\partial \log u_{s_L,k}}{\partial y_{1,p}} \frac{\partial \log u_{s_R,j}}{\partial y_{1',p}}. \tag{C.9}$$

C.3 Matching of loop variables

We now want to relate $(\dagger\dagger\dagger)$ with $(\star\star\star)$, *i.e.* the parts proportional to $X_{p,j}/Y_j$ in the tree and loop answers, respectively. In this case, it turns out that these two factors will not match at integrand level, but we will show that they differ by a total derivative.

Let's start by looking at the tree-level glue term $(\dagger\dagger\dagger)$, in particular to the piece proportional to $X_{p,J}$ with $J \in \{2, \dots, 2n\}$:

$$X_{p,J} \left(\underbrace{\frac{\partial \log u_{s_L,J}}{\partial y_{1,p}} \sum_{k \in \{1, \dots, 2n\}} \frac{\partial \log u_{s_R,k}}{\partial y_{1',p}}}_{(1)} + \underbrace{\frac{\partial \log u_{s_R,J}}{\partial y_{1',p}} \sum_{k \in \{2, \dots, 1'\}} \frac{\partial \log u_{s_L,k}}{\partial y_{1,p}}}_{(2)} \right) \Big|_{y_{1,p}=y_{1',p}=0}. \tag{C.10}$$

Let's start by analyzing term **(1)**:

$$X_{p,J} \frac{\partial \log u_{s_L,J}}{\partial y_{1,p}} \sum_{k \in \{1, \dots, 2n\}} \frac{\partial \log u_{s_R,k}}{\partial y_{1',p}} \Big|_{y_{1,p}=y_{1',p}=0} = X_{p,J} \frac{\partial \log u_{s_L,J}}{\partial y_{1,p}} \times \frac{\partial \log \left(\prod_{k \in \{1, \dots, 2n\}} u_{s_R,k} \right)}{\partial y_{1',p}} \Big|_{y_{1,p}=y_{1',p}=0}. \quad (\text{C.11})$$

Now inside the second logarithm we have the product of all the u -variables corresponding to curves that start somewhere on the tree part and eventually end in the following path: from t to $1'p$ and exit in road p, s_R . This means that this product is effectively the u -variable of the curve of the smaller surface obtained by cutting through road $t, U_{s_R,t}$, that goes from road p, s_R to road t . In particular, this means that this product is **independent** of y_t . Now the u -variable for this curve on this smaller surface is really simple:

$$\prod_{k \in \{1, \dots, 2n\}} u_{s_R,k} \equiv U_{s_R,t} = \frac{1}{(1 + y_{1',p})} \Rightarrow \frac{\partial \log \left(\prod_{k \in \{1, \dots, 2n\}} u_{s_R,k} \right)}{\partial y_{1',p}} \Big|_{y_{1,p}=y_{1',p}=0} = -1. \quad (\text{C.12})$$

So we can rewrite **(C.10)** as follows:

$$X_{p,J} \left(\underbrace{-\frac{\partial \log u_{s_L,J}}{\partial y_{1,p}}}_{(1)} + \underbrace{\frac{\partial \log u_{s_R,J}}{\partial y_{1',p}} \sum_{k \in \{2, \dots, 1'\}} \frac{\partial \log u_{s_L,k}}{\partial y_{1,p}}}_{(2)} \right) \Big|_{y_{1,p}=y_{1',p}=0}. \quad (\text{C.13})$$

Before looking at term **(2)**, let's look at what we have on the loop-side. From **(7.20)**, we have that the term in **(*)** proportional to Y_J is:

$$Y_J \frac{\partial \log u_{Y_J}}{\partial y_1} \Big|_{y_1=0}. \quad (\text{C.14})$$

Since Y_J does not intersect Y_1 , we can't use the u -equations to compute this derivative. Instead, we consider all curves that, just like Y_J , enter the fat graph in $J, J+1$ and go until road 1, and from there continue to anywhere. Let's denote this set of curves by \mathcal{C} . This is of course an infinite family of curves since they can self-intersect infinitely often. Now, exactly for the same reason as before, have that:

$$\partial_{y_1} \left(u_{Y_J} \times \prod_{X \in \mathcal{C}} u_X \right) = 0 \Rightarrow \partial_{y_1} \log u_{Y_J} = -\partial_{y_1} \sum_{X \in \mathcal{C}} \log u_X. \quad (\text{C.15})$$

Now since we want to evaluate the derivative at $y_1 = 0$, the contribution coming from $X \in \mathcal{C}$ that intersects Y_1 more than once is zero. Therefore we have:

$$\partial_{y_1} \log u_{Y_J} \Big|_{y_1=0} = -\partial_{y_1} \log \prod_{k \in \{1, \dots, 2n\}} u_{J,k} \Big|_{y_1=0}, \quad (\text{C.16})$$

where for $k \in \{1, \dots, J-1\}$ these correspond to curves that self-intersect once; while for $k \in \{J, \dots, 2n\}$ these are curves that do not intersect but still go around the loop (see

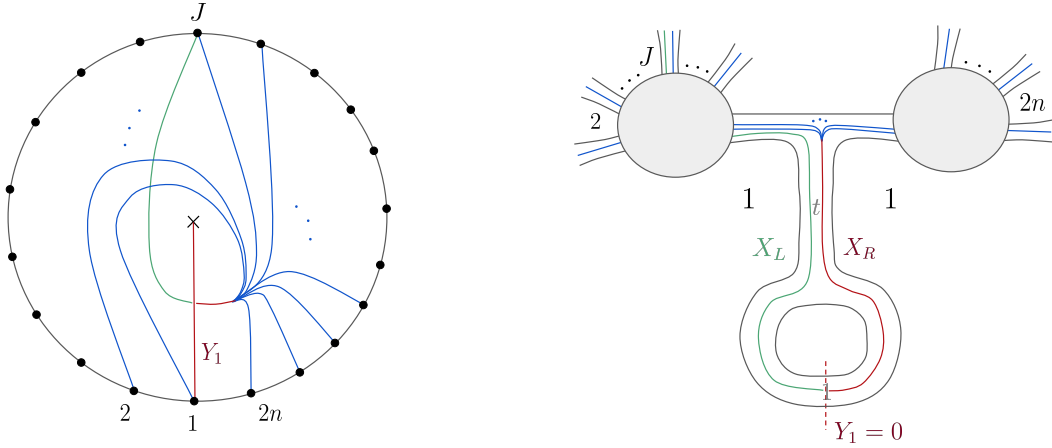


Figure 36: Extending curve Y_J – curves that intersect Y_1 only once.

figure 36, left). So this product of curves can be interpreted as a curve that starts on road $(J, J + 1)$, goes around the loop once, and ends in t (union of curve green and red). In particular, after cutting the loop surface, this curve breaks into X_L and X_R (see figure 36, right). X_R is effectively a curve of the smaller surface that starts in the tadpole road. Therefore, using the result from section C.2, we can write the derivative of the logarithm as follows:

$$\left. \frac{\partial \log u_{Y_J}}{\partial y_1} \right|_{y_1=0} = \left. \frac{\partial \log u_{X_{J,1}}}{\partial y_1} \cdot \frac{\partial \log u_{X_{1,t}}}{\partial y_1} \right|_{y_1=0} = \left. \frac{\partial \log u_{X_L}}{\partial y_1} \cdot \frac{\partial \log u_{X_R}}{\partial y_1} \right|_{y_1=0}. \quad (\text{C.17})$$

Once again, to relate to the tree-level variables, we consider the extension of curves X_L and X_R , to the scaffolded cut surface in the same way we did previously. While $u_{X_{1,t}}$ becomes $U_{s_R,t}$ giving a trivial contribution, as shown in (C.12), $u_{X_{J,1}}$ becomes $u_{s_L,J}$, allowing us to write

$$\left. \frac{\partial \log u_{Y_J}}{\partial y_1} \right|_{y_1=0} = - \left. \frac{\partial \log u_{s_L,J}}{\partial y_1} \right|_{y_1=0}, \quad (\text{C.18})$$

which precisely matches part of the tree-level contribution. So currently the difference between the tree-gluing and the loop cut for $(\dagger\dagger\dagger)$ is simply term (2):

$$X_{p,J} \left(\frac{\partial \log u_{s_R,J}}{\partial y_{1',p}} \sum_{k \in \{2, \dots, 1'\}} \frac{\partial \log u_{s_L,k}}{\partial y_{1,p}} \right) \Big|_{y_{1,p}=y_{1',p}=0}. \quad (\text{C.19})$$

Let's now try to use the u -equations to simplify (2). We start by once more turning the sum into a product inside the logarithm:

$$X_{p,J} \frac{\partial \log u_{s_R,J}}{\partial y_{1',p}} \cdot \frac{\partial \log \prod_{k \in \{2, \dots, 1'\}} u_{s_L,k}}{\partial y_{1,p}} \Big|_{y_{1,p}=y_{1',p}=0}. \quad (\text{C.20})$$

As opposed to (1), this product of u 's **cannot** be identified as the u of a smaller surface. So instead, in order to simplify this result we use the extended u -equations:

$$\prod_{k \in \{2, \dots, 1'\}} u_{s_L, k} + u_{1, p} u_{1, s_R} = 1, \quad (\text{C.21})$$

which allows us to write:

$$\frac{\partial \log \prod_{k \in \{2, \dots, 1'\}} u_{s_L, k}}{\partial y_{1, p}} \Big|_{y_{1, p} = y_{1', p} = 0} = -u_{1, s_R} \cdot \frac{\partial u_{1, p}}{\partial y_{1, p}} \Big|_{y_{1, p} = y_{1', p} = 0} = -\frac{\partial u_{1, p}}{\partial y_{1, p}} \Big|_{y_{1, p} = y_{1', p} = 0}. \quad (\text{C.22})$$

Finally to compute $\partial_{y_{1, p}} u_{1, p}$, we use (2.17) which allows us to write $y_{1, p}$ in terms of u 's in the following way:

$$y_{1, p} = \frac{u_{1, p} \prod_{k \in \{2, \dots, 2n\}} u_{p, k}}{u_{s_L, s_R} u_{s_L, 1'}} \Rightarrow 1 = \frac{\partial u_{1, p}}{\partial y_{1, p}} \prod_{k \in \{2, \dots, 2n\}} u_{p, k} \Big|_{y_{1, p} = y_{1', p} = 0}, \quad (\text{C.23})$$

and so we can rewrite (C.20) as

$$X_{p, J} \frac{\partial \log u_{s_R, J}}{\partial y_{1', p}} \cdot \frac{1}{\prod_{k \in \{2, \dots, 2n\}} u_{p, k}} \Big|_{y_{1, p} = y_{1', p} = 0}. \quad (\text{C.24})$$

Using, once again, the u -equations we can find an expression for $\partial_{y_{1', p}} \log u_{s_R, J}$ in terms of the remaining u variables as follows:

$$\begin{aligned} u_{s_R, J} + u_{1', p} \prod_{\substack{a \in \{1, \dots, J-1\} \\ b \in \{J+1, \dots, 1'\}}} u_{a, b} \times \prod_{k \in \{J+1, \dots, 2n\}} u_{p, k} &= 1 \\ \Rightarrow \frac{\partial \log u_{s_R, J}}{\partial y_{1', p}} &= - \underbrace{\frac{\partial \log u_{1', p}}{\partial y_{1', p}}}_{=1} \times \prod_{\substack{a \in \{1, \dots, J-1\} \\ b \in \{J+1, \dots, 1'\}}} u_{a, b} \times \prod_{k \in \{J+1, \dots, 2n\}} u_{p, k}, \end{aligned} \quad (\text{C.25})$$

which we can further simplify with the help of the generalized u -equations that tell us

$$\prod_{\substack{a \in \{1, \dots, J-1\} \\ b \in \{J+1, \dots, 1'\}}} u_{a, b} = 1 - u_{p, J} u_{s_R, J} \Rightarrow \prod_{\substack{a \in \{1, \dots, J-1\} \\ b \in \{J+1, \dots, 1'\}}} u_{a, b} \Big|_{y_{1, p} = y_{1', p} = 0} = 1 - u_{p, J} \Big|_{y_{1, p} = y_{1', p} = 0}. \quad (\text{C.26})$$

In summary, we have that the tree-level contribution that is not present in the loop side is:

$$X_{p, J} \left(\frac{1 - u_{p, J}}{u_{p, J}} \cdot \frac{1}{\prod_{k \in \{2, \dots, J-1\}} u_{p, k}} \right) \Big|_{y_{1, p} = y_{1', p} = 0}. \quad (\text{C.27})$$

In subsection C.6, we show that the above difference between loop integrand and the forward limit of the tree is actually a total derivative and thus vanishes after integration.

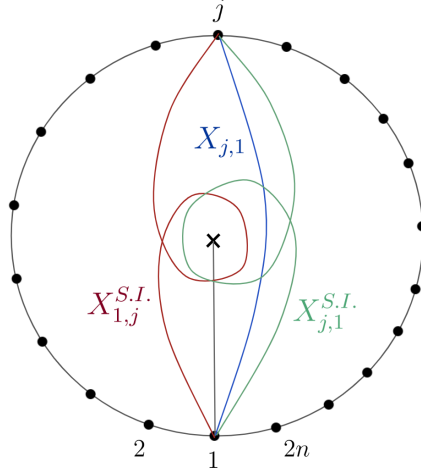


Figure 37: Curves contributing to $X_{1,j}$ term.

C.4 Matching of curves $X_{1,j}$

Now we want to see how $(\dagger\dagger\dagger)$ matches $(\star\star\star)$. Let's start with the tree side. Since $X_{1,2} = X_{1',2n} = 0$ we have that $(\dagger\dagger\dagger)$ is :

$$\sum_{j \in \{3, \dots, 2n-1\}} -X_{1,j} \left(\underbrace{\frac{\partial \log u_{s_L,1'}}{\partial y_{1,p}}}_{=-1} \frac{\partial \log u_{s_R,j}}{\partial y_{1',p}} + \frac{\partial \log u_{s_L,j}}{\partial y_{1,p}} \frac{\partial \log u_{s_R,1}}{\partial y_{1',p}} \right) \Bigg|_{y_{1,p}=y_{1',p}=0}. \quad (\text{C.28})$$

Now on the loop side, we have to consider the contributions of three different curves, see figure 37. Let's start by looking at the contribution coming from the two self-intersecting curves. From the word for curve $X_{1,j}^{S.I.}$, we get the following u -variable:

$$\begin{aligned} \underline{j1^{S.I.}} : M_1 M_L(y_t) M_L(y_1) M_2 &= \begin{bmatrix} x & 0 \\ z & 1 \end{bmatrix} \begin{bmatrix} y_t & y_t \\ 0 & 1 \end{bmatrix} \begin{bmatrix} y_1 & y_1 \\ 0 & 1 \end{bmatrix} \begin{bmatrix} a & b \\ c & d \end{bmatrix} \\ \Rightarrow u_{j,1}^{S.I.} &= \frac{(d + by_1 + dy_1)(c + cy_t z + ay_1 y_t z + cy_1 y_t z)}{(c + ay_1 + cy_1)(d + dy_t z + by_1 y_t z + dy_1 y_t z)} \Rightarrow \frac{\partial \log u_{j,1}^{S.I.}}{\partial y_1} \Bigg|_{y_1=0} = \frac{(bc - ad)}{cd(1 + y_t z)}. \end{aligned} \quad (\text{C.29})$$

Now proceeding like we did in section C.2, we can show that:

$$\frac{\partial \log u_{j,1}^{S.I.}}{\partial y_1} \Bigg|_{y_1=0} = - \frac{\partial \log u_{s_R,1}}{\partial y_{1',p}} \frac{\partial \log u_{s_L,j}}{\partial y_{1,p}}. \quad (\text{C.30})$$

Doing exactly the same thing for $X_{1,j}^{S.I.}$ we get:

$$\frac{\partial \log u_{1,j}^{S.I.}}{\partial y_1} \Bigg|_{y_1=0} = \frac{\partial \log u_{s_R,j}}{\partial y_{1',p}}. \quad (\text{C.31})$$

This means that the contribution coming from the two self-intersecting curves perfectly matches the tree-level gluing term. However, on the loop side, we still have a contribution from the non-self-intersecting curve $X_{j,1}$ (see figure 37), for which the u -variable is:

$$\begin{aligned} \underline{j1}: \quad M_1 M_R(y_1) M_2 &= \begin{bmatrix} x & 0 \\ z & 1 \end{bmatrix} \begin{bmatrix} y_1 & 0 \\ 1 & 1 \end{bmatrix} \begin{bmatrix} a & b \\ c & d \end{bmatrix} = \begin{bmatrix} axy_1 & bxy_1 \\ c + a(1 + zy_1) & d + b(1 + zy_1) \end{bmatrix} \\ \Rightarrow u_{j,1} &= \frac{b(a + c + ay_1 z)}{a(b + d + by_1 z)} \quad \Rightarrow \left. \frac{\partial \log u_{j,1}}{\partial y_1} \right|_{y_1=0} = \frac{bz(ad - bc)}{a(b + d)^2}, \end{aligned} \quad (\text{C.32})$$

which can be expressed in terms of the scaffolded-tree variables as follows:

$$\left. \frac{\partial \log u_{j,1}}{\partial y_1} \right|_{y_1=0} = -z \frac{\partial \log u_{s_R,j}}{\partial y_{1',p}}, \quad (\text{C.33})$$

with z being the F -polynomial appearing in M_1 . So on the loop side, we have an extra term:

$$\sum_{j=3, \dots, 2n-1} -z X_{1,j} \frac{\partial \log u_{s_R,j}}{\partial y_{1',p}}. \quad (\text{C.34})$$

Now, one can easily check that z is exactly the F -polynomial corresponding to the curve that turns consistently right until y_t , and thus has the following simple form:

$$z = (1 + y_t(1 + y_{1,m}(1 + \dots))). \quad (\text{C.35})$$

Finally, we note that this F -polynomial appears in the expression of u_{Y_1} , allowing us to write:

$$\frac{1}{z} = \frac{y_1}{u_{Y_1}} \Big|_{y_1=0} = \prod_{k \in \{2, \dots, 2n\}} u_{Y_k} \Big|_{y_1=0} = \prod_{k \in \{2, \dots, 2n\}} u_{p,k} \Big|_{y_1=0}, \quad (\text{C.36})$$

where we use (2.17) in the first equality. In summary, the extra term in the loop side is:

$$\sum_{j=3, \dots, 2n-1} -X_{1,j} \frac{\partial \log u_{s_R,j}}{\partial y_{1',p}} \frac{1}{\prod_{k \in \{2, \dots, 2n\}} u_{p,k}}. \quad (\text{C.37})$$

C.5 Matching the tadpole part

From the tree-level side ($\dagger\dagger\dagger\dagger$), we have the following

$$-X_{1,1'} \frac{\partial \log u_{s_L,1'}}{\partial y_{1,p}} \frac{\partial \log u_{s_R,1}}{\partial y_{1',p}} \Big|_{y_{1,p}=y_{1',p}=0} = X_{1,1'} \frac{\partial \log u_{s_R,1}}{\partial y_{1',p}} \Big|_{y_{1,p}=y_{1',p}=0}. \quad (\text{C.38})$$

From the loop side, we have two contributions, one from the regular tadpole curve, and one from the tadpole that self-intersects once. To obtain the contribution from the latter we can use directly (C.31), setting $j = 1$ to get:

$$X_{1,1} \frac{\partial \log u_{1,1}^{S.I.}}{\partial y_1} \Big|_{y_1=0} = X_{1,1} \frac{\partial \log u_{s_R,1}}{\partial y_{1',p}}, \quad (\text{C.39})$$

which precisely matches the tree glue result. As for the contribution from the non-self-intersecting curve, proceeding exactly in the same way as we did for $X_{j,1}$, we get:

$$-X_{1,1} \frac{\partial \log u_{s_R,1}}{\partial y_{1',p}} = -X_{1,1} \frac{\partial \log u_{s_R,1}}{\partial y_{1',p}} \frac{1}{\prod_{k \in \{2, \dots, 2n\}} u_{p,k}}. \quad (\text{C.40})$$

C.6 Difference between loop-cut and tree-gluing as a total derivative

So in summary the difference between the loop cut and the tree-level glue is:

$$\begin{aligned} & \prod \frac{1}{y_i^2} \left(\sum_{j=1, \dots, 2n} (X_{1,j} - X_{p,j}) \frac{\partial \log u_{sR,j}}{\partial y_{1',p}} \frac{1}{\prod_{k \in \{2, \dots, 2n\}} u_{p,k}} + 1 \right) \prod_C u_C^{X_C} \\ &= \prod \frac{1}{y_i^2} \left(- \sum_{j=1, \dots, 2n} (X_{1,j} - X_{p,j}) \frac{1 - u_{p,j}}{\prod_{k \in \{2, \dots, j\}} u_{p,k}} + 1 \right) \prod_C u_C^{X_C}. \end{aligned} \quad (\text{C.41})$$

The claim is that (C.41) is equal to the following total derivative:

$$- \frac{\partial}{\partial y_t} \left(\prod \frac{1}{y_i^2} \frac{\prod_{k \in \{1, \dots, m-1\}} u_{p,k} u_{1',k}}{u_{p,1} \prod_{j \in \{2, \dots, 2n\}} u_{p,j}^2} \prod_C u_C^{X_C} \right) \Big|_{y_{1,p}=y_{1',p}=0}, \quad (\text{C.42})$$

where m is the region indicated in figure 34.

Let's now proceed to the proof this result. We start by using (2.17), $y_i = \prod_X u_X^{g_X^{(i)}}$, to write y_t in terms of u 's as follows

$$y_t = \left(\frac{\prod_{k \in \{1, \dots, m-1\}} u_{1',k}}{\prod_{j \in \{m, \dots, 2n\}} u_{p,j}} \right), \quad (\text{C.43})$$

and so we can simplify expression (C.42) by defining Q as

$$Q = \frac{\prod_{k \in \{1, \dots, m-1\}} u_{p,k} u_{1',k}}{u_{p,1} \prod_{j \in \{2, \dots, 2n\}} u_{p,j}^2} = \frac{y_t}{\prod_{j \in \{2, \dots, 2n\}} u_{p,j}} = \frac{y_t}{1 - u_{1,1'}}, \quad (\text{C.44})$$

where we use the u -equations in the last equality. Therefore the claim is equivalent to

$$-Q \frac{\partial \log u_{p,J}}{\partial y_t} \Big|_{y_{1,p}=y_{1',p}=0} = \frac{1 - u_{p,J}}{u_{p,J}} \cdot \frac{1}{\prod_{k \in \{2, \dots, J-1\}} u_{p,k}} \Big|_{y_{1,p}=y_{1',p}=0}. \quad (\text{C.45})$$

It is sufficient to prove (C.45) under a specific triangulation since the integrated result is triangulation-independent. For example, taking the scaffolding triangulation with a ray-like triangulation inside the gluon n -gon: $\{X_{1,p'}, X_{1,p}, X_{1,3}, X_{3,5}, \dots, X_{2n-1,1'}, X_{1,1'}, X_{3,1'}, \dots, X_{2n-1,1'}\}$, allow us to write Q as

$$Q = \frac{y_t(1 + y_t)}{u_{p,2}}. \quad (\text{C.46})$$

Then one can prove (C.45) indeed holds after some tedious algebra involving the 2×2 matrices defining the u variables.

References

- [1] N. Arkani-Hamed and J. Trnka, *The Amplituhedron*, *JHEP* **10** (2014) 030, [[arXiv:1312.2007](#)].
- [2] N. Arkani-Hamed, Y. Bai, and T. Lam, *Positive Geometries and Canonical Forms*, *JHEP* **11** (2017) 039, [[arXiv:1703.04541](#)].
- [3] A. Hodges, *Eliminating spurious poles from gauge-theoretic amplitudes*, *JHEP* **05** (2013) 135, [[arXiv:0905.1473](#)].
- [4] N. Arkani-Hamed, H. Thomas, and J. Trnka, *Unwinding the Amplituhedron in Binary*, *JHEP* **01** (2018) 016, [[arXiv:1704.05069](#)].
- [5] N. Arkani-Hamed, Y. Bai, S. He, and G. Yan, *Scattering Forms and the Positive Geometry of Kinematics, Color and the Worldsheet*, *JHEP* **05** (2018) 096, [[arXiv:1711.09102](#)].
- [6] N. Arkani-Hamed, S. He, G. Salvatori, and H. Thomas, *Causal diamonds, cluster polytopes and scattering amplitudes*, *JHEP* **11** (2022) 049, [[arXiv:1912.12948](#)].
- [7] N. Arkani-Hamed, H. Frost, G. Salvatori, P.-G. Plamondon, and H. Thomas, *All Loop Scattering as a Counting Problem*, [arXiv:2309.15913](#).
- [8] N. Arkani-Hamed, H. Frost, G. Salvatori, P.-G. Plamondon, and H. Thomas, *All Loop Scattering For All Multiplicity*, [arXiv:2311.09284](#).
- [9] N. Arkani-Hamed, S. He, T. Lam, and H. Thomas, *Binary geometries, generalized particles and strings, and cluster algebras*, *Phys. Rev. D* **107** (2023), no. 6 066015, [[arXiv:1912.11764](#)].
- [10] N. Arkani-Hamed, S. He, and T. Lam, *Stringy canonical forms*, *JHEP* **02** (2021) 069, [[arXiv:1912.08707](#)].
- [11] N. Arkani-Hamed, J. L. Bourjaily, F. Cachazo, A. B. Goncharov, A. Postnikov, and J. Trnka, *Grassmannian Geometry of Scattering Amplitudes*. Cambridge University Press, 4, 2016.
- [12] N. Arkani-Hamed, Q. Cao, J. Dong, C. Figueiredo, and S. He, *Hidden zeros for particle/string amplitudes and the unity of colored scalars, pions and gluons*, [arXiv:2312.16282](#).
- [13] N. Arkani-Hamed, Q. Cao, J. Dong, C. Figueiredo, and S. He, *NLSM \subset $Tr(\phi^3)$* , [arXiv:xxxx.xxxx](#).
- [14] N. Arkani-Hamed, H. Frost, G. Salvatori, P.-G. Plamondon, and H. Thomas, *The combinatorial string, to appear*.
- [15] R. P. Feynman, *Quantum theory of gravitation*, *Acta Phys. Polon.* **24** (1963) 697–722.
- [16] S. Caron-Huot, *Loops and trees*, *JHEP* **05** (2011) 080, [[arXiv:1007.3224](#)].
- [17] *work in progress*.
- [18] N. Arkani-Hamed, H. Frost, G. Salvatori, P.-G. Plamondon, and H. Thomas, *The curvy world of curves, to appear*.
- [19] Z. Koba and H. B. Nielsen, *Reaction amplitude for n mesons: A Generalization of the Veneziano-Bardakci-Ruegg-Virasora model*, *Nucl. Phys. B* **10** (1969) 633–655.
- [20] F. C. S. Brown, *Multiple zeta values and periods of moduli spaces $M_{0,n}(\mathbb{R})$* , *Annales Sci. Ecole Norm. Sup.* **42** (2009) 371, [[math/0606419](#)].

- [21] G. Veneziano, *Construction of a crossing - symmetric, Regge behaved amplitude for linearly rising trajectories*, *Nuovo Cim. A* **57** (1968) 190–197.
- [22] C. R. Mafra, O. Schlotterer, and S. Stieberger, *Complete N-Point Superstring Disk Amplitude II. Amplitude and Hypergeometric Function Structure*, *Nucl. Phys. B* **873** (2013) 461–513, [[arXiv:1106.2646](#)].
- [23] C. R. Mafra and O. Schlotterer, *Non-abelian Z-theory: Berends-Giele recursion for the α' -expansion of disk integrals*, *JHEP* **01** (2017) 031, [[arXiv:1609.07078](#)].
- [24] J. J. M. Carrasco, C. R. Mafra, and O. Schlotterer, *Abelian Z-theory: NLSM amplitudes and α' -corrections from the open string*, *JHEP* **06** (2017) 093, [[arXiv:1608.02569](#)].
- [25] M. Mirzakhani, *Simple geodesics and Weil-Petersson volumes of moduli spaces of bordered Riemann surfaces*, *Invent. Math.* **167** (2006), no. 1 179–222.
- [26] E. Witten, *The Feynman $i\epsilon$ in String Theory*, *JHEP* **04** (2015) 055, [[arXiv:1307.5124](#)].
- [27] *work in progress*.
- [28] M. B. Green, J. H. Schwarz, and E. Witten, *Superstring Theory: Volume 1, Introduction*. Cambridge university press, 1988.
- [29] S. He, F. Teng, and Y. Zhang, *String amplitudes from field-theory amplitudes and vice versa*, *Phys. Rev. Lett.* **122** (2019), no. 21 211603, [[arXiv:1812.03369](#)].
- [30] S. He, F. Teng, and Y. Zhang, *String Correlators: Recursive Expansion, Integration-by-Parts and Scattering Equations*, *JHEP* **09** (2019) 085, [[arXiv:1907.06041](#)].
- [31] F. Cachazo, S. He, and E. Y. Yuan, *Scattering Equations and Matrices: From Einstein To Yang-Mills, DBI and NLSM*, *JHEP* **07** (2015) 149, [[arXiv:1412.3479](#)].
- [32] F. Cachazo, S. He, and E. Y. Yuan, *Scattering of Massless Particles in Arbitrary Dimensions*, *Phys. Rev. Lett.* **113** (2014), no. 17 171601, [[arXiv:1307.2199](#)].
- [33] F. Cachazo, S. He, and E. Y. Yuan, *Scattering of Massless Particles: Scalars, Gluons and Gravitons*, *JHEP* **07** (2014) 033, [[arXiv:1309.0885](#)].
- [34] *work in progress*.
- [35] N. Arkani-Hamed, F. Cachazo, and J. Kaplan, *What is the Simplest Quantum Field Theory?*, *JHEP* **09** (2010) 016, [[arXiv:0808.1446](#)].
- [36] F. Cachazo, S. He, and E. Y. Yuan, *New Double Soft Emission Theorems*, *Phys. Rev. D* **92** (2015), no. 6 065030, [[arXiv:1503.04816](#)].
- [37] *work in progress*.
- [38] N. Arkani-Hamed, J. L. Bourjaily, F. Cachazo, S. Caron-Huot, and J. Trnka, *The All-Loop Integrand For Scattering Amplitudes in Planar $N=4$ SYM*, *JHEP* **01** (2011) 041, [[arXiv:1008.2958](#)].
- [39] A. Edison, S. He, H. Johansson, O. Schlotterer, F. Teng, and Y. Zhang, *Perfecting one-loop BCJ numerators in SYM and supergravity*, *JHEP* **02** (2023) 164, [[arXiv:2211.00638](#)].
- [40] H. Kawai, D. C. Lewellen, and S. H. H. Tye, *A Relation Between Tree Amplitudes of Closed and Open Strings*, *Nucl. Phys. B* **269** (1986) 1–23.
- [41] Z. Bern, J. J. M. Carrasco, and H. Johansson, *New Relations for Gauge-Theory Amplitudes*, *Phys. Rev. D* **78** (2008) 085011, [[arXiv:0805.3993](#)].